

國立臺灣師範大學生命科學系 博士論文

脊髓小腦運動失調症之族群遺傳分析與
CTG 三核苷重複擴增的分子致病研究
**Genetic studies of spinocerebellar ataxias
and molecular impacts of CTG
trinucleotide expansion**

研究生:林 玄 原

Hsuan-Yuan Lin

指導教授:李 桂 楨 博士

Guey-Jen Lee-Chen

中華民國九十六年六月

誌謝

謹將本論文獻給在天上的父親，雖然您來不及參與我的成長與學習，但在
我心目中，您還是影響我一生最深刻的人。

師大的六年時光，是我一生中成長最多的日子。最要感謝的是恩師李桂楨
老師引領我進入遺傳學與分子生物學的領域，並從中享受到研究的成就與樂
趣；蘇銘燦老師在實驗構思上的靈活與謝秀梅老師基因轉殖小鼠實驗的細心指
導，都讓我在研究生涯中進步良多。此外，承蒙陳瓊美醫師之悉心指導，以及
陳儀莊老師之指正引導，始能使本論文更臻完善。

實驗室的和諧氣氛，也是讓我能夠在六年之間學習到這麼多的一個重要因
素。除了要感謝瑞宏學長與政光學長在實驗上的教導，也很榮幸能與國保及承
岳同學這麼多年，李姐、秀觀學姊、欣杰學長、怡辰、志信、霽茹、芷英、雅
仝、懿婷、玢璘、淑宜、宜欣、士寰、襄銘、若芸、慧茹、郡潔、金珏、玄
竺、佩瑛、昇翰、國修、郁芳.....等夥伴，日常的吃喝玩樂實在是少不了你
們，研究所的生活也因為你們而多彩多姿。實驗室附近的鄰居：建智學長、慶
孝學長、淑寧學姊、哲維學長、柏安學長、芳足學姊、雅津、金祝、永祥、聖
文、鎮寬、俊彥.....，感謝你們在實驗上的教導、藥品器材上的接濟與這份濃
烈的友情；實在是很難想像一般人覺得會唸得很辛苦的研究所生涯，能夠結交
到這麼多的貼心知己，尤其是哲維學長可以為朋友兩肋插刀的情誼更是一生中
難求的。還要感謝翎絢、振銘、管小姐、景勝與陸泉在動物實驗上的大力幫
忙，才能使得這部份的實驗能夠順利進行。

當然除了老師與夥伴們外，要感謝媽媽從小對我的栽培，以及姊姊與哥哥
在背後的支持；親愛的老婆-婉芳的體諒與貼心，成就了我的研究所生涯。也要
感謝婉芳的爸爸、媽媽、阿宏及哈弟的關懷與支持，讓我享受到更多家人的溫
暖。

要感謝的人實在太多了，礙於篇幅，未能於文中提及的好友也請見諒。最後要特別感謝 Confocal Microscope Lab, Instrumentation Center, NTU 在共軛焦顯微鏡使用上的協助，使得細胞螢光染色實驗得以順利完成。

本論文感謝 財團法人罕見疾病基金會提供論文獎助金。

Index

Index.....	I
Abstract (Chinese)	V
Abstract	VII
List of figures and tables.....	IX
Introduction.....	1
Spinocerebellar ataxia type 1 (SCA1)	3
Spinocerebellar ataxia type 2 (SCA2)	3
Spinocerebellar ataxia type 3 (SCA3)	4
Spinocerebellar ataxia type 6 (SCA6)	5
Spinocerebellar ataxia type 7 (SCA7)	5
Spinocerebellar ataxia type 8 (SCA8)	6
Spinocerebellar ataxia type 10 (SCA10)	6
Spinocerebellar ataxia type 12 (SCA12)	7
Spinocerebellar ataxia type 17 (SCA17)	7
Organization of SCA8 gene	9
The role of KLHL1 protein.....	10
Natural antisense transcripts	11
Myotonic dystrophy type 1 (DM1).....	11
Internal ribosome entry segment (IRES)	12
Animal models of SCA8	13
Aims	15
Materials and methods	16
Subjects	16
Genomic DNA extraction	16
Polymerase chain reaction (PCR) and genotyping	17
Gel extraction.....	17
Statistical analyses	18
SCA8 cDNA cloning	18

Site-directed mutagenesis	19
pEF-SCA8 constructs.....	19
KLHL1 cDNA cloning and pEF-KLHL1-EGFP construct.....	20
pCMV-(CAG) ₃₆ -IRES-EGFP construct.....	20
pCMV-ORF1-EGFP construct	20
pCMV-SCA8-EGFP constructs.....	21
pCMV-K-ORF3-EGFP constructs.....	21
Preparation of electro-competent cells	21
Ligation	22
Electroporation.....	22
Minipreparation of plasmid DNA.....	23
Midipreparation of plasmid DNA.....	23
Cell cultivation.....	24
Transfection	24
Fluorescence activated cell sorting (FACS) analysis	25
Immunofluorescence analysis.....	25
Cell lysate preparation	26
Cytoplasmic and nuclear proteins preparation.....	27
Western blotting (immunoblotting)	27
RNA isolation	28
Establishment of SCA8 stably expressing Flp-In T-REx 293 cell lines	29
Cell proliferation assessment (WST-1 assay).....	29
Transgene construction and SCA8 transgenic mouse generation	30
Transgenic mouse genotyping	30
Characterization of transgene copy numbers of transgenic mouse lines	31
RNA isolation from mouse brain tissues and reverse transcription- polymerase chain reaction (RT-PCR).....	31

Rotarod test	31
Immunohistochemical analysis	32
RNA cleanup	33
Microarray analysis	33
Real-time RT-PCR (Quantitative RT- PCR)	34
Protein samples preparation for proteomic analysis	35
Minimal labeling with CyDye Fluors for 2-D difference gel electrophoresis (DIGE)	35
IPG strip rehydration and first-dimension isoelectric focusing (IEF)	36
Second-dimension SDS-PAGE	36
Gel staining with SYPRO Ruby	37
Image analysis	37
In-gel digestion	37
Mass Spectrometry	38
Results	39
Trinucleotide or pentanucleotide repeat distributions	39
Frequency of SCAs and genetic and clinical features of patients	39
Frequency of large normal alleles	40
SCA8 alleles with 75 to 92 repeats in PD patients	40
SCA17 allele with 46 repeats in PD patient	41
Regulation of KLHL1 and CAG repeat-containing RNA expression by SCA8	41
SCA8 encodes translatable ORF1 and ORF3	43
ORF1 and expanded poly-leucine-containing ORF3 proteins form aggregates	44
Aggregated ORF1 and ORF3 proteins are localized in both nuclei and cytoplasm	44

Generation and characterization of isogenic and inducible SCA8 cell lines	45
Generation and characterization of SCA8 transgenic mice	47
Expression of SCA8 transcripts in SCA8 transgenic lines	47
Behavior assessment of transgenic mice by performance on the accelerating rotarod	48
SCA8 transgene does not cause the morphological abnormalities of Purkinje cells	48
SCA8 transgenic mice exhibit the clasping phenotype	49
Proteomic analysis of SCA8 transgenic mice	50
Discussion	51
References	62

摘要

脊髓小腦運動失調症（SCAs）為一群顯性遺傳的神經退化性疾病，目前已確定的各型中，絕大多數是由致病基因中的三核苷酸或五核苷酸重複擴增所致。本論文首先建立了臺灣地區族群的 SCAs 致病基因之遺傳資料庫，並且檢測尚未確定的病例。在我們的檢測結果中，臺灣 SCAs 族群當中最多的為 SCA3；且臺灣的族群分佈頻率與日本及高加索人群極為相似。此外，我們亦發現五名帕金森氏症患者具有 SCA8 或是 SCA17 基因的突變，顯示這兩種基因的突變可能以非小腦症狀的表現型來顯現。

SCA8 與其他的 SCAs 不同之處在於其雖然也是由三核苷酸重複擴增所造成，但其致病基因中的三核苷酸為 CTG，且位於非轉譯區，而非像其他型 SCAs 絕大多數為轉譯區中的 CAG 擴增。此外，SCA8 基因所轉錄 RNA 的 5'端，與 *KLHL1* 基因之 mRNA 的 5'端互補，即為 *KLHL1* 基因的反意 RNA。本論文的第二部份為利用細胞與基因轉殖小鼠模式來探討 SCA8 的可能致病機轉。在細胞模式中，我們發現 CTG 擴增的 SCA8 對於 *KLHL1* 基因表現的抑制較不若正常 SCA8 來得強；此外，雖然之前的研究認為 SCA8 基因並不會進行轉譯，但我們的研究證實了 SCA8 基因中的開放解讀架構（open reading frame, ORF）確實可以轉譯成蛋白質，且 CTG 擴增的

SCA8 與 *ORF1* 都會形成細胞內不可溶的包涵體。因此，*SCA8* 的反意調控與可轉譯的開放解讀架構都可能與致病過程相關。我們亦建立 *SCA8* 的基因轉殖小鼠模式，雖然行為測定與小腦組織形態上都未發現異狀，但卻出現四肢緊抱（*clasp*ing）的現象。因此，此現象或許可提供作為致病機轉或是藥物研究之指標。

Abstract

Spinocerebellar ataxias (SCAs) comprise a heterogeneous neurodegenerative disorders that are dominantly inherited. Among the identified SCAs, the trinucleotide or pentanucleotide mutations have been shown to cause most SCAs. However, the prevalence of SCAs varies among populations. In the first part, in order to set up a database of the trinucleotide- and pentanucleotide-repeat expansions leading to SCA, we have assessed the repeat size at the SCA1, SCA2, MJD/SCA3, SCA6, SCA8, SCA10, SCA12, SCA17, and DRPLA loci. MJD/SCA3 (46%) was the most common autosomal dominant SCA in the Taiwanese cohort, followed by SCA6 (18%) and SCA1 (3%). The frequencies of large normal alleles are closely associated with the prevalence of SCA1, SCA2, MJD/SCA3, SCA6, and DRPLA among Taiwanese, Japanese, and Caucasians. In addition, abnormal expansion of *SCA8* and *SAC17* genes were detected in patients with PD, suggesting these two mutations might manifest as non-cerebellar symptoms.

Unlike most SCAs caused by expansion of a coding CAG trinucleotide repeat, *SCA8* has been shown to link to CTG triplet repeat expansion in the 3' untranslated region of *SCA8* gene on 13q21. The 5' end of the *SCA8* transcript overlaps the transcription and translation start sites, as well as the first splice donor sequence of the *Kelch-like 1 (KLHL1)* gene of the complementary strand. The aim of the other part is to uncover the plausible mechanisms using cell and transgenic mouse as model systems. *In vitro* studies demonstrated that the suppressive activity for *KLHL1* was significantly different for *SCA8* transcripts carrying 157 combined repeats,

and that *SCA8* RNA was translatable. Both the expressed GFP-tagged ORF1 and poly-leucine-expansion ORF3 proteins formed aggregates. Thus, *SCA8 trans* effects and poly-leucine-containing aggregates might be correlated with the pathogenesis of *SCA8*. In addition, the *SCA8* overexpression transgenic mouse model showed no difference of motor activity and histopathological morphology of Purkinje cells between transgenic mice and their control littermates. However, hind-limb clasping was observed in transgenic mice with 157 repeats during tail suspension. Although no marked pathological phenotypes were found in our model, the clasping phenotype might be used to be a characteristic evaluation index for drugs screening as in Huntington's disease mice.

List of figures and tables

Figure 1. Frequency distribution of tri- or pentanucleotide repeat lengths	84
Figure 2. Structure of <i>SCA8</i> gene	85
Figure 3. Schematic diagrams of pEF- <i>SCA8</i>	86
Figure 4. Schematic diagrams of pCMV-ORF1-EGFP.....	87
Figure 5. Regulation of the <i>KLHL1</i> and CAG repeat-containing transcript expression by <i>SCA8</i>	88
Figure 6. Expression analysis of <i>SCA8</i> ORF1 and ORF3 in HEK293 ...	89
Figure 7. Distribution of <i>SCA8</i> -ORF1 and ORF3 proteins.....	90
Figure 8. Subcellular localization of <i>SCA8</i> ORF1-EGFP and ORF3- EGFP proteins	91
Figure 9. Observation of ORF1-EGFP distribution form continuous focal planes.....	92
Figure 10. Observation of <i>SCA8</i> -157R-EGFP distribution form continuous focal planes	93
Figure 11. Expression analysis of <i>SCA8</i> ORF1 and ORF3 in IMR-32 ..	94
Figure 12. Diagram of Flp-In system	95
Figure 13. Characterization of isogenic and inducible <i>SCA8</i> cell lines ..	96
Figure 14. The effects of staurosporin, MG-132, and paraquat	97
Figure 15. Schematic diagram of <i>SCA8</i> transgene and genotype confirmations	98
Figure 16. Estimation of the expression of <i>SCA8</i> transgene by RT-PCR	99
Figure 17. Rotarod performance of <i>SCA8</i> transgenic mice	100
Figure 18. Immunohistochemical analyses of the <i>SCA8</i> transgenic mouse cerebella.	101
Figure 19. The clasping phenotype of <i>SCA8</i> transgenic mouse	102
Figure 20. Real-time RT-PCR analyses.....	103
Figure 21. Real-time RT-PCR analyses.....	104

Figure 22. Real-time RT-PCR analyses.....	105
Figure 23. Two-dimensional difference gel electrophoresis gels.....	106
Table 1. Genetics of SCAs.....	107
Table 2. Primers and conditions for PCR amplification of tri- or pentanucleotide repeat region in SCA genes	108
Table 3. Trinucleotide and pentanucleotide repeat lengths in nine disease genes.....	109
Table 4. Prevalence and frequency of large normal alleles	110
Table 5. Expanded trinucleotide repeat sequences and numbers in PD patients	111
Table 6. Summary of copy numbers, RNA expression, and clasping phenotype of SCA8 transgenic mice.....	112
Table 7. List of TaqMan gene expression assays	113
Table 8. Summary of microarray analysis at the age of 20-month	114
Table 9. Summary of relative changes of protein abundance.....	115
Table 10. MALDI-TOF analysis of the protein spots	116

Introduction

The word “ataxia” derived from Greek word, “*a taxis*” in the late 19th century and refers to “without order or incoordination”. This word is used to describe the symptom of incoordination that may be caused by trauma, infections, other diseases, Vitamin E deficiency or neurodegenerative changes. In addition to environmental and dietary factors, ataxia could also be caused inherently.

In 1863, Dr. Nikolaus Friedreich first described six patients with a recessively inherited ataxia in which the age of onset was below 20-year-old and it is known as Friedreich's ataxia. Thirty years later, Dr. Pierre Marie noticed another dominantly inherited form clinically distinct from that described by Friedreich and began between thirty and forty years of age, and patients described here is recently affirm as having spinocerebellar ataxia type 3 (SCA3)/Machado-Joseph disease (MJD) (Uchihara et al. 2004). Therefore, ataxias at that time were roughly divided into Friedreich's ataxia and Marie's ataxia, based on the age of onset.

These ataxias were not further clearly subclassified until in the 1980s, after Dr. Harding classifying autosomal dominant cerebellar ataxias (ADCAs) into three clinical subgroups types, including ADCA type I, type II, and type III. ADCA type I is characterized by a progressive cerebellar syndrome, with additional but variable associated features of supranuclear ophthalmoplegia, optic atrophy, mild dementia, peripheral neuropathy or extrapyramidal dysfunction. SCA1, SCA2, SCA3, SCA4, SCA8, SCA12, SCA17, dentatorubral pallidolusian atrophy (DRPLA) and recently defined SCA27

and SCA28 fit in with this type. ADCA type II shows cerebellar ataxia accompanied with pigmentary macular dystrophy and only SCA7 is included. ADCA type III is a pure cerebellar syndrome and comprises SCA5, SCA6, SCA10, SCA11, SCA14, SCA15, SCA22, and SCA26. SCA13 does not fall within any categories described above.

Although each SCA is primarily categorized in terms of the clinical symptoms, different SCAs may sometimes have overlapping signs and it is difficult to distinguish simply on the basis of clinical grounds. However, with the advance of molecular biotechnology, mutation analyses have linked various genetic loci to the subtypes of SCA and afforded the genetic classification of clinical subtypes. Dissimilar to most inherited diseases caused by point mutation, deletion, insertion or translocation of causing gene, identified SCAs are largely caused by the unexpected prolongation of tandem nucleotide repeats. Among the mapped SCAs, SCA1, SCA2, SCA3/MJD, SCA6, SCA7, SCA17, and DRPLA have been shown to be associated with the expansions of coded CAG repeats translated into polyglutamine stretch that adds a toxic gain of function to the respective proteins (Orr et al. 1993; Kawaguchi et al. 1994; Koide et al. 1994; Imbert et al. 1996; Pulst et al. 1996; David et al. 1997; Zhuchenko et al. 1997; Koide et al. 1999), and SCA8, SCA10, and SCA12 are associated with expansions of 3' UTR CTG, intronic ATTCT, and promoter CAG, respectively (Holmes et al. 1999; Koob et al. 1999; Matsuura et al. 2000). Nevertheless, SCA5, SCA14 and SCA27 have been found caused by missense mutations (van de Warrenburg et al. 2003; Yabe et al. 2003; Stevanin et al. 2004; Alonso et al. 2005; Brusse et al. 2006; Ikeda et al. 2006) rather than tandem repeats

expansions. Some SCAs involved in this study will be discussed briefly in the following and the genetic summary of SCAs is listed in **Table 1**.

Spinocerebellar ataxia type 1 (SCA1)

SCA1 is the first mapped SCA in which the mutant gene *SCA1* localized on chromosome 6p23. It has been found that *SCA1* gene carries more than 40 CAG trinucleotide repeat units in affected individuals (Orr et al. 1993; Banfi et al. 1994) and it is now believed that expanded CAG-encoded polyglutamine (polyQ) tract within ataxin-1, the *SCA1* product, gains a novel function. SCA1 usually begins in the 3rd and 4th decade of life accompanied with symptoms such as ataxia, slow saccades, increased tendon reflexes at knee, and difficulty speaking and swallowing. In the view of molecular mechanisms, ataxin-1 interacts with glyceraldehyde-3-phosphotase dehydrogenase (GAPDH) (Koshy et al. 1996), cerebellar Purkinje-enriched leucine-rich acidic nuclear protein (LANP) (Matilla et al. 1997), calcium binding protein calbindin D28k (CaB) (Vig et al. 1998; Vig et al. 2000), proteasome and chaperon proteins (Cummings et al. 1998). Most associated proteins are recruited to nuclear aggregates formed under the expression of mutant ataxin-1 and this could be explained the fact that aberrant interactions involve in the pathogenesis.

Spinocerebellar ataxia type 2 (SCA2)

The typical clinical features of SCA2 include limb and gait ataxia, slow saccades, and hyporeflexia, while levodopa-responsive parkinsonism is occasionally presented or dominant in the family (Gwinn-Hardy et al. 2000; Shan et al. 2001; Furtado et al. 2002; Ragothaman et al. 2004). SCA2 is caused by the expansion of unstable CAG repeats in *SCA2* gene encoding

ataxin-2. The most common normal ataxin-2 allele contains 22 glutamines. The range of glutamine repeats in mutant ataxin-2 varies from 33 to 77 with 37 glutamines being most common. Wild type ataxin-2 is primarily localized with the Golgi apparatus, whereas expression of mutant ataxin-2 disrupts the normal morphology of the Golgi complex (Huynh et al. 2003) and this dispersion can be reduced by the overexpression of parkin, an E3 ubiquitin ligase mutated in an autosomal recessive form of parkinsonism. In addition, ataxin-2 serves as a substrate of parkin for ubiquitination and degradation, and mutant ataxin-2 aggregates mask these effects of parkin by sequestering it (Huynh et al. 2007). Thus, the correlation between ataxin-2 and parkin needs to be further investigated to uncover the pathogenesis of SCA2 and related parkinsonism.

Spinocerebellar ataxia type 3 (SCA3)

SCA3 is the most common dominantly inherited ataxia worldwide and also called Machado-Joseph disease (MJD), named for affected families of Azorean extraction, characterized principally by ataxia, spasticity, and ocular movement abnormalities. The mutation leading to SCA3/MJD is linked to chromosome 14q32.1, and the range of CAG repeats in mutant alleles is 45-86 repeats (Kawaguchi et al. 1994). The disease protein, ataxin-3, of 42kDa is smallest of the polyQ disease so far. Ataxin-3 consists of a structured N-terminus with deubiquitinating activity, two ubiquitin-interacting motifs (UIMs) and a C-terminal polyQ tract (Masino et al. 2003). *In vitro* and *in vivo* studies have shown that expression of expanded ataxin-3 induces cell death and results in accumulation of ubiquitinated intranuclear inclusions selectively in neurons of affected brain regions (Paulson et al.

1997) in which the recruitment of ubiquitin might act via UIM motifs (Donaldson et al. 2003).

Spinocerebellar ataxia type 6 (SCA6)

SCA6 is caused by a very mild CAG repeat expansion in *CACNA1A* gene encoding the α_{1A} subunit of voltage-gated calcium channels type P/Q (Zhuchenko et al. 1997). However, other mutations in this gene have been found to cause familial hemiplegic migraine (FMH) and episodic ataxia type 2 (EA2) (Ophoff et al. 1996), suggesting these diseases are allelic disorders. The clinical features of SCA6 include nystagmus, dysarthria, and ataxia, while in some cases signs of brainstem and pyramidal tract are also involved. It is believed that polyQ expansion in this calcium channel influences the trafficking of Ca^{2+} and a previous study has indicated that polyQ elongation caused a proportional negative shift of voltage-dependent inactivation, suggesting reduced Ca^{2+} influx may be associated with neuronal death in cerebellum (Toru et al. 2000).

Spinocerebellar ataxia type 7 (SCA7)

SCA7 is unique to SCAs for the phenotype of retinal degeneration in addition to typical cerebellar symptoms. SCA7 was mapped to Chromosome 3p14-p21.1 (Benomar et al. 1995). Normal SCA7 alleles contain 4-35 CAG repeats, while pathological alleles contain over 38 CAG repeats. Ataxin-7, encoded by *SCA7* gene, is nuclear localized and associates with the nuclear matrix and the nucleolus (Kaytor et al. 1999). In addition, ataxin-7 was considered as a component of the TATA-binding protein-free TAF-containing complex (TFTC) and the SPT3-TAF9-GCN5 acetyltransferase complex (STAGA) (Helmlinger et al. 2004), which both belong to histone

acetyltransferase (HAT) complexes, or related complexes. Although mutant ataxin-7 did not disturb the assembly of these complexes, it inhibited the histone acetylation function in a dominant-negative manner (Helmlinger et al. 2004; McMahon et al. 2005; Palhan et al. 2005). Taken together, the spatial and proteins interaction patterns help to explain some aspects of SCA7 pathogenesis.

Spinocerebellar ataxia type 8 (SCA8)

SCA8 was first described in 1999 as a novel autosomal SCA caused by CTG triplet repeats expansion in the nontranslated *SCA8* gene locating on chromosome 13q21 (Koob et al. 1999). Dysarthria, eye move disorder, and ataxia are commonly observed in patients. Incomplete penetrance is an interesting trait observed in SCA8 that expanded CTG repeats do not always cosegregate with clinical features. In addition, intergenerational transmission of CTG alleles is unstable and shows a strong bias toward expansions in maternal transmission (Koob et al. 1999; Day et al. 2000; Moseley et al. 2000). Further description of SCA8 will be presented in the following.

Spinocerebellar ataxia type 10 (SCA10)

SCA10, characterized by ataxia, dysarthria and seizure not found in other SCAs (Grewal et al. 1998; Rasmussen et al. 2001; Grewal et al. 2002), is caused by expansion of ATTCT pentanucleotide repeat in intron 9 of a novel gene, *SCA10*, on chromosome 22q13.3. Although little is known about ataxin-10, the protein product of *SCA10*, has been localized to cytoplasmic and perinuclear compartments, and knocking it down induces severe neuronal loss (Marz et al. 2004). In addition, overexpression of ataxin-10 enhanced intracellular glycosylation activity via interaction with *O*-Linked β -N-

acetylglucosamine transferase (OGT) (Marz et al. 2006). Accordingly, ataxin-10 might play a vital role in cell.

Spinocerebellar ataxia type 12 (SCA12)

SCA12 was first described in pedigrees of German American and Indian descent (Holmes et al. 1999; Fujigasaki et al. 2001b). Patients usually begin with action tremor in their 3rd decade, followed clinical symptoms such as ataxia, hyperreflexia, dysarthria and bradykinesia (Holmes et al. 1999; O'Hearn et al. 2001; Srivastava et al. 2001). The causing mutation lies 5' untranslated region (UTR) of the gene *PPP2R2B*, which produces regulatory B subunit of serine/threonine phosphatase, PP2A. PP2A is implicated in various cell process including cell growth and differentiation, DNA replication, microtubule assembly, and apoptosis (Price and Mumby 1999; Virshup 2000). Down regulation of PP2A in brain has been shown to disrupt the balance of phosphorylation/dephosphorylation state, resulting in accumulation of hyperphosphorylated tau, a microtubule-associated protein (Gong et al. 2000). It is speculated that expansion of CAG repeat misregulates the expression of downstream gene, which in turn affects the phosphatase activity of PP2A (Holmes et al. 2003).

Spinocerebellar ataxia type 17 (SCA17)

TATA-box binding protein (TBP) is well-known for its role in the initiation of RNA transcription, but it is now also considered associated with SCA17. SCA17 was first described in a Japanese family and the clinical features consist of ataxia, dementia, hyperreflexia, parkinsonian, and postural reflex disturbance (Koide et al. 1999; Fujigasaki et al. 2001a; Nakamura et al. 2001). Normal individuals carry 25-42 CAG repeats in *TBP* gene, while

those have 43-48 CAG repeats show an incomplete penetrance (Fujigasaki et al. 2001a; Nakamura et al. 2001; Silveira et al. 2002). Immunocytochemical analysis in SCA17 patients showed neuronal intranuclear inclusion bodies (Nakamura et al. 2001), and most neuronal nuclei were diffusely stained with 1C2 antibody, which recognizes expanded polyglutamine tracts (Nakamura et al. 2001). Expression of the full-length TBP protein resulted in repeat-length-dependent inclusion formation *in vitro*, and overexpression of expanded TBP increased Cre-dependent transcriptional activity, suggesting that mutant TBP might be involved in aberrant transcription activity (Reid et al. 2003). TBP is also found colocalize to neurofibrillary tangle structures in Alzheimer's disease (AD) (Reid et al. 2004), implying that ubiquitously expressed TBP might contribute to other diseases.

“Anticipation” refers to the phenomena that the disease begins at an earlier age and worsens while it is transmitted to the next generation. This phenomena is often found in diseases caused by trinucleotide repeat expansion, including Huntington's disease, myotonic dystrophy, SCA1, SCA2, SCA3, SCA6, SCA7, SCA8, SCA10, SCA12, SCA17, SCA22, and DRPLA, as the next generations often have more repeats and more severe symptoms.

The prevalence of SCAs varies among populations. Such differences were closely associated with the distributions of large normal alleles in Japanese and Caucasian populations (Takano et al. 1998). The frequency of SCA has been assessed in Chinese patients, with 5% for SCA1, 6% for SCA2, 48% for MJD/SCA3, and 0% for SCA6, SCA7, and DRPLA (Tang et al. 2000). A study of ethnic Chinese in Taiwan also revealed MJD/SCA3 as the most

common type (47%), followed by SCA6 (11%), SCA2 (11%), SCA1 (5%), SCA7 (3%), DRPLA (1%), and SCA8 (0%) (Soong et al. 2001). However, 22% of SCA patients in this study did not have mutations in the above 7 SCA genes, and there has been no report on SCA10, SCA12, and SCA17 among Chinese populations. In addition, and with the exception of the MJD/SCA3 and SCA6 genes, the distribution of SCA repeats in the Chinese population has not been well documented.

Among the growing numbers of the neurodegenerative disorder, expanded repetitive DNA sequences contribute some aspects to the pathogenesis. The expanded sequence might occur either within or outside of the coding region, and the latter includes the regions of introns, 3' untranslated, and 5' untranslated region (UTR). The autosomal inherited spinocerebellar ataxia type 8 (SCA8) is an example in which trinucleotide CTG repeat expansion occurs in the 3' UTR of the *SCA8* gene that lacks a significant open reading frame. SCA8 was first described in a large family characterized by the symptoms including limb ataxia, dysarthria, and horizontal nystagmus (Koob et al. 1999). The CTG repeat length is mitotically unstable, and often interrupted by CTA repeats (CTG/CTA combined repeats) (Koob et al. 1999; Moseley et al. 2000; Silveira et al. 2000). In addition, the intergenerational changes in CTG repeat number are typically larger for SCA8 than for the other SCAs, and most cases are resulted from maternal expansive transmission (Koob et al. 1999).

Organization of SCA8 gene

Human *SCA8* gene spans around 32 kb in length on chromosome 13q21 and is composed of up to six exons that are alternatively spliced (**Figure 2A**).

The 5' end of *SCA8* transcript is variably spliced exon D, D', D'', D4, D5, which in turn joins to the variable exon C3, the invariable exons C2, C1, the alternative exon B, and terminates at either exon B or A (Nemes et al. 2000; Benzow and Koob 2002). Since the last exon is the region where CTG repeats reside, the expanded CTG tract might not be included in *SCA8* transcripts, accounting for the incomplete penetrance in some way. Another attractive feature of *SCA8* gene is that exon D is transcribed in the opposite direction through the first exon of *KLHL1* transcript (Nemes et al. 2000) (**Figure 2A**). The similar distribution patterns in the brain and the conserved sense/antisense organization of *SCA8* and *KLHL1* (Benzow and Koob 2002) indicate that endogenous *SCA8* transcripts might act as a natural, or so-called *cis*-encoded antisense transcripts of *KLHL1*, which further results in *SCA8* neuropathogenesis.

The role of KLHL1 protein

KLHL1 protein is highly homologous to the *Drosophila* kelch protein, which is responsible for maintaining actin organization of ring canals connecting the oocyte to supporting nurse cells during oogenesis (Xue and Cooley 1993; Robinson and Cooley 1997). *KLHL1* spans a genomic size of over 400 kb and comprises of 11 exons encoding the amino-terminal region (NTR) following by the BTB/POZ (for Broad-Complex, Tramtrack and Bric a brac/Poxvirus and Zinc-finger domain) dimerization domain and the six actin-binding Kelch motif repeats (KREPs) separating by the intervening amino acid sequence (IVS) (Robinson and Cooley 1997). In addition, *KLHL1* protein interacts with the α_{1A} subunit of voltage-gated calcium channels type P/Q, the product of *SCA6* gene, by increasing its current

density and channel availability for opening (Aromolaran et al. 2007), indicating that KLHL1 might have a role for modulating calcium channel.

Natural antisense transcripts

Natural antisense transcripts (NATs) are endogenous RNAs complementary to sequences of already known function. Although some are transcribed from a locus that is different from the locus of the sense RNA, most antisense transcripts are issued from the same locus. They were first found in prokaryotes and have been considered regulating the expression of specific genes, which are often down regulated. In the last two decades, more and more NATs have been described in eukaryotes, including human. It is widely accepted that NATs might function as templates for translation or regulators of sense gene expression (Dolnick 1993; Li et al. 1996). Apart from being translation templates, NATs could exert its regulational effects via at least three mechanisms. First, the overlapping segments form double strand, which leads to the prevention of translation or the digestion to small fragments (Lai 2002). Second, NATs involve epigenetic regulations such as the methylation of promoters by some unknown mechanisms and the conversion of the chromosome structure (Wutz et al. 1997; Tufarelli et al. 2003). Third, sense and antisense RNAs form two voluminous RNA pol II complexes on opposite strands, leading to RNA polymerases clash in the overlapping region, which would ultimately interfere the activity of one or both protein complexes (Prescott and Proudfoot 2002).

Myotonic dystrophy type 1 (DM1)

Myotonic dystrophy type 1 (DM1) is also caused by a CTG trinucleotide repeat expansion in the 3' UTR of its disease-causing gene, *DMPK* (Buxton

et al. 1992; Harley et al. 1992; Kitsu et al. 1992; Mahadevan et al. 1992). The CTG repeat expansion within the *DMPK* gene primarily affects the neuromuscular system, while cardiac conduction defects, smooth muscle involvement, mental changes, hypersomnia, ocular cataracts, insulin dependent diabetes and testicular atrophy are also involved. At least three hypotheses have been proposed to explain the possible mechanisms of DM1. First, haploinsufficiency has been proposed to explain the dominant nature of DM. However, *DMPK* levels in adult and congenital patients were not significantly changed (Narang et al. 2000), and neither heterozygous nor homozygous *DMPK* knock out mice show the severely multisystemic DM phenotypes (Berul et al. 1999), suggesting that haploinsufficiency might not be directly involved in DM. Second, the CTG expansion is likely to disrupt the chromatin structure nearby the *DMPK* and further affect the transcription *DMPK* and its neighboring genes (Otten and Tapscott 1995). Third, the mutant *DMPK* transcripts tend to be retained within the nucleus in distinct foci, which in turn sequester the RNA-binding proteins, including CUG-binding proteins (CUGBPs), muscleblind (MBNL) protein family, and some other transcription factors, or affect the transport of other CAG repeats-containing RNA (Taneja et al. 1995; Fardaei et al. 2002; Ebraldize et al. 2004). In the view of being mediated by CTG expansion, the molecular similarity between SCA8 and DM1 should provide an opportunity to further define the molecular pathogenesis of SCA8.

Internal ribosome entry segment (IRES)

Initiation of translation of most eukaryotic mRNAs normally depends on the 5' m⁷GpppN cap structure of mRNAs, which recruits 43S ribosome preinitiation complex via interaction with the cap binding protein eIF4E

(Sonenberg 1994). The translation machinery then migrates downstream until it meets the first AUG codon in the optimal context for initiation of translation (Kozak 1991). This scanning model predicts that any mRNA with long 5'-untranslated region (5'-UTR) and complex secondary structures may not be translated efficiently. In an alternative mechanism of translation initiation, the ribosome can be directly recruited to an internal site on the mRNA that can be some considerable distance from the cap structure (Hellen and Sarnow 2001). The latter mechanism requires the formation of a complex RNA structural element termed an internal ribosome entry segment (IRES). In the presence of *trans*-acting factors, IRES allows the internal ribosome entry (Stoneley and Willis 2004). Up to date, many eukaryotic cellular mRNAs have been suggested to contain such IRES activities (see <http://www.rangueil.inserm.fr/IRESdatabase>). Although reported non-coding (Koob et al. 1999), small ORFs in the *SCA8* transcripts were noted. Among them, a 102 amino acids containing-ORF1 and a 41 amino acids plus a poly-leucine tract containing-ORF3 may be translated if *SCA8* RNA possesses a cap independent IRES activity. Our previous study had demonstrated the possible IRES activity within *SCA8* (Lin et al. submitted). Therefore, if small ORFs could be translated, the linkage between translatable ORFs and pathogenesis remains to be further investigated.

Animal models of SCA8

Animal models play a crucial role in studying pathological mechanisms of human diseases. Several models have been established to investigate *SCA8*. Ectopic expression of *SCA8* in the *Drosophila* retina induces late-onset and progressive neurodegeneration, and the neuronally expressed RNA binding protein, *staufen* is found to be recruited to the *SCA8* RNA with the presence

of 3' CUG-containing region, suggesting that SCA8 may be resulted from RNA-mediated molecular pathway (Mutsuddi et al. 2004). Recently targeted deletion of a single *Sca8* ataxia locus allele in mice leads to degeneration of Purkinje cell function, indicating partial loss of *Klh11* function with the pathogenesis of the disease (He et al. 2006). In addition, using a transgenic mouse model in which the human *SCA8* mutation is present on a BAC, a newly discovered gene, *ataxin 8 (ATXN8)*, which encodes a nearly pure polyglutamine expansion protein in the CAG direction, was reported (Moseley et al. 2006). The studies of BAC *SCA8* transgenic mice revealed 1C2-positive intranuclear inclusions in Purkinje and brainstem neurons, indicating polyglutamine expansion protein in the CAG direction with the pathogenesis of the disease (Moseley et al. 2006). However, BAC clones usually insert to the chromosome with relatively low copies, leading to lower expression of transgene. Hence, reinforcing transgene expression under the control of the specific promoter in replace of expressing low copies of artificial chromosome could sometimes get severe phenotypes and a earlier age of onset.

Aims

The first aim of this study was to set up a database of the trinucleotide- and pentanucleotide-repeat expansions leading to SCA, we have assessed the repeat size at the SCA1, SCA2, MJD/SCA3, SCA6, SCA8, SCA10, SCA12, SCA17, and DRPLA loci in 198 normal controls and 334 patients with ataxia and Parkinson's disease (PD) in Taiwanese. In addition, we also compared the frequencies of large normal alleles with the relative frequencies of SCA1, SCA2, MJD/SCA3, SCA6, and DRPLA among Taiwanese, Japanese, and Caucasians. Secondly, in order to uncover the molecular mechanisms underlying SCA8, we used *in vitro* cellular system to investigate the plausible pathogenesis, including the antisense effects between KLHL1 and SCA8, and the translatable open reading frame in SCA8. We also generated stable and inducible SCA8 cell lines carrying various CTA/CTG combined repeats to find out the repeats effects on stresses. In addition, to get insight the pathogenesis of SCA8 and for further potential therapy screening, we also generated transgenic mice harboring the human SCA8 cDNA carrying either normal or expanded CTA/CTG combined repeats under control of cerebellar Purkinje cell specific promoter, *Pcp2/L7* promoter.

Materials and methods

Subjects

Seventy patients with ataxia, including 39 patients from 28 families with autosomal dominant cerebellar ataxia and 31 patients with sporadic ataxia and 264 patients with idiopathic PD, were enrolled in this study. Clinical diagnoses of ataxia and PD were made according to the published criteria. These 334 patients were recruited from the neurology clinics of Chang Gung Memorial Hospital. In addition, 198 unrelated subjects without neurodegenerative disorders were recruited as normal controls. All examinations were performed after obtaining informed consent from patients and control individuals.

Genomic DNA extraction

Genomic DNA extraction from whole blood is carried out using DNA Extraction Kit (Cat. No.200600, Stratagene). Three volume of 1x Solution 1 was mixed well with the blood sample and incubated on ice for 5 minutes. After centrifugation at 2,000 rpm for 10 minutes, the supernatant was removed and the pellet was resuspended in 2 ml of Solution 2. Then 10 μ l of pronase is added to the suspension and incubated at 60°C for several hours, or at 37°C overnight for several days. The suspension was placed on ice for 10 minutes, followed by mixing with 0.8 ml of Solution 3 and stood on ice for 10 minutes. The protein precipitate was pelleted by centrifugation at 3,400 rpm for 15 minutes at 4°C, and the supernatant containing nucleic acid was treated with 6 μ l of RNase at 37°C for 15 minutes. DNA precipitate was separated out by mixing with 2.5 ml of isopropanol, transferred to a fresh tube, and centrifuged at 14,000 rpm for 1 minute. The pellet was rinsed once

with 70% ethanol and air-dried. DNA was dissolved in adequate volume of ddH₂O and the concentration was determined using the spectrophotometer.

Polymerase chain reaction (PCR) and genotyping

Molecular analyses of tri- or pentanucleotide repeat loci of SCA1, SCA2, SCA3, SCA6, SCA8, SCA10, SCA12, SCA17, and DRPLA were carried out by polymerase chain reaction (PCR) with the primers and under the conditions listed in **Table 2**. Briefly, 100 ng of genomic DNA, 0.4 μM of each primer of which the forward primer was fluorescence labeled, 100-200 μM dNTPs, 0.8-1.5 mM MgCl₂, 10 mM of Tris pH 8.3, 50 mM KCl, 0.5 U Taq polymerase, and 10% dimethylsulfoxide were prepared in a final volume of 25 μl. Amplified products were analyzed in a linear polyacrylamide gel on an automated MegaBACE Analyzer and allele sizes were determined by comparing migration relative to molecular weight standards. DNA sequencing was performed to accurately assess repeat size and the presence of interruptions.

Gel extraction

After separation on the agarose gel, DNA fragment was recovered using Gel-MTM Extraction System (Cat. No. EG1001, Viogene). First, the gel slice was completely dissolved in 0.5 ml GEX Buffer at 60°C for 5 to 10 minutes. Then the dissolved gel mixture was applied to the Gel-MTM column and centrifuged for 1 minute. The column was washed with 0.5 ml of WF Buffer followed with centrifugation for 1 minute, and washed with 0.7 ml of WS Buffer followed with centrifugation for 1 minute. The residual ethanol was removed by one more centrifugation for 1 minute. DNA was dissolved in 30 μl of ddH₂O for 5 minutes and eluted by centrifugation for 1 minute.

Statistical analyses

Possible differences between the normal and patient groups in normal repeat frequency distributions were assessed using a non-parametric Mann–Whitney *U*-test. Allele frequencies at each locus were estimated by the gene count method. Statistical analyses of differences in the frequency of large normal alleles (those corresponding to 5 to approximately 10% of the upper tails) for each locus were performed with the Fisher's exact test.

SCA8 cDNA cloning

Human cerebellar polyadenylated RNA (Clontech) was reverse transcribed into cDNA by using the SuperScript™ II reverse transcriptase (Invitrogen). Sense and antisense primers used for amplification of full length *SCA8* cDNA were (5'-ATCCTTCACCTGTTGCCT) and (5'-GCTTGTGAGGACTGAGAATG), respectively. The 1.3-kb full-length, (CTA)₁₁(CTG)₁₂ combined repeats (23R) containing cDNA (including exons D, C2, C1, B, and A) (*SCA8*-23R) (**Figure 2B**) (Nemes et al. 2000) was cloned into pGEM-T Easy vector (Promega) and sequenced. The *Nla*III-*Dra*I fragment containing (CTA)₁₁(CTG)₁₂ repeats was replaced with a 290bp fragment from the PCR clone of a patient with *SCA8* CTG₈₈ expansion [(CTA)₈CCACTACTGCTACTGCTA(CTG)₆₄CTA(CTG)₉] (*SCA8*-88R). The trinucleotide repeat number is further expanded to [(CTA)₈CCACTACTGCTACTGCTA(CTG)₆₇CTA(CTG)₆₅CTA(CTG)₉] combined 157 repeats by ligation of *Fnu*4HI partially digested fragments (*SCA8*-157R) (項, 2005). To construct the CTA/CTG deleted *SCA8*, a *Dra*I site was introduced to the 5' end of repeats by site-directed mutagenesis [primer 5'-CCCTGGGTCCTTCATGTTAGAAAACCTGG-

CTTTAAA(CTA)₈C] as described below and the *Dra*I fragment containing CTA/CTG combined repeats was removed (SCA8-0R).

Site-directed mutagenesis

Site-directed mutagenesis was carried out using QuikChange™ XL Site-Directed Mutagenesis Kits (Cat. No.200517, Stratagene). The reaction was set up in 25 µl of volume including 2.5 µl of 10 × reaction buffer, 10 ng of template DNA, 62.5 ng of both sense and antisense primers, 50 µM dNTPs, 1.5 µl of QuickSolution and 0.5 µl of *PfuTurbo* DNA polymerase. The reaction was temperature cycled with the condition: 1 cycle of denaturation at 95°C for 1 minute, 18 cycles of reaction comprising denaturation at 95°C for 50 seconds, annealing at 60°C for 50 seconds, and elongation at 68°C for 12 minutes, followed by elongation at 68°C for 7 minutes. Following cycling, the reaction was cooled and 0.5 µl of *Dpn*I (10 U/µl) was added to digest the parental DNA template at 37°C for 1 hour. Then 5 µl of the reaction was taken to transform the competent cells and the site-directed mutant DNA was extracted from the cultured clones and sequenced.

pEF-SCA8 constructs

To generate SCA8 expression constructs driven by the human polypeptide chain elongation factor 1α promoter (the EF promoter), SCA8 cDNA bearing 0 to 157 CTA/CTG combined repeats was placed in the *Not*I restricted site of pEF-IRES/hrGFP vector (Chung et al. 2002) in which the *Kpn*I fragment containing 3' region of the IRES sequence and the humanized *Renilla* green fluorescent protein (hrGFP) gene were removed to result in pEF-SCA8-0R, 23R, 88R, and 157R constructs (**Figure 3A**). These constructs were sequenced and verified by restriction mapping.

KLHL1 cDNA cloning and pEF-KLHL1-EGFP construct

The 3.2 kb *KLHL1* cDNA was amplified also from human cerebellar polyadenylated RNA using sense (5'-CATGTCAGGCTCTGGGCGAA-AAG) and antisense (5'-TGGGCGATGAGAATATGAAGTCTG) primers. After cloning into pGEM-T Easy and sequencing, the 2.2 kb *KLHL1* coding sequences and the EGFP gene from pEGFP-N1 were fused in-frame and inserted into the *NotI* site of the modified pEF-IRES/hrGFP vector in which hrGFP had been removed by *KpnI* restriction to generate pEF-KLHL1-EGFP (**Figure 3B**). The construct was verified by DNA sequencing and restriction mapping.

pCMV-(CAG)₃₆-IRES-EGFP construct

The 1.1 kb *TATA binding protein (TBP)* cDNA containing 36 CAA/CAG repeats [(CAG)₃(CAA)₃(CAG)₉CAACAGCAA(CAG)₁₆CAACAG] was amplified using sense (5'-CTGGTTTGCCAAGAAGAAAGTG) and antisense (5'-AGGCAAGGGTACATGAGAGCCA) primers (by 王政光). After cloning and sequencing, the 5' 254-bp cDNA fragment was placed between the *EcoRI* and *PstI* sites of the pIRES2-EGFP vector (Clontech) (洪, 2005). The resulting pCMV-(CAG)₃₆-IRES-EGFP contains the 5' region of *TBP* cDNA upstream to the IRES and EGFP gene (**Figure 3C**). The construct was verified by DNA sequencing.

pCMV-ORF1-EGFP construct

The ORF1 translation termination sequence of *SCA8* cDNA (in pGEM-T Easy vector) was removed and a *SmaI* restricted site (underlined) added by PCR using primer 5'-GCGCCCGGGACACTTCAACTTCCTATACATACA.

The *EcoRI* (in MCS of pGEM-T Easy vector)-*SmaI* fragment containing *SCA8* ORF1 was in-frame fused to the *EGFP* gene in the pEGFP-N1 vector (Clontech) (between the *EcoRI* and *BstUI* sites). The Kozak sequence of enhanced green fluorescence protein (EGFP) gene was removed by site-directed mutagenesis (primer 5'-CGGGCCCGGGATCCACCGGTCGCC Δ -GTGAGCAAGGGCGAGGAGCTG, Δ = ACCATG) (by 蕭欣杰). The resulting pCMV-ORF1-EGFP construct (**Figure 4A**) was verified by DNA sequencing and restriction mapping.

pCMV-SCA8-EGFP constructs

The translation termination sequence of *SCA8* ORF3 (with 0R, 23R, 88R and 157R) was removed by *AflIII* restriction. A linker sequence (5'-CGACTCGCG) was added between the filled-in *AflIII* site and the *BstUI* site of pEGFP-N1 vector to fuse *SCA8* ORF3 and Kozak-deleted EGFP gene in-frame. The resulting pCMV-SCA8-EGFP constructs (**Figure 4B**) were verified by DNA sequencing and restriction mapping.

pCMV-K-ORF3-EGFP constructs

To generate pCMV-K-ORF3-EGFP, *SCA8* cDNA sequences 1~1032 in pCMV-SCA8-23R-EGFP and pCMV-SCA8-157R-EGFP were removed and the bases in front of AUG start codon were modified to match the Kozak consensus sequence (CACC) (by Dr. 蘇銘燦). The resulting pCMV-K-ORF3-23R-EGFP and pCMV-K-ORF3-157R-EGFP constructs (**Figure 4C**) were verified by DNA sequencing and restriction mapping.

Preparation of electro-competent cells

The day before preparation, bacteria (TOP 10F', Cat. No.50-0059, Invitrogen) were cultured overnight in 100 ml of LB broth containing tetracycline. On the day, bacterial culture was aliquot into four 1-liter flasks, each containing 225 ml of LB broth, and inoculated with shaking at 37°C until the OD₆₀₀ reached 0.7 ~ 0.8. Cells were chilled on ice for 10 minutes and pelleted by centrifugation at 4,000 rpm at 4°C for 5 minutes. The supernatant was removed and cells were resuspended and pooled in 250 ml of cold ddH₂O for pellet from 500 ml culture. Cells were centrifuged at 4,500 rpm at 4°C for 5 minutes and washed with 250 ml of cold ddH₂O twice. The supernatant was poured off and cells were resuspended in 1 ml of ddH₂O containing 20% glycerol. Finally, cells were aliquot into eppendorf tubes in 40 µl amounts and stored at -80°C.

Ligation

The adequate amount of insert DNA fragment was mixed with vector, 0.5 µl of 10 × Ligation Buffer, 0.5 µl of PEG 4000 Solution, and 1.25 U of T4 DNA ligase (Cat. No.EL0331, Fermentas) in a volume of 5 µl. The ligation reaction was incubated at room temperature for 1 hour or 16°C overnight.

Electroporation

The ligation reaction was inactivated at 65°C for 10 minutes and kept on ice after spinning down. Immediately prior electroporation, 1 µl ligation sample was mixed with 20 µl aliquot of electro-competent cells and then added to the 1 mm-gap cuvette (Cat. No.4307-000-569, Eppendorf). The electroporation was carried out using MicroPulser Electroporator (BIO-RAD) with 1.25 Kvolts under the manual program. Chilled LB broth (500 µl) which contains no antibiotics was added immediately to the cuvette. The

content of curvette was then transferred to the tube, incubated at 37°C for at least 30 minutes, and plated on LB medium with appropriate antibiotic for incubation at 37°C for 16-18 hours.

Minipreparation of plasmid DNA

A single bacterial colony was transferred into 1ml of LB broth containing the appropriate antibiotic. After overnight incubation at 37°C with vigorous shaking, the bacteria were harvested by 14,000 rpm centrifugation for 1 minute. The bacterial pellet was resuspended in 70 µl of Solution I (50 mM glucose – 25 mM Tris-HCl pH 8.0 – 10 mM EDTA pH8.0) by vigorous vortexing. Then 140 µl fresh Solution II (0.2 N NaOH – 1% SDS) was added into the bacterial suspension and the contents was mixed by inverting several times followed mixing with 105 µl Solution III (3 M potassium acetate). The cell debris and genomic DNA were precipitated at 14,000 rpm for 5 minutes, and the supernatant containing plasmid DNA was transferred to a fresh tube. The plasmid DNA pellet was precipitated after mixing with 0.8 volume of isopropanol and centrifuged at 14,000 rpm for 5 minutes. The DNA pellet was washed in 70% ethanol and dried in the air. The plasmid DNA was dissolved in 40 µl ddH₂O containing 10 µg/ml RNase and checked by 0.8% agarose gel electrophoresis.

Midipreparation of plasmid DNA

Large-scale isolation of plasmid DNA was performed with Midi-V100™ Ultrapure Plasmid Extraction System (Viogene). A single bacterial colony was incubated in 65 ml of LB broth containing the appropriate antibiotic at 37°C for 20 hours and then the bacteria cells were harvested by

centrifugation at 8000 g for 5 minutes. The cell pellet was resuspended in 4 ml of VP1 Buffer containing RNase. The cell suspension was mixed with 4 ml of VP2 Buffer and with 4 ml of VP3 Buffer, sequentially. The cell debris was centrifuged at 12,000 g for 15 minutes and the supernatant was applied to a Midi-V100™ column, which was pre-equilibrated with 10 ml of VP4 Buffer. The column was washed with 15 ml of VP5 Buffer and the plasmid DNA was eluted with 5 ml of VP6 Buffer. Then DNA was precipitated by mixing with 3.75 ml of isopropanol, allotted to 1.5 ml tube, and centrifuged at 14,000 rpm for 10 minutes. After removing the supernatant, DNA pellet was dissolved in 63 µl of ddH₂O for each tube and combined to a tube. To eliminate residual salt, DNA was precipitated by mixing with 20 µl of 5 M NaCl and 1000 µl of pure ethanol, followed by centrifugation at 14,000 rpm for 5 minutes. The supernatant was removed and DNA was allowed to dry in the air. Finally, DNA was dissolved in 400 µl of ddH₂O and the concentration was determined using the spectrophotometer.

Cell cultivation

Human embryonic kidney (HEK) 293 (ATCC No. CRL-1573) and IMR-32 (ATCC No. CCL-127) cell lines were maintained in DMEM supplement with 10% fetal calf serum (FCS), 1.0 mM sodium pyruvate, 1.5 g/L sodium bicarbonate, 100 U/ml penicillin, and 100 U/ml streptomycin, at 37°C in an atmosphere containing 5% CO₂.

Transfection

The rapid transfection process was carried out without plating cells the day before transfection. For transfection performed in the 12-well plate, 2 µg of

DNA and 2 ~ 4 μ l of LipofectamineTM 2000 reagent (LF2000) (Cat. No.11668-019, Invitrogen) were first diluted into 100 μ l Opti-MEM[®] I Reduced Serum Medium (Cat. No.31985-062, Invitrogen), respectively, and incubated for 5 minutes at room temperature. Then DNA and LF2000 were combined in the well and incubated for 20 minutes at room temperature. At the meanwhile of DNA-LF2000 complexes formation, the cell suspension of appropriate number per well was prepared in 10% FCS-DMEM without antibiotics. The cell suspension was added to the DNA-LF2000, mixed gently by rocking back and forth, and incubated at 37°C for at least 24 hours for further expression studies.

Fluorescence activated cell sorting (FACS) analysis

HEK293 cells cultivated in DMEM containing 10% FCS were transfected with the various cDNA constructs using a lipofection procedure. pEGFP-N1 was used as a negative control to show the specificity of SCA8 *trans* RNA interference. Forty-eight hours later, cells were harvested for fluorescence activated cell sorting (FACS) analysis. The amounts of GFP expressed were analyzed in a FACSCalibur flow cytometer (Becton-Dickinson), equipped with an argon laser operating at 530 nm. A forward scatter gate was established to exclude dead cells and cell debris from the analysis. 10⁴ cells were analyzed in each sample.

Immunofluorescence analysis

The transfection process was performed as described above. Before transfection, circular coverslips of which the diameter was 15 mm were sterilized and coated with poly-L-lysine as noted below. Coverslips were first washed in 70% ethanol for 30 minutes twice, incubated in 0.1 N HCl

overnight, sterilized by autoclaving and stored in 95% ethanol. Coverslips were then placed in each well of 12-well culture plate and coated with poly-L-lysine (100 µg/ml, Sigma) for 1 hour at room temperature. After removing poly-L-lysine, coverslips were briefly washed with sterile ddH₂O twice, allowed to dry completely, and ready for use after sterilizing under UV light for at least 1 hour. After transfection, cells were allowed to grow on coverslips for at least 1 day depending on the confluence and/or the gene expression level. For immunofluorescence analysis, cells were rinsed briefly in PBS and fixed in 4% paraformaldehyde in PBS for 15 minute at room temperature. After washing twice with PBS, cells were permeabilized with 0.25% Triton X-100 in PBS for 10 minutes, followed by washing in PBS three times. The intracellular nonspecific binding of the antibodies was blocked with PBS containing 1% BSA for at least 1 hour. Cells were then incubated with the primary antibodies for 1 hour at room temperature or overnight at 4°C, washed in PBS three times, and a second incubation with fluorescence-conjugated antibodies for another 1 hour at room temperature, followed by washing in PBS three times. The nuclei were stained using 0.05% DAPI (4'-6-diamidino-2-phenylindole) and the coverslip was mounted on glass slides in Vectashield (Cat. No.H-1400, Vector). The stained cells were observed with Leica TCS confocal laser scanning microscope.

Cell lysate preparation

Cells were harvested by centrifugation at 1,000 g for 5 minutes followed with cold PBS washing twice. The cell pellet was resuspended in 200 µl RIPA buffer (10 mM Tris pH7.5 – 150 mM NaCl – 5 mM EDTA pH8.0 – 0.1% SDS – 1% DOS – 1% NP-40) containing the protease inhibitor mixture,

sonicated 15 pulses three times, and sat on ice for 30 minutes. Protein extracts were centrifuged at maximum speed at 4°C for 30 min and the supernatant was transferred to a fresh tube. The protein concentration was determined using the Bio-Rad Protein Assay (Cat. No.500-0006, Bio-Rad).

Cytoplasmic and nuclear proteins preparation

Separation and preparation of cytoplasmic and nuclear extracts was performed using NE-PER Nuclear and Cytoplasmic Extraction Reagents (Cat. No.78833, Pierce). Transfected cells ($1 \sim 2 \times 10^6$) were harvested, resuspended in 100 μ l of ice-cold CER I containing protease inhibitor, and incubated on ice for 10 minutes. Then 5.5 μ l of ice-cold CER II was added to the cell suspension, mixing by vortexing for 5 seconds, and incubated on ice for 1 minute. After vortexing for another 5 seconds, cell extract was centrifuged at 4° C for 5 minutes at maximum speed, and the supernatant, which embraces the cytoplasmic fraction, was transferred to a fresh, pre-chilled tube and stored at -80°C. The pellet was resuspended in 50 μ l of ice-cold NER, vortexing for 15 seconds, and incubated on ice with vortexing for 15 seconds every 10 minutes, for a total of 40 minutes. The insoluble fraction was precipitated by centrifugation at 4°C for 10 minutes at maximum speed and the supernatant was used for nuclear fraction. The protein concentration was determined using the Bio-Rad Protein Assay. For subcellular location determination, the protein extracts were reacted with antibodies against poly ADP-ribose polymerase (PARP) (sc-7150, Santa Cruz Biotechnology), the nuclear marker, and α -tubulin (sc-5286, Santa Cruz Biotechnology), the cytoplasmic marker, respectively.

Western blotting (immunoblotting)

Equal amount of cell lysates were denatured in 1 × sample buffer (50 mM Tris pH 6.8 – 2% SDS – 10% Glycerol – 2.5% β-mercaptoethanol – 0.005% bromophenolblue) at 95°C for 10 minutes and separated by SDS-PAGE according to the molecular weight and electrophoretic transferred to nitrocellulose membrane (Schleicher and Schuell) using XCell II™ Blot Module (Cat. No. EI9051, Invitrogen) in transfer buffer (25 mM Tris – 0.2 M glycine – 20% methanol) at 45 V for 1 hour. The membrane was blocked in PBS containing 10% non-fat milk for at least 1 hour at room temperature or overnight at 4°C. The membrane was rinsed with washing buffer (10 mM Tris, pH 8.0 – 0.05% tween-20) and incubated with primary antibodies at room temperature for at least 1 hour. The membrane was washed three times with washing buffer for 5 minutes. Then the membrane was incubated with appropriate secondary antibodies conjugated horse radish peroxidase for 1 hour and washed three times with washing buffer. The immune complexes were detected with SuperSignal® West Femto Maximum Sensitivity Substrate (Cat. No.34096, Pierce).

RNA isolation

Total RNA was extracted using Trizol reagent (Cat. No. 15596-018, Invitrogen) according to the manufacturer's specifications. After PBS washing, 1ml of Trizol reagent was added to the culture dishes and cells were scraped from the culture dish. The cell suspension was incubated on ice for 5 minutes, mixed well with 1/5 volume of chloroform and incubated on ice for another 5 minutes. RNA was separated from DNA and proteins by centrifugation at 4°C for 15 minutes. The colorless, upper aqueous phase was carefully removed to a fresh tube avoiding the material that collected at the interface, and mixed with 0.8 volume of isopropanol. The mixture was

sat at -20°C for at least 1 hour and centrifuged at 4°C for 15 minutes to precipitate RNA. The supernatant was discarded and RNA pellet was rinsed with 70% DEPC-H₂O. RNA was air dried and dissolved in adequate volume of DEPC-H₂O. The quality and quantity of RNA samples were determined by the agarose electrophoresis and the absorbance at 260 nm, respectively.

Establishment of SCA8 stably expressing Flp-In T-REx 293 cell lines

The generation of SCA8 stably expressing Flp-In T-REx 293 cell lines is based on the Flp-In™ T-REx™ system (Invitrogen). For constructing stably SCA8 expressing vectors, fSCA8-0, 23, 88, and 157R were restricted by *NotI* and inserted to *NotI* site of pcDNA5/FRT expressing vector. Then each of these expressing vectors and pOG44 were co-transfected into the Flp-In T-REx 293 cell with the molar ratio of 1:9. One day after transfection, the medium was replaced with fresh one. Next day, cells were split into fresh medium with the density not more than 25% confluent. Once cells attached to the dish, the culture medium was replaced with the selective medium containing 100 µg/ml of Hygromycin and 15 µg/ml of Blasticidin. After 1 month of Hygromycin selection with replacement of fresh selective medium every 4 days, genomic DNA was isolated from each cell line and verified by PCR with sense (5'-GCTTGTGAGGACTGAGAATG) and antisense (5'-CCCTGGGTCCTTCATGTTAG) primer pair. To induce expression of SCA8 integrating into the FRT site, cells were treated with 1 µg/ml doxycycline (dox) for varying periods of time.

Cell proliferation assessment (WST-1 assay)

The extent of cell proliferation was determined with PreMix WST-1 Cell Proliferation Assay System (Takara). After doxycycline induction and drugs

treating, the cells are added PreMix WST-1 in a final 1:10 dilution and incubated for 4 hours. The cell viability is determined by measuring the formazan dye formation, cleaved by the succinate-tetrazolium reductase which is active in the viable cells, at 450 nm using microplate reader.

Transgene construction and SCA8 transgenic mouse generation

Full length SCA8 cDNAs carrying 23 and 157 combined repeats were subcloned into the *NotI* site of pCEV expression vector in which SCA8 expression is under the control of the cerebellar Purkinje cells specific *pcp2/L7* promoter. The transgene constructs were purified as described above and verified. The transgene fragments containing *pcp2/L7* promoter, SCA8 cDNA, and SV40 polyadenylation signal were excised with *SphI/BamHI* digestion and injected into FVB mouse pronuclei to generate transgenic mice (the service of transgenic core facility, Institute of Molecular Biology, Academia Sinica).

Transgenic mouse genotyping

The genomic DNAs from transgenic founders and offspring were isolated from tail biopsies and PCR genotyped using transgene-specific primers TG-F (5'-TATGGTGAGAGCAGAGATGG) and TG-R (5'-CATGTCAGGCTC-TGGGCGAAAAG). Briefly, 0.5-1.0 cm of tail biopsies were minced in 200 μ l of tail solution (50 mM EDTA – 1% SDS – 50 mM Tris-HCl pH 8.0 – 100 mM NaCl – 0.35 mg/ml protease K) and incubated at 65°C for 4 hours or at 37°C overnight. The mixture then was mixed with 80 μ l of 5 M potassium acetate and sat at 4°C for 1 hour followed by centrifugation at 14,000 rpm at 4°C for 30 minutes. The supernatant was transferred to the fresh tube and mixed well with 500 μ l of pure ethanol. DNA was pelleted by

centrifugation at 14,000 rpm for 5 minutes and then washed with 70% ethanol. DNA pellet was air-dried, dissolved in 50 µl of ddH₂O. 0.5 µl of DNA was used as the template for PCR, and the amplified fragment spans from the pcp2/L7 promoter to the exon D of the human *SCA8*. The GAPDH fragment was PCR amplified with primers GAPDH-F (5'-CCCTTCATTGACCTCAACTA) and GAPDH-R (5'-CCAAAGTTGTCATGGATGAC), as the internal control.

Characterization of transgene copy numbers of transgenic mouse lines

The transgene copy numbers were determined using PCR. Briefly, copy standards were prepared by mixing non-transgenic tail DNA with a known amount of 1, 10, 50, and 100 copies of transgene DNA. The intensity of PCR amplified fragment with TG-F and TG-R primers was compared to copy standards to estimate the copy numbers.

RNA isolation from mouse brain tissues and reverse transcription-polymerase chain reaction (RT-PCR)

The brain tissues were dissected and 1 ml of Trizol reagent (Invitrogen) was added to isolate total RNA from half of the cerebellum. The procedure of isolation of RNA was as described above. After RNase-free DNase (Stratagene) treatment, 1 µg of RNA was reverse transcribed into cDNA using the SuperScriptTM III reverse transcriptase (Invitrogen). The RT-F (5'-CTTTTCGCCCAGAGCCTGACATG) and RT-R (5'-CTAACATGAAGGACCCAGGG) primers were used to amplify cDNA fragments to assess the expression of transgene transcripts.

Rotarod test

The rotarod is used to measure the ability of equilibrium and motor improvement with training. Mice are placed on the 38 cm-diameter rotarod (IITC Life Science) for three trials per day for four consecutive days with the rotarod undergoing a linear acceleration from 2 to 20 rpm over the first 5 min and maintaining at a maximum speed for another 5 min. The mice were allowed to rest for at least 60 min between trials to avoid fatigue and exhausting. Mice were scored for their latency to fall for each trial and averages of the three trials of the last day.

Immunohistochemical analysis

Avertin-anesthetized mice were perfused with 0.9% saline followed with 4% paraformaldehyde fixation. The brain tissue was dissected and incubated with 4% paraformaldehyde overnight. Then the tissue was transferred in order from 10% sucrose solution for 1 hour, 20% sucrose solution for 2 hour, to 30% sucrose solution for 2 days. The brain was cryosectioned and sections were rinsed in 0.1 M phosphate saline buffer three times (10 min/wash). Endogenous peroxidase activity was blocked by incubation with 3% H₂O₂ for 30 min. Sections were then washed in phosphate saline buffer three times (10 min/wash). Nonspecific epitopes were then blocked by incubation in 5% normal goat serum and 0.1% Triton X-100 in phosphate saline buffer for 2 h. Sections were incubated in primary antibodies overnight at room temperature and then washed three times in phosphate saline buffer for 10 min/wash. Secondary antibodies were applied to the sections by a linking reagent (DAKO) for 1h. Immunostainings were highlighted using substrate-chromogen solution and DAB oxidation. All sections were mounted on coated slides and cover-slipped for light microscopy.

RNA cleanup

Isolated RNA was cleaned up using RNeasy Mini Kit (Cat. No.74104, Qiagen). As described in the manufacture, the volume of RNA sample was first adjusted to 100 μ l with DEPC-H₂O, mixed with 350 μ l Buffer RLT containing 1% β -mercaptoethanol, followed with 250 μ l of ethanol. The mixture was then applied to the RNeasy mini column and centrifuged for 15 seconds at $\geq 8,000g$. The column was transferred into a new collection tube, added 500 μ l Buffer RPE, and centrifuged for 15 seconds at $\geq 8,000g$. Another 500 μ l Buffer RPE was added to the column and centrifuged for 2 minutes at $\geq 8,000g$. And another centrifugation for 1 minute was carried out to eliminate residual ethanol. Finally, 20 μ l of DEPC-H₂O was added the column which has been transferred to a new tube, stayed at room temperature for 3 minutes, and centrifuged at $\geq 8,000 g$ for 1 minute. To obtain a more yield, another 15 μ l of DEPC-H₂O can be added to perform the second elution. The quality and quantity of cleaned-up RNA samples were determined by the agarose electrophoresis and the absorbance at 260 nm, respectively.

Microarray analysis

We are indebted to the conduction of microarray assay of Genomic Medicine Research Core Laboratory in Chang Gung Memorial Hospital. The cleaned-up RNA was first reverse transcribed to the first-strand cDNA followed by the second-strand cDNA synthesis. Then the double-stranded cDNA was purified and serves as a template in the subsequent *in vitro* transcription reaction coupled with biotin labeling. The biotinylated cRNA targets were then purified, fragmented, and hybridized to MOE430A

(Affymetrix). The array was incubated for 16 hours at 45°C, then automatically washed and stained. The array image was scanned and the acquired signal intensities were normalized. One-way ANOVA and fold-change analysis were performed to determine which genes were differentially expressed between transgenic and control littermates. The cut-off values of up-regulated and down-regulated transcripts were set as 1.5 and 0.7 fold changes, respectively.

Real-time RT-PCR (Quantitative RT-PCR)

6.25 µg of total RNA, isolated from either SCA8 transgenic or wild-type littermates as mentioned above, was treated with RNase-free DNase (Stratagene) in 25 µl of reaction volume and then 1 µg of DNase-treated RNA was used as a template to synthesize the first-strand cDNA using High Capacity cDNA Reverse Transcription Kit (Cat. No.4368814, Applied Biosystems) with random primers. Specific primers for each studied gene and for mouse endogenous control, Gapdh, were listed in **Table 7** and obtained from Applied Biosystems. Real-time quantitative PCR experiments were performed in the ABI PRISM® 7000 Sequence Detection System (Applied Biosystems). Amplification was performed on a cDNA amount equivalent to 50 ng total RNA with 1x TaqMan® universal PCR Master mix (Cat. No.4304437, Applied Biosystems) and 1x specific Applied Biosystems Assay-on-Demand (AOD). The PCR condition was: initiation step at 50°C for 2 minutes, denaturation at 95°C for 10 minutes, then 40 cycles of denaturing at 95°C for 15 seconds and combined annealing and extension at 60°C for 1 minute. Experimental samples and no-template controls were all run in duplicate. Results from duplicate reactions were averaged and used as the value for each biological replicate.

Protein samples preparation for proteomic analysis

Half of dissected cerebella from transgenic mice and wild type littermates were homogenized in 200 μ l of Lysis solution (8 M urea – 4% CHAPS) and sat on ice for 20 minutes. Protein extracts were centrifuged at maximum speed at 4°C for 30 min and the supernatant was transferred to a fresh tube. To separate proteins in the crude extracts from contaminating substances, the protein extracts were applied to the 2-D Clean-Up Kit (Cat. No.80-6484-51, Amersham Biosciences). According to the instruction, the supernatant was mixed well with 3 volumes of precipitant and incubated on ice for 15 minutes. Then the mixture of protein and precipitant was mixed with co-precipitant followed by the centrifugation at 4°C for 10 minutes. The supernatant was removed as much as possible and 40 μ l co-precipitant was layered on the pellet. After sitting on ice for 5 minutes, the mixture was centrifuged for 5 minutes and the supernatant was discarded. The pellet was piled with 25 μ l of ddH₂O and dispersed by vortexing. Then 1 ml of chilled wash buffer and 5 μ l of wash additive was added to the protein pellet. The mixture was incubated at -20°C for at least 30 minutes to 1 week with occasional vortex for 20-30 seconds. Protein was pelleted by centrifugation at at maximum speed for 5 minutes. The supernatant was discarded and the pellet was allowed to air dry for no more than 5 minutes. Finally, the protein pellet was resuspended in 200 μ l of Lysis solution with sonication. The quantity of cleaned-up protein sample was determined using 2-D Quant Kit (Cat. No.80-6483-56, Amersham Biosciences)

Minimal labeling with CyDye Fluors for 2-D difference gel electrophoresis

(DIGE)

For 2-D DIGE, protein samples were labeled with CyTM2, Cy3 and Cy5 fluors (Cat. No.25-8010-65, Amersham Biosciences) after protein quantization. 50 µg of protein samples were mixed with 400 pmol CyDye and incubated on ice for 30 minutes in the dark. Then the labeling reaction was quenched by adding 1µl of 10 mM lysine and leaving on ice for 10 minutes in the dark.

IPG strip rehydration and first-dimension isoelectric focusing (IEF)

For the first dimension, the protein sample was mixed with rehydration buffer(8 M Urea – 2% CHAPS – 40 mM DTT – 0.5% IPG buffer –0.002% bromophenol blue) to make up for the volume 250 µl (for 13-cm strips). Then the sample mixture was loaded in the strip holders evenly and a pH 3-10, 13-cm ImmobilineTM DryStrip (Amersham Biosciences) was faced down to absorb the protein. Strips were rehydrated at 20°C for 12 hours on IPGphor II (Amersham Biosciences). Then protein samples were separated according to each isoelectric point (pI) with the running program: Step 500 V for 4 hours, Grad 1000 V for 1 hour, Grad 8000V for 3 hours, and Step 8000V for 38000 Vhours.

Second-dimension SDS-PAGE

After IEF steps, strips were equilibrated in SDS Equilibration buffer (2% SDS – 50 mM Tris-HCl pH 8.8 – 6 M Urea – 30% Glycerol –0.002% bromophenol blue) containing 1% (wt/vol) dithiothreitol (DTT) for 15 minutes with shaking followed by the second equilibration in SDS Equilibration buffer containing 2.5% (wt/vol) iodoacetamide for 15 minutes

with shaking. The strip then was transferred to the top of an 18 × 16 cm, 1.5 cm thick, 12.5% polyacrylamide gel and sealed with melting agarose (0.5% dissolved in 1x SDS running buffer). Gels were run at 30 mA for the first 15 minutes followed by 60 mA for 4.5~5 hours until the bromophenol blue dye reached the bottom.

Gel staining with SYPRO Ruby

Gels were rinsed with ddH₂O and then fixed in 40% methanol and 10% acetic acid overnight. Then they were washed with ddH₂O for 10 minutes 3 times, followed by staining with SYPRO Ruby protein gel stain (Cat. No.S12000, Molecular Probe) overnight. Before visualizing the gel image, the gel was washed with 10% methanol and 7% acetic acid for 30 minutes and rinsed with ddH₂O for 5 minutes twice. The gels were imaged on the Molecular Dynamics Typhoon 9210 (Amersham Biosciences) using optimal excitation/emission wavelength.

Image analysis

ImageMaster™ 2D Platinum Software (Amersham Biosciences) was used for analyzing the DIGE images. Briefly, the DIGE images underwent spot detection and quantitation with an average of 2200 spots per gel detected. Next, the matched images were analyzed and based on the Student's *t*-test feature, only those statistically significant spots ($p < 0.05$) were accepted. The volume ratio of matched spots with greater than 1.3 was considered significantly differentially expressed.

In-gel digestion

Differentially expressed protein spots were picked with Ettan™ Spot Picker (GE Healthcare) from the SYPRO Ruby stained gel which had been matched to DIGE gels. The picked gel spots were rinsed with 100 µl of ddH₂O, and then washed with 100 µl of 50 mM ammonium bicarbonate (NH₄HCO₃)/acetonitrile (ACN) (1:1, v/v) for 15 minutes. Next, the solvent was removed and the gel particle was covered with 50 µl of ACN with vortexing for 1 minute. ACN was then removed, and replaced with 50 µl of 50 mM NH₄HCO₃ for 5 minutes. ACN was added and the mixture was incubated for 15 minutes. The solvent was removed and replaced with 50 µl of ACN with vortexing for 1 minute, and then ACN was removed. The gel piece was vacuum dried for 30 minutes. The gel piece was incubated with 8 µl of freshly diluted trypsin (2.5 ng/µl in NH₄HCO₃) at 37°C overnight. Next day, the gel piece covered with at least 3 µl of solvent was sonified for 10 minutes and the supernatant was recovered. The gel was then covered with 3 µl of 50% ACN with 1% trifluoroacetic acid and sonified for another 10 minutes. The supernatant was recovered and pooled together.

Mass Spectrometry

Trypsinized protein fragments were identified using the MALDI-TOF MS (conduction of Genomic Medicine Research Core Laboratory in Chang Gung Memorial Hospital). The MALDI spectra used for protein identification from trypsinized fragments were searched against the National Center for Biotechnology Information (NCBI) protein databases using the MASCOT search engine (www.matrixscience.com).

Results

Trinucleotide or pentanucleotide repeat distributions

Figure 1 shows the frequency distributions of (CAG/CTG/ATTCT) repeat lengths at the nine loci in neurodegenerative patients and controls. Expansions of SCA types 1, 3, and 6 were detected in clinically defined patients with dominant SCA. Excluding known SCAs, the frequency distributions of normal alleles in patient group were not significantly different from those in the control group at the nine loci studied ($P > 0.05$) (**Table 3**), and the CAG repeats at SCA types 1, 2, 3, 6, and DRPLA are generally polymorphic within the region smaller than 40 repeats in each group. In the case of *SCA8* locus, the frequency distribution subclasses into three groups. The small group closely distributed around an allele with 18 CTGs; the second class comprised CTG repeat sizes of 22 to 39 units, and the third one of extremely large normal alleles were found in one *SCA3* patient (65 units) and four PD patients (75-92 units). At the *SCA10* locus, almost all alleles with the pentanucleotid ATTCT repeats range form 10 to 20 repeats and 14 repeat is the most frequent in each group. The frequencies of most *SCA12* alleles distribute smaller than 20 repeats, with one group distributing around 10 repeats and the other ranging from 13 to 18 repeats. At the *SCA17* locus, alleles vary from 30 to 43 in the control group and from 28 to 46 in the patient group, while alleles with 36 are predominant (>50%) in each group.

Frequency of SCAs and genetic and clinical features of patients

Analysis of loci involved in the SCAs showed that 26 unrelated patients (67%) had ataxia due to CAG expansion. SCA3 was the most common types of dominant SCA in Taiwan, accounting for 18 cases (46%), followed by SCA6 (7 cases, 18%) and SCA1 (1 case, 3%). The genes responsible for remaining 13 cases (33%) of dominant SCA remain to be determined. For SCA3, the mean age at onset was 36 years (SD, 12.74) and mean expanded allele sizes was 71 repeats (SD, 4.99) in 18 patients from 10 families. For SCA6, the mean age at onset and mean expanded allele sizes in 7 patients from 5 families were 48 years (SD, 10.02) and 23 repeats (SD, 0.79), respectively. For the SCA1 patient, the age at onset was 39 years and the expanded allele was 49 repeats.

Frequency of large normal alleles

When alleles corresponding to 5~10% of the upper tails (large normal alleles) at the nine loci were compared, no significant difference was found between the patient group and the control group. Nevertheless, we observed close associations between prevalences and frequencies of large normal alleles of SCA types 1, 2, 3, 6, and DRPLA in Taiwanese, Japanese and Caucasian families (**Table 4**).

SCA8 alleles with 75 to 92 repeats in PD patients

Although no expansion of SCA type 8 was detected in patients with dominant SCA, abnormal expansions were detected in four patients with PD (1.5%) (**Table 5**). The four patients met the criteria for PD, which included the presence of two of the four cardinal signs (resting tremor, cogwheel rigidity, bradykinesia or postural instability), improvement of symptoms with L-dopa therapy, and no evidence of secondary parkinsonism caused by

other neurologic disease or known drugs or toxins, or of atypical parkinsonism. DNA sequencing analysis revealed that these potentially pathogenic alleles had 75, 82, 88, and 92 combined repeats with a pure uninterrupted CTG repeat tract or interruptions (**Table 5**).

SCA17 allele with 46 repeats in PD patient

Abnormal CAG expansion in the SCA17 *TBP* gene was detected in one patient with PD (**Table 5**). The patient met the criteria for PD as described above. DNA sequencing analysis revealed that allele in the patient had CAG/CAA combined 46 repeats (**Table 5**).

Regulation of KLHL1 and CAG repeat-containing RNA expression by SCA8

The natural overlapping organization of the *SCA8* and *KLHL1* coding regions (Benzow and Koob 2002), and the similar distributions has been suggested that *SCA8* may function as a natural antisense regulator of *KLHL1* (Nemes et al. 2000). To test this hypothesis, we constructed the human *SCA8* cDNA with 0, 23, 88, or 157 combined repeats driven by the EF promoter (pEF-*SCA8*) as well as *KLHL1* cDNA tagged with EGFP (pEF-*KLHL1*-EGFP) (**Figure 3A, 3B**). Since human embryonic kidney-derived HEK293 cells express many neuron-specific mRNAs (Shaw et al. 2002), and were frequently used to study other repeat expansion diseases (Handa et al. 2005), they were used in this study as a *in vitro* cell model. After co-transfecting of pEF-*SCA8* and pEF-*KLHL1* into HEK293 cells for two days, FACS was performed to evaluate the expression of the *KLHL1* fusion gene. The *KLHL1*-EGFP fusion protein production from cells co-transfected with *SCA8* carrying 0 ~ 157 combined repeats was significantly reduced (29%, 35%, 38% and 55% of the levels of *KLHL1* fusion gene, $P < 0.05$) (**Figure**

5B). The difference between co-transfecting *SCA8* carrying 0 and 157 repeats constructs were significant (29% vs. 55%, $P = 0.03$). The results suggest that *SCA8* may function as a negative regulator of *KLHL1* in an inversely CUG repeats-dependent manner.

The expanded CUG repeats within *DMPK* transcripts were able to interact with CAG repeats located within the *TBP* or androgen receptor mRNA (Hamshire and Brook 1996; Sasagawa et al. 1999). To examine if *SCA8* RNA could pair with CAG repeats from the *TBP* gene transcript, we placed the 5' *TBP* (CAG)₃₆-containing cDNA fragment upstream to the IRES-mediated translation of EGFP gene [pCMV-(CAG)₃₆-IRES-EGFP] (**Figure 3C**). After co-transfecting equal amount of pCMV-(CAG)₃₆-IRES-EGFP and pEF-*SCA8*-0R, -23R, -88R, or 157R constructs into HEK293 cells for two days, EGFP protein production detected was 97%, 84%, 80% ($P > 0.05$), and 71% ($P = 0.01$) of the levels in cells transfecting pCMV-(CAG)₃₆-IRES-EGFP and pEF vector (**Figure 5C**). The difference between co-transfecting *SCA8* carrying 0 and 157 repeats constructs were also significant (97% vs. 71%, $P = 0.04$). These results suggested that *SCA8* RNA may down regulate the protein expression of CAG repeat-containing RNA gene, and the length of CUG repeats affects this down-regulation.

To examine the specificity of *SCA8 trans* RNA interference, pEGFP-N1 (**Figure 3D**) was used to co-transfect with pEF-*SCA8* constructs. As shown in **Figure 5A**, 93%, 98%, 98% and 106% of the levels of the EGFP protein expression were detected as compared to that of co-transfecting pEGFP-N1 and pEF vector ($P > 0.05$). The difference between co-transfecting *SCA8*

carrying 0 and 157 repeats constructs were not significant (93% vs. 106%, $P = 0.09$). The results demonstrated the specific regulation of *SCA8* on *KLHL1*.

SCA8 encodes translatable ORF1 and ORF3

Although reported non-coding (Koob et al. 1999), small ORFs in the *SCA8* transcripts were noted (**Figure 2B**). Among them, a 102 amino acids containing-ORF1 and a 41 amino acids plus a poly-leucine tract containing-ORF3 may be translated if *SCA8* RNA possesses a cap independent IRES activity. To investigate if indeed the *SCA8* ORF1 and ORF3 are translated, *EGFP* gene was fused in-frame with the C terminal of the *SCA8* ORF1 (pCMV-ORF1-EGFP) as well as ORF3 carrying 23 combined repeats (pCMV-SCA8-23R-EGFP) (**Figure 4A, 4B**). The predicted ORF1 and ORF3 contain 102 amino acids and 41 amino acids plus a poly-leucine tract (23 leucines), respectively (**Figure 4D**). The constructs were expressed in HEK293 cells driven by the cytomegalovirus (CMV) promoter. After two days the levels of EGFP protein were evaluated by FACS analysis. As shown in **Figure 6A**, the 3%, 38% and 52% IRES-dependent EGFP production was seen in cells transfected with pCMV-SCA8-23R-EGFP, pCMV-ORF1-EGFP and pIRES2-EGFP constructs as compared to the control pEGFP-N1 construct (cap-dependent EGFP expression). Additionally, equal amounts of cell lysates were separated and immunoblotted with GFP antibody. As shown in **Figure 6B**, while no specific polypeptide was detected in mock-transfected HEK293 cells, a 50 kDa protein was detected in pCMV-ORF1-EGFP transfected cells, as compared to a 27 kDa protein in pEGFP-N1-transfected cells. Probably due to very low IRES-dependent expression of ORF3-23R-EGFP (**Figure 6A**), no ORF3-EGFP fusion protein was detected in Western blot.

ORF1 and expanded poly-leucine-containing ORF3 proteins form aggregates

To further investigate the expression of SCA8 ORF1 and ORF3 proteins, confocal microscopy examination of ORF-GFP fluorescence was carried out after transfection of pCMV-ORF1-EGFP and pCMV-SCA8-23R-EGFP constructs (**Figure 4A, 4B**) into HEK293 cells. In addition, in order to investigate the effects of expanded CTG repeats on protein expression and distribution, ORF3 carrying 0, 88 and 157 combined repeats were prepared too. As shown in **Figure 7**, strong GFP fluorescence was distributed diffusely in cells expressing EGFP-N1. With SCA8 ORF1 fused at the N terminus of GFP (ORF1-EGFP), small and dispersed aggregates appeared both in the nucleus and cytoplasm (accounting for $80 \pm 8\%$ of transfected cells), in addition to showing diffuse cytoplasmic expression. Cells expressing ORF3-0R-EGFP gave much weaker but similar fluorescence pattern to that of GFP only. For cells expressing ORF3-23R-EGFP, weak but more or less unevenly distributed cytoplasmic fluorescence was observed. Moreover, cytoplasmic microaggregates, mostly perinuclear, were seen in cells transfected with ORF3-88R-EGFP (41 amino acids plus Leu₈ProLeu₇₉) and ORF3-157R-EGFP (Leu₈ProLeu₁₄₈). These results demonstrate that in addition to be translated, the expressed GFP-tagged ORF1 and poly-leucine-expansion ORF3 proteins formed aggregates.

Aggregated ORF1 and ORF3 proteins are localized in both nuclei and cytoplasm

As IRES activity of SCA8 is too low to detect ORF3-EGFP fusion protein in immunoblot, constructs were designed to force expression of ORF3-EGFP proteins by cloning the ORF3 immediately downstream of an eukaryotic

translation initiation Kozak consensus sequence (pCMV-K-ORF3-23R-EGFP and pCMV-K-ORF3-157R-EGFP) (**Figure 4C**). Fluorescence observation of K-ORF3 showed intensely expressing EGFP pattern, and most cells expressing either pCMV-K-ORF3-23R-EGFP or pCMV-K-ORF3-157R-EGFP formed aggregates, probably due to overexpression of ORF3-EGFP (data not shown). To examine the subcellular localization of SCA8 ORF proteins, HEK293 cells were transfected with pCMV-ORF1-EGFP, pCMV-K-ORF3-23R-EGFP and pCMV-K-ORF3-157R-EGFP constructs and performed cell fractionation studies. Protein blot analysis (**Figure 8**) shows that the GFP-tagged ORF3-157R protein migrates as a smear at the top of the gel. The ORF3-157R-EGFP fusion protein is found mostly in the nuclei. Although ORF3-23R-EGFP protein also migrates as a larger protein product, a band of around 30 kDa could be detected. The expressed ORF3-23R-EGFP protein localized in both nuclear and cytoplasmic extracts. The expressed 50 kDa ORF1-EGFP protein localized mostly in the cytoplasm. In addition, confocal microscopy analysis of ORF1 and ORF3 distributions from continuous focal planes also demonstrated that ORF1 was abundantly cytoplasmic (**Figure 9**), while ORF3-157R aggregates were formed closely associated with the nucleus (**Figure 10**). Aggregates formation was also observed when neuroblastoma IMR-32 cells were transfected ORF1 and expanded SCA8 (data not shown). And overexpression of ORF3-157R-EGFP fusion protein led to stalling in the stacking gel as well (**Figure 11**).

Generation and characterization of isogenic and inducible SCA8 cell lines

Transient transfection often results in overexpression of gene of interest since multiple copies are gained in transfected cells. Additionally, copy

numbers of transfected gene vary from cell to cell, and it could integrate at different loci on chromosomes in the presence of antibiotics selection. In order to establish isogenic and inducible cell line expressing *SCA8* gene carrying 0~157 CTA/CTG combined repeats, we adopted the Flp-In T-REx system (Invitrogen) to generate stable HEK293 cell lines. As shown in **Figure 12**, the FRT locus ensures a single defined site of chromosomal integration via homologous recombination mediated by the Flp recombinase, and in the T-REx form of these cells, expression from this locus is controlled in a Tet-on-inducible fashion by the addition of either tetracycline or the related antibiotic doxycycline. The integration of *SCA8* gene into Flp-In T-REx HEK293 cells was verified by PCR (**Figure 13A**), and the RNA expression level was determined by real-time PCR assays (**Figure 13B**). The addition of doxycycline (1 $\mu\text{g/ml}$, 2 days) resulted in 20-30 times induction of *SCA8* RNA, indicating that the expression of integrated *SCA8* was tetracycline/doxycycline-dependent regulated. To find out whether *SCA8* isogenic cell lines with more CTA/CTG combined repeats are more susceptible to the stress, these cell lines were treated with various concentrations of staurosporine (apoptotic stimulus), MG-132 (proteasome inhibitor), or paraquat (source of free radicals) for one day and cell proliferation was assessed with WST-1 assay. As shown in **Figure 14**, the addition of low dosages of staurosporine (0~15 nM) or MG-132 (0~0.5 μM) did not cause significant differences of death among cell lines. However, when isogenic HEK293 cell lines with expanded *SCA8* combined repeat tracts were exposed to high dosages of staurosporine (30~50 nM) or MG-132 (0.75~1.0 μM), the viability of these cell lines decreased significantly. Unexpectedly, treatment of the high dosage of staurosporine or MG-132 also caused more death to the cell line with *SCA8* carrying 0 CTG repeats. In

addition, neither low nor high dosage had significant effects on all cell lines. Taken together, isogenic HEK293 cell lines with mutant *SCA8* were more sensitive to staurosporine and MG-132, but not paraquat.

Generation and characterization of SCA8 transgenic mice

To generate transgenic murine models expressing human *SCA8* within the cerebellum, we subcloned human *SCA8* cDNA with exons D, C2, C1, B, and A bearing either normal-range 23 or expanded 157 CTG/CTA combined repeats downstream to the cerebellar Purkinje-specific *pcp2/L7* promoter (**Figure 15A**). The transgene genotyping was performed with PCR reaction specifically amplified the region from *pcp2/L7* promoter to the exon D of human *SCA8* gene (**Figure 15B**). The transgene copy numbers of two *SCA8*-23R (17 and 24) and five *SCA8*-157R (7, 11, 17, 19 and 62) transgenic lines were estimated by comparison of transgene PCR products to the PCR products of copy number standards (**Figure 15C**). As summarized in the figure, the copy numbers are ranged from 1 to 30 among these transgenic lines.

Expression of SCA8 transcripts in SCA8 transgenic lines

From each group we chose 2 lines (23R-17, 23R-24, 157R-11, 157R-62) for further breeding and analyses. The human *SCA8* transgene can be successfully transmitted from generations 1 to 5 in these lines. Since *SCA8* gene is considered not having translatable peptide products, we assessed the expression of transgene in the level of transcripts by RT-PCR. As the result shown in **Figure 16**, all the transgenic lines we examined expressed the human *SCA8* in the cerebellum (lane C). In the brain region other to the cerebellum (lane B), however, transgene transcripts also could be detected,

implying that expression of human *SCA8* transgene might not be restricted to the cerebellum.

Behavior assessment of transgenic mice by performance on the accelerating rotarod

To evaluate the motor performance and the equilibrium ability, the trained mice were placed on the accelerating rotarod from 2 to 20 rpm over the first 5 min and maintaining at a maximum speed for another 5 min to score their latency on the rod. However, at the early life, neither *SCA8*-23R (**Figure 17A**) nor *SCA*-157R (**Figure 17B**) lines showed a different latency compared to their wild-type littermates. Although we also tested the older ones, the sample size was too small to tell the difference from sample variance. We also examined the body weights and the grabbing force of these transgenic mice, but no significant difference was detected (data not shown).

SCA8 transgene does not cause the morphological abnormalities of Purkinje cells

To examine if the *SCA8* transgene causes the morphological changes of the cerebellum, the histological analysis was performed with the calbindin D28k antibody to assess the numbers and the arrangement of the cerebellar Purkinje cells. However, at the age of 2-year-old, no markedly loss or shrinkage of Purkinje cells was observed in 23R-24 (**Figure 18A, 18C**) or 157R-62 (**Figure 18B, 18D**) lines. All these cells formed a continuous cellular sheet along the outer margin of granular layer of the cerebellar cortex, indicating that the ectopic expression of human *SCA8* bearing either

normal or expanded CTG repeats in the cerebellum of the mouse does not cause unusual orientation, or ectopic localization of Purkinje cells.

SCA8 transgenic mice exhibit the clasping phenotype

Although *SCA8* transgenic mice did not show abnormalities in both histopathological and behavioral analyses, it is striking that our *SCA8* transgenic mice exhibit a special paw clasping phenotype when suspended by the tail (**Figure 19A**), similar to that observed in HD transgenic murine model R6/2 (**Figure 19B**) (Mangiarini et al. 1995; Juvonen et al. 2000; Worth et al. 2000). The clasping phenotype of our *SCA8* transgenic mice progresses an alternating clasping and releasing of the feet, instead of maintaining holding all feet together. The founders of 157R-11 and -62 first exhibited this clasping phenotype at about 1 year of age, and some of their offspring showed the same phenotypes at younger age. However, less than 50% of the transgenic offspring displayed this phenotype, suggesting that an incomplete penetrance of *SCA8* transgene might also exist in our transgenic model as in the human patients.

To investigate whether human *SCA8* gene with expanded CTG tract would affect global RNA expression, total RNAs from cerebella of *SCA8*-23 and 157R transgenic mice at the age of 20 month and age-matched wild-type littermate control were genome-wide analyzed using MOE430A chips from Affymetrix. After normalization, differentially expressed genes were selected using one-way ANOVA and fold-change analysis. All the probe sets that showed greater than 1.5- fold or smaller than 0.7-fold changes with were considered significantly differentially expressed (**Table 7**). The candidate genes found from the microarray assays were further validated by

real-time PCR. Among 11 candidate genes, the expression patterns of *Calml4*, *Igf2*, *Igfbp2*, *Ttr*, *Pthlh*, and *Rbp1* were in accordance with the microarray analyses, although the patterns of remaining 5 genes seemed no significant differences (**Figure 20**, **21**, and **22**).

Proteomic analysis of SCA8 transgenic mice

Although RNA plays an intermediate role between DNA and protein synthesis, differences of transcript level could not account for overall changes in different disease states or treatments. Since most cellular functions are exerted by the protein units, the protein patterns of SCA8 transgenic mice was performed to search deranged proteins. The resulting 2-D DIGE gel images were matched and analyzed, and expression levels of 13 protein spots were significantly changed (**Figure 23**), and relative changes of protein abundance are summarized in **Table 9**. Using MALDI-TOF spectrometry and MASCOT search engine, 5 out 13 protein spots were identified as mitochondrial ATP synthase D chain (spot 1565), calbindin (spot 1525), calretinin (spot 1473), heterogeneous nuclear ribonucleoprotein K (spot 841), and serum albumin precursor (spot 761) (**Table 10**).

Discussion

SCAs are a heterogeneous group of inherited neurodegenerative disorder, which the cerebellum is primarily affected. Most of them are associated with unstably expanded tandem repeats in pathogenic genes. In this study, we analyzed the frequency distributions of 9 SCAs in Taiwanese, including recently identified SCA8, SCA10, SCA12, and SCA17, which were not surveyed before 2004. Our data showed that the genes responsible for 33% of dominant SCA in Taiwanese remain to be determined, similar to the previous studies in which pathogenic genes were unknown for approximately 20-40% of SCAs (Moseley et al. 1998; Takano et al. 1998; Soong et al. 2001). The prevalences of SCA1 (4%), SCA3 (36%), SCA8 (0%), and DRPLA (0%) in our study were similar to those reported: SCA1 5%, SCA3 47-48%, SCA8 0%, and DRPLA 0-1% in Taiwanese and Chinese (Soong et al. 2001; Tang et al. 2000). Although the SCA2 alleles were reported as 6% in Chinese (Tang et al. 2000) and 11% in Taiwanese (Soong et al. 2001), no SCA2 allele was detected in our study, probably due to differences in the number of sampled chromosomes, sampled individuals and/or sampled populations. In addition, similar prevalence and frequency distributions of large normal alleles of SCA1, SCA3, SCA6, and DRPLA (**Table 4**) indicate that mutations of these genes might origin from the common ancestor, while the larger normal alleles have more chance to mutate (Leeflang et al. 1995).

Abnormal expansions ranging from 75 to 92 repeats of *SCA8* alleles were detected in four patients with PD (**Table 5**). The expanded *SCA8* alleles ranging from 68 (Stevanin et al. 2000) to more than 1000 repeats (Ikeda et al.

2004) were characterized in familial and sporadic ataxia patients. In addition, the larger expanded allele has been reported in patients with psychiatric disorders and other neurological disorders, such as PD, Friedreich's ataxia and AD (Izumi et al. 2003; Juvonen et al. 2000; Sobrido et al. 2001; Stevanin et al. 2000; Tazon et al. 2002; Vincent et al. 2000; Worth et al. 2000). *SCA8* transcripts distribute throughout the brain in spite of details not being verified (Benzow and Koob 2002). Additionally, no survey was conducted to investigate the interaction between *SCA8* and other gene transcripts. It cannot be excluded that *SCA8* transcripts could interact with products of disease genes on the pathogenic pathways of PD, and *vice versa*. Thus, PD phenotypes may be the manifestation of expanded *SCA8* alleles in these four PD patients. Although no large expanded allele was found in our normal controls, *SCA8* mutation has been found in rare instances in healthy control individuals, suggesting that association between expansion mutation at *SCA8* and *SCA* is not straightforward. However, in most instances the expanded allele closely correlates with *SCA8* disease, and rarely identical haplotypes existed between affected and normal chromosomes (Ikeda et al. 2004), implying CTG expansion should play a predominant role in pathogenesis.

Abnormal CAG expansions in the *SCA17 TBP* gene were detected in a PD patient (46 repeats) (**Table 5**). The *TBP* alleles range from 30 to 43 repeats in our normal controls. In the general population, the reported normal *TBP* alleles range in size from 25 to 44 repeats (Gostout et al. 1993; Zuhlke et al. 2001) and the expanded alleles in patients with ataxia from 43 to 63 repeats (Koide et al. 1999; Fujigasaki et al. 2001a; Nakamura et al. 2001; Silveira et al. 2002; Zuhlke et al. 2003), but with reduced penetrance (Zuhlke et al.

2003). Recently Huntington's disease-like phenotype due to CAG repeat expansion in the *TBP* gene was reported (Stevanin et al. 2003). In addition, non-cerebellar symptoms may develop in some specific SCA types (Gwinn-Hardy et al. 2000; Gwinn-Hardy et al. 2001; O'Hearn et al. 2001), as well as the PD manifestation of *SCA8* mutation described in this study. As *TBP* is a critical factor regulating the initiation of transcription and ubiquitously expressed in all cells, the 46-repeat allele in PD patient may be linked to the neurological manifestations observed.

The overlapping organization and evolutionary conservation of *SCA8* and *KLHL1* genes (Nemes et al. 2000; Benzow and Koob 2002) hint the close relation of them. KLHL1 protein is the homologue of *Drosophila* kelch protein, functioning as maintaining cytoskeleton order, and it is recently reported that KLHL1 enhances neurite outgrowth mediated via the interaction with glycogen synthase kinase 3 β (Seng et al. 2006) and modulates P/Q-type calcium channel function (Aromolaran et al. 2007). Nevertheless, no studies focused on the *trans* antisense effect of *SCA8* to *KLHL1*. We co-expressed *KLHL1* and *SCA8* carrying various numbers of CTG repeats to investigate whether *SCA8* regulates the expression of *KLHL1* and whether this regulation is mediated in a CTG repeats-dependent manner. The expression of *KLHL1* was reduced as expected when *SCA8* was expressed in the same cells (29 ~ 55% of the levels of *KLHL1*-EGFP gene, **Figure 4B**), suggesting that *SCA8* is a negative regulator of *KLHL1*. The synthesis of overlapping transcripts potentially interferes with the RNA processing at different levels. Epigenetic modification, transcriptional interference, impaired splicing, or RNA export as well as mechanisms triggered by double-stranded RNA such as RNA editing and RNA

interference/micro-RNA synthesis may represent consequences of antisense transcription (Werner and Berdal 2005). Among the identified natural antisense transcripts, the 5' end overlapping *SCA8/KLHL1* organization is similar to the relation between homeobox-containing transcription factor *Msx1* gene and its antisense (*Msx1-AS*) compartment, while non-coding *Msx1-AS* RNA is complementary to region extending from 3' end of exon 2 to the middle of intron 1 (more than 2 kb) (Blin-Wakkach et al. 2001). Although the precise mechanism for *Msx1* sense–AS RNA interactions remains unclear, the nature that complementary region extends across intron 1 and exon 2 implying the duplex RNA might be an obstacle to splicing. However, the overlapping region of *SCA8/KLHL1* does not comprise the exon-intron boundary and the levels of both *KLHL1* and *SCA8* transcripts were not significantly reduced by RT-PCR and gel semi-quantitation (洪, 2005), the repression of *KLHL1* by *SCA8* was likely mediated through post-transcriptional interferences such as nuclear retention and translational blockage.

SCA8 was first defined as a non-coding CUG-expanded RNA disease (Koob et al. 1999). Although the precise transcription start site remains to be determined, *SCA8* has been proven to be an intact transcript which have up to six exons and alternative polyadenylation sites. But sequence analysis performed formerly revealed no significant translatable ORFs existing in any of splice isoforms (Nemes et al. 2000). The standard translation initiation recruits eIF4F to the 5' m⁷GpppN cap of mRNA, followed by the ribosome binding and scanning for the proper region to start translation. On the other hand, some eukaryotic mRNAs and viral RNAs have the ability to recruit the translational machinery to the internal portion of RNAs mediated through

the IRES elements. Judged from the structure of *SCA8* transcripts and the long 5' UTR containing a G/C rich region (Nemes et al. 2000), which could serve as a recognition site of *trans* interacting factors, the translational ability of *SCA8* remains to be uncovered. In our previous study, sequence analysis revealed the existence of three small ORFs in the *SCA8* transcripts and *SCA8* RNA was demonstrated to possess the bipartite cap independent IRESs using dicistronic constructs (Lin et al. submitted). Owing to short intervention between ORF1 and ORF2, ORF2 is considered non-translatable through the IRES activity. Thus, GFP tagged ORF1 and ORF3 were transiently transfected into HEK293 cells to verify if indeed the *SCA8* transcripts are translatable. Both GFP-tagged ORF1 and ORF3 are expressed, while ORF3 expressing at much lower level (3% of the cap-dependent expression) and could not be detected on the immunoblotting (**Figure 5**). The strength of IRES is mediated by the arrangement of ORFs (Hennecke et al. 2001) and physiological conditions leading to greatly reduced cap-dependent protein synthesis (Fernandez et al. 2001; Kim and Jang 2002; Sherrill et al. 2004). Therefore, the relatively lower expression level of *SCA8* ORF3 compared to ORF1 might be due to the genomic arrangement, or the robust expression of ORF3 would occur under cellular stresses.

Although the expression level of *SCA8* ORF3 was very low in our *in vitro* system, the uneven cytoplasmic distribution of ORF3-23R-EGFP could be observed (**Figure 6**). Since overexpression of EGFP alone resulted in diffusely distribution of green fluorescence, the uneven distribution of ORF3-23R-EGFP should be derived from the content of ORF3. Additionally, with the increase of CTG repeats, more and larger protein aggregates formed (**Figure 6**) and stalled in the stacking layer of polyacrylamide gel (**Figure 7**),

further indicating that CTG-encoding polyleucine is prone to aggregate. Cytoplasmic and intranuclear accumulation of mutant disease proteins are often found in neurodegenerative diseases, including Huntington's disease, SCA1, SCA2, SCA3, SCA7, SCA17, and DRPLA (Scherzinger et al. 1997; Skinner et al. 1997; Koyano et al. 2000; Paulson et al. 1997; Holmberg et al. 1998; Nakamura et al. 2001; Miyashita et al. 1998), but the role of mutant protein aggregates remains controversial. Although so far no diseases are linked to mutant polyleucine proteins, recently it was found that the polyleucine stretch conferred more toxicity than the polyglutamine stretch and showed a high propensity for aggregation distributing closely around the nucleus (Dorsman et al. 2002; Oma et al. 2004). But the threshold of polyleucine to induce cellular abnormality was not determined. Polyglutamine diseases arise when the hydrophobic glutamine tract in the pathogenic protein elongates over a threshold length, which is usually around 30-40 glutamine residues. Besides, expression of 30-residue polyleucine in COS-7 cells resulted in perinuclear as well as cytoplasmic aggregates (Oma et al. 2004), suggesting polyleucine stretch is more hydrophobic than polyglutamine stretch. Consequently, with the same amount of hydrophobic amino acids when beyond the threshold, polyleucine stretch would lead to more aggregates. On the other hand, considering SCA8 genes with 23 CTG repeats non-pathogenic, the relatively low expression level in our cellular system as well as in neurons of both healthy and affected individuals (Benzow and Koob 2002) may prevent the SCA8 phenotypes in spite of the uneven distributions. With the increase of CTG repeats, long polyleucine stretch renders ORF3 more hydrophobicity, which might in turn serve as a nucleus for aggregate growth, one of widely accepted processes involved in aggregates formation (Harper and Lansbury

1997; Ferrone 1999). However, whether mutant ORF3 aggregates cause cell death was not surveyed in this study, and the role of soluble ORF1 aggregates should also be determined in the future.

In an effort to understand the effect of long CTG repeat tracts on cell survival under specific stresses, we had developed a number of otherwise isogenic HEK293 derived cell lines expressing transcripts with various numbers of CTG repeats. In this study, the finding that isogenic HEK293 cell lines with mutant *SCA8* were more sensitive to high dosage of staurosporine is consistent with that staurosporine enhanced cytotoxicity caused by expanded polyglutamine protein (Cooper et al. 1998). Although staurosporine is an apoptosis-inducing agent, it also affects the cell cycle and causes cell cycle arrest in the G1 phase (Orr et al. 1998), the increased susceptibility to cell death induced by it may be mediated in part through effects on the cell cycle. In addition, isogenic HEK293 cells with mutant *SCA8* were also increased cell susceptibility to the proteasome inhibitor, MG-132. There is evidence that ataxins 1, 3 and 7, are susceptible to be ubiquitinated and targeted by the proteasome for degradation and clearance (Cummings et al. 1999; Matilla et al. 2001; Chai et al. 2004). However, mutant ataxins form misfolded structure, which in turn impare the recognition and degradation process by the proteasome. Accordingly, intracellular aggregates produced by the expanded *SCA8* gene might derange proteasome function, although no appropriate methods could detect the aggregate formation now.

We have developed a *SCA8* transgenic mouse model in which human *SCA8* gene is expressed under the control of cerebellar Purkinje cell-specific

promoter, *pcp2/L7*. Although human *SCA8* and mouse analog are evolutionary conserved, the mouse *SCA8* gene does not consist of exons C, B, and A (Benzow and Koob 2002), in which the last one contains the CTG trinucleotide repeats relevant to the pathogenesis of *SCA8*. Thus, we introduced human *SCA8* with either normal-ranged 23 or expanded 157 CTG/CTA combined repeats into mouse genome to see if the expanded CTG repeats would lead the mice to manifest the *SCA8* phenotypes. In our *SCA8* transgenic mouse model, however, we cannot detect histological abnormalities in the Purkinje cells (**Figure 13**). Biomarkers of other cell types could be further used to examine the cerebellum, such as glial fibrillary acidic protein (GFAP), a marker for the microglia, used to detect the activated astrocytes. In the previous studies of anti-addictive drug, Ibogaine, GFAP was served as a useful biomarker for neurotoxicity (O'Callaghan et al. 1996; Xu et al. 2000). In addition, abundant reactive microglia have been shown to surround the β -amyloid plaques in the AD brain (McGeer and McGeer 1995), suggesting that microglia also plays a role in the neurodegenerative disorders.

Previously in our study of HEK293 cell model, RNA FISH experiments revealed ribonuclear foci formation in cells carrying expanded 88 and 157 combined repeats (Lin et al. 2007). In our mouse model, we haven't examined the formation of ribonuclear foci, which now are considered as a hallmark of affected muscle in DM1 and DM2 patients. A CTG expansion in the 3'-UTR of *DMPK* gene, sequesters CUGBPs from their normal cellular functions, leading to abnormal RNA splicing of several genes. It is suggested that decreased levels of muscleblind (MBNL) and increased levels of CUGBP are relevant to the formation of CUG-containing ribonuclear foci

and might mediate the RNA-induced toxicity (de Haro et al. 2006). Yet the precise role of the ribonuclear foci remains to be determined since even though ribonuclear foci and the CUG binding protein, MBNL, are colocalized, no pathological phenotypes can be detected in *Drosophila* MBNL null models (Houseley et al. 2005). Since SCA8 and DM1 share molecular similarity and no ribonuclear foci formation has been reported in SCA8 patients or other models, we are going to determine whether the CUG-containing ribonuclear foci could be detected in our SCA8 transgenic mouse model using RNA-FISH strategy.

Although *Pcp2/L7* promoter restricts the expression of its downstream gene to Purkinje and retinal bipolar cells, the expression of the *SCA8* transgene in our model can be found in other regions of the brain. Endogenous *Pcp2/L7* protein is expressed exclusively in Purkinje cells and retinal bipolar neurons (Nordquist et al. 1988; Oberdick et al. 1988; Berrebi et al. 1991). It has been shown that 3.1-kb stretch of sequence upstream of *Pcp2/L7* restricted the gene expression to Purkinje cells (Vandaele et al. 1991), while the 5' upstream region of *Pcp2/L7* DNA direct the gene activity both in Purkinje and retinal bipolar cells (Oberdick et al. 1990). Further investigations indicates that the nonspecific expression was resulted from the control of a 2.88-kb *Pcp2/L7* DNA fragment upstream from exon 4 (Barski et al. 2000), suggesting that the regulatory element for specific expression might not be included in this region. Since *SCA8* transgene in our model is controlled only by a 0.85-kb fragment upstream from exon 2, it may not be surprising that the expression is not restricted to the cerebellum. Nevertheless, the expression pattern in other tissues should be further determined.

The clasping phenotype has been used as an evaluation criterion to study the disease progression in HD mice (Reddy et al. 1999; van Dellen et al. 2001) in spite of the causing mechanisms remaining unclear. This dystonic posturing of the hind limbs in our SCA8 transgenic mouse model is worth a target for uncovering the disease pathway and drugs screening for relieving the distress.

In this study, gene expression profiles in SCA8 transgenic mice were examined by using microarray and proteomic analyses to identify potential mechanisms responsible for the pathogenesis of SCA8. Although no significantly behavioral abnormality was observed in SCA8 transgenic mice, from the results of microarray assay and real-time quantitative RT-PCR, we found that expressions of *Calml4*, *Igf2*, *Igfbp2*, *Ttr*, *Pthlh*, and *Rbp1* were deranged. *Igf2* (insulin-like growth factor 2), *Igfbp2* (insulin-like growth factor binding protein 2), and *Ttr* (transthyretin) had been found to be implicated in Alzheimer's disease (Stein and Johnson 2002), the most common neurodegenerative disease, and increased expressions of *Igf2* and *Ttr* were linked to the protection of neurons from β -amyloid induced toxicity (Dore et al. 1997; Serot et al. 1997). Thus, decreased levels of these proteins in SCA8 transgenic mice might lead to more harmful effects caused by mutant SCA8. Proteomic analysis showed that expressions of calbindin and calretinin were decreased in SCA8-157R transgenic mice. These proteins belong to the large family of EF-hand calcium-binding proteins (Rogers and Resibois 1992) and calcium-binding proteins-expressing neurons are thought to be resistant to injury-promoting perturbations in calcium homeostasis (Mattson et al. 1991). In addition, reduced immunoreactivity to calcium-binding proteins was shown in other SCAs (Kumada et al. 2000; Vig et al.

1996; Vig et al. 1998; Vig et al. 2000; Yang et al. 2000), suggesting that down-regulation of calbindin and calretinin might increase cerebellar susceptibility to neurotoxicity. Although 2-D electrophoresis offers an efficient and fast tool to investigate the protein profile, MALDI-TOF analysis only provides predicted candidate proteins and could not reflect the actual biological status of them. Therefore, immunoblotting and IHC should be performed for further validation of these candidate proteins.

References

- 洪葦苓 (2005) 第八型脊髓小腦運動失調症:CTG 三核苷重複的遺傳分析與細胞模式研究。國立臺灣師範大學生命科學系碩士論文
- 項聖文 (2005) 第八型脊髓小腦運動失調症之果蠅模式建立與致病機制研究。國立臺灣師範大學生命科學系碩士論文
- Alonso I, Costa C, Gomes A, Ferro A, Seixas AI, Silva S, Cruz VT, Coutinho P, Sequeiros J, Silveira I (2005) A novel H101Q mutation causes PKC γ loss in spinocerebellar ataxia type 14. *J Hum Genet* 50: 523-9
- Aromolaran KA, Benzow KA, Koob MD, Piedras-Renteria ES (2007) The Kelch-like protein 1 modulates P/Q-type calcium current density. *Neuroscience* 145: 841-50
- Banfi S, Servadio A, Chung MY, Kwiatkowski TJ, Jr., McCall AE, Duvick LA, Shen Y, Roth EJ, Orr HT, Zoghbi HY (1994) Identification and characterization of the gene causing type 1 spinocerebellar ataxia. *Nat Genet* 7: 513-20
- Barski JJ, Dethleffsen K, Meyer M (2000) Cre recombinase expression in cerebellar Purkinje cells. *Genesis* 28: 93-8
- Benomar A, Krols L, Stevanin G, Cancel G, LeGuern E, David G, Ouhabi H, Martin JJ, Durr A, Zaim A, et al. (1995) The gene for autosomal dominant cerebellar ataxia with pigmentary macular dystrophy maps to chromosome 3p12-p21.1. *Nat Genet* 10: 84-8
- Benzow KA, Koob MD (2002) The KLHL1-antisense transcript (KLHL1AS) is evolutionarily conserved. *Mamm Genome* 13: 134-41

- Berrebi AS, Oberdick J, Sangameswaran L, Christakos S, Morgan JJ, Mugnaini E (1991) Cerebellar Purkinje cell markers are expressed in retinal bipolar neurons. *J Comp Neurol* 308: 630-49
- Berul CI, Maguire CT, Aronovitz MJ, Greenwood J, Miller C, Gehrman J, Housman D, Mendelsohn ME, Reddy S (1999) DMPK dosage alterations result in atrioventricular conduction abnormalities in a mouse myotonic dystrophy model. *J Clin Invest* 103: R1-7
- Blin-Wakkach C, Lezot F, Ghoul-Mazgar S, Hotton D, Monteiro S, Teillaud C, Pibouin L, Orestes-Cardoso S, Papagerakis P, Macdougall M, Robert B, Berdal A (2001) Endogenous Msx1 antisense transcript: In vivo and in vitro evidences, structure, and potential involvement in skeleton development in mammals. *Proc Natl Acad Sci U S A* 98: 7336-41
- Buxton J, Shelbourne P, Davies J, Jones C, Van Tongeren T, Aslanidis C, de Jong P, Jansen G, Anvret M, Riley B, et al. (1992) Detection of an unstable fragment of DNA specific to individuals with myotonic dystrophy. *Nature* 355: 547-8
- Brusse E, de Koning I, Maat-Kievit A, Oostra BA, Heutink P, van Swieten JC (2006) Spinocerebellar ataxia associated with a mutation in the fibroblast growth factor 14 gene (SCA27): A new phenotype. *Mov Disord* 21: 396-401
- Chai Y, Berke SS, Cohen RE, Paulson HL (2004) Poly-ubiquitin binding by the polyglutamine disease protein ataxin-3 links its normal function to protein surveillance pathways. *J Biol Chem* 279: 3605-11
- Chung S, Andersson T, Sonntag KC, Bjorklund L, Isacson O, Kim KS (2002) Analysis of different promoter systems for efficient transgene expression in mouse embryonic stem cell lines. *Stem Cells* 20: 139-45

- Cooper JK, Schilling G, Peters MF, Herring WJ, Sharp AH, Kaminsky Z, Masone J, Khan FA, Delanoy M, Borchelt DR, Dawson VL, Dawson TM, Ross CA (1998) Truncated N-terminal fragments of huntingtin with expanded glutamine repeats form nuclear and cytoplasmic aggregates in cell culture. *Hum Mol Genet* 7: 783-90
- Cummings CJ, Mancini MA, Antalffy B, DeFranco DB, Orr HT, Zoghbi HY (1998) Chaperone suppression of aggregation and altered subcellular proteasome localization imply protein misfolding in SCA1. *Nat Genet* 19: 148-54
- Cummings CJ, Reinstein E, Sun Y, Antalffy B, Jiang Y, Ciechanover A, Orr HT, Beaudet AL, Zoghbi HY (1999) Mutation of the E6-AP ubiquitin ligase reduces nuclear inclusion frequency while accelerating polyglutamine-induced pathology in SCA1 mice. *Neuron* 24: 879-92
- David G, Abbas N, Stevanin G, Durr A, Yvert G, Cancel G, Weber C, Imbert G, Saudou F, Antoniou E, Drabkin H, Gemmill R, Giunti P, Benomar A, Wood N, Ruberg M, Agid Y, Mandel JL, Brice A (1997) Cloning of the SCA7 gene reveals a highly unstable CAG repeat expansion. *Nat Genet* 17: 65-70
- Day JW, Schut LJ, Moseley ML, Durand AC, Ranum LP (2000) Spinocerebellar ataxia type 8: clinical features in a large family. *Neurology* 55: 649-57
- de Haro M, Al-Ramahi I, De Gouyon B, Ukani L, Rosa A, Faustino NA, Ashizawa T, Cooper TA, Botas J (2006) MBNL1 and CUGBP1 modify expanded CUG-induced toxicity in a *Drosophila* model of myotonic dystrophy type 1. *Hum Mol Genet* 15: 2138-45

- Dolnick BJ (1993) Cloning and characterization of a naturally occurring antisense RNA to human thymidylate synthase mRNA. *Nucleic Acids Res* 21: 1747-52
- Dore S, Kar S, Quirion R (1997) Insulin-like growth factor I protects and rescues hippocampal neurons against beta-amyloid- and human amylin-induced toxicity. *Proc Natl Acad Sci U S A* 94: 4772-7
- Dorsman JC, Pepers B, Langenberg D, Kerkdijk H, Ijszenga M, den Dunnen JT, Roos RA, van Ommen GJ (2002) Strong aggregation and increased toxicity of poly-leucine over polyglutamine stretches in mammalian cells. *Hum Mol Genet* 11: 1487-96
- Donaldson KM, Li W, Ching KA, Batalov S, Tsai CC, Joazeiro CA (2003) Ubiquitin-mediated sequestration of normal cellular proteins into polyglutamine aggregates. *Proc Natl Acad Sci U S A* 100: 8892-7
- Ebraldize A, Wang Y, Petkova V, Ebraldise K and Junghans RP (2004) RNA leaching of transcription factors disrupts transcription in myotonic dystrophy. *Science* 303: 383-7
- Fardaei M, Rogers MT, Thorpe HM, Larkin K, Hamshere MG, Harper PS, Brook JD (2002) Three proteins, MBNL, MBLL and MBXL, co-localize in vivo with nuclear foci of expanded-repeat transcripts in DM1 and DM2 cells. *Hum Mol Genet* 11: 805-14
- Fernandez J, Yaman I, Mishra R, Merrick WC, Snider MD, Lamers WH, Hatzoglou M (2001) Internal ribosome entry site-mediated translation of a mammalian mRNA is regulated by amino acid availability. *J Biol Chem* 276: 12285-91
- Fernandez J, Yaman I, Sarnow P, Snider MD, Hatzoglou M (2002) Regulation of internal ribosomal entry site-mediated translation by

- phosphorylation of the translation initiation factor eIF2alpha. *J Biol Chem* 277: 19198-205
- Ferrone F (1999) Analysis of protein aggregation kinetics. *Methods Enzymol* 309: 256-74
- Fujigasaki H, Martin JJ, De Deyn PP, Camuzat A, Deffond D, Stevanin G, Dermaut B, Van Broeckhoven C, Durr A, Brice A (2001a) CAG repeat expansion in the TATA box-binding protein gene causes autosomal dominant cerebellar ataxia. *Brain* 124: 1939-47
- Fujigasaki H, Verma IC, Camuzat A, Margolis RL, Zander C, Lebre AS, Jamot L, Saxena R, Anand I, Holmes SE, Ross CA, Durr A, Brice A (2001b) SCA12 is a rare locus for autosomal dominant cerebellar ataxia: a study of an Indian family. *Ann Neurol* 49: 117-21
- Furtado S, Farrer M, Tsuboi Y, Klimek ML, de la Fuente-Fernandez R, Hussey J, Lockhart P, Calne DB, Suchowersky O, Stoessl AJ, Wszolek ZK (2002) SCA-2 presenting as parkinsonism in an Alberta family: clinical, genetic, and PET findings. *Neurology* 59: 1625-7
- Gong CX, Lidsky T, Wegiel J, Zuck L, Grundke-Iqbal I, Iqbal K (2000) Phosphorylation of microtubule-associated protein tau is regulated by protein phosphatase 2A in mammalian brain. Implications for neurofibrillary degeneration in Alzheimer's disease. *J Biol Chem* 275: 5535-44
- Gostout B, Liu Q, Sommer SS (1993) "Cryptic" repeating triplets of purines and pyrimidines (cRRY(i)) are frequent and polymorphic: analysis of coding cRRY(i) in the proopiomelanocortin (POMC) and TATA-binding protein (TBP) genes. *Am J Hum Genet* 52: 1182-90

- Grewal RP, Tayag E, Figueroa KP, Zu L, Durazo A, Nunez C, Pulst SM (1998) Clinical and genetic analysis of a distinct autosomal dominant spinocerebellar ataxia. *Neurology* 51: 1423-6
- Grewal RP, Achari M, Matsuura T, Durazo A, Tayag E, Zu L, Pulst SM, Ashizawa T (2002) Clinical features and ATTCT repeat expansion in spinocerebellar ataxia type 10. *Arch Neurol* 59: 1285-90
- Gwinn-Hardy K, Chen JY, Liu HC, Liu TY, Boss M, Seltzer W, Adam A, Singleton A, Koroshetz W, Waters C, Hardy J, Farrer M (2000) Spinocerebellar ataxia type 2 with parkinsonism in ethnic Chinese. *Neurology* 55: 800-5
- Gwinn-Hardy K, Singleton A, O'Suilleabhain P, Boss M, Nicholl D, Adam A, Hussey J, Critchley P, Hardy J, Farrer M (2001) Spinocerebellar ataxia type 3 phenotypically resembling parkinson disease in a black family. *Arch Neurol* 58: 296-9
- Hamshere MG, Brook JD (1996) Myotonic dystrophy, knockouts, warts and all. *Trends Genet* 12: 332-4
- Handa V, Goldwater D, Stiles D, Cam M, Poy G, Kumari D, Usdin K (2005) Long CGG-repeat tracts are toxic to human cells: implications for carriers of Fragile X premutation alleles. *FEBS Lett* 579: 2702-8
- Harley HG, Brook JD, Rundle SA, Crow S, Reardon W, Buckler AJ, Harper PS, Housman DE, Shaw DJ (1992) Expansion of an unstable DNA region and phenotypic variation in myotonic dystrophy. *Nature* 355: 545-6
- Harper JD, Lansbury PT, Jr. (1997) Models of amyloid seeding in Alzheimer's disease and scrapie: mechanistic truths and physiological consequences of the time-dependent solubility of amyloid proteins. *Annu Rev Biochem* 66: 385-407

- He Y, Zu T, Benzow KA, Orr HT, Clark HB, Koob MD (2006) Targeted deletion of a single Sca8 ataxia locus allele in mice causes abnormal gait, progressive loss of motor coordination, and Purkinje cell dendritic deficits. *J Neurosci* 26: 9975-82
- Hellen CU, Sarnow P (2001) Internal ribosome entry sites in eukaryotic mRNA molecules. *Genes Dev* 15: 1593-612
- Helmlinger D, Hardy S, Sasorith S, Klein F, Robert F, Weber C, Miguet L, Potier N, Van-Dorsselaer A, Wurtz JM, Mandel JL, Tora L, Devys D (2004) Ataxin-7 is a subunit of GCN5 histone acetyltransferase-containing complexes. *Hum Mol Genet* 13: 1257-65
- Hennecke M, Kwissa M, Metzger K, Oumard A, Kroger A, Schirmbeck R, Reimann J, Hauser H (2001) Composition and arrangement of genes define the strength of IRES-driven translation in bicistronic mRNAs. *Nucleic Acids Res* 29: 3327-34
- Holmberg M, Duyckaerts C, Durr A, Cancel G, Gourfinkel-An I, Damier P, Faucheux B, Trottier Y, Hirsch EC, Agid Y, Brice A (1998) Spinocerebellar ataxia type 7 (SCA7): a neurodegenerative disorder with neuronal intranuclear inclusions. *Hum Mol Genet* 7: 913-8
- Holmes SE, O'Hearn EE, McInnis MG, Gorelick-Feldman DA, Kleiderlein JJ, Callahan C, Kwak NG, Ingersoll-Ashworth RG, Sherr M, Sumner AJ, Sharp AH, Ananth U, Seltzer WK, Boss MA, Vieria-Saecker AM, Epplen JT, Riess O, Ross CA, Margolis RL (1999) Expansion of a novel CAG trinucleotide repeat in the 5' region of PPP2R2B is associated with SCA12. *Nat Genet* 23: 391-2
- Holmes SE, O'Hearn E, Margolis RL (2003) Why is SCA12 different from other SCAs? *Cytogenet Genome Res* 100: 189-97

- Houseley JM, Wang Z, Brock GJ, Soloway J, Artero R, Perez-Alonso M, O'Dell KM, Monckton DG (2005) Myotonic dystrophy associated expanded CUG repeat muscleblind positive ribonuclear foci are not toxic to *Drosophila*. *Hum Mol Genet* 14: 873-83
- Huez I, Creancier L, Audigier S, Gensac MC, Prats AC, Prats H (1998) Two independent internal ribosome entry sites are involved in translation initiation of vascular endothelial growth factor mRNA. *Mol Cell Biol* 18: 6178-90
- Huynh DP, Yang HT, Vakharia H, Nguyen D, Pulst SM (2003) Expansion of the polyQ repeat in ataxin-2 alters its Golgi localization, disrupts the Golgi complex and causes cell death. *Hum Mol Genet* 12: 1485-96
- Huynh DP, Nguyen DT, Pulst-Korenberg JB, Brice A, Pulst SM (2007) Parkin is an E3 ubiquitin-ligase for normal and mutant ataxin-2 and prevents ataxin-2-induced cell death. *Exp Neurol* 203: 531-41
- Ikeda Y, Dick KA, Weatherspoon MR, Gincel D, Armbrust KR, Dalton JC, et al. (2006) Spectrin mutations cause spinocerebellar ataxia type 5. *Nat Genet* 38: 184-90
- Imbert G, Saudou F, Yvert G, Devys D, Trottier Y, Garnier JM, Weber C, Mandel JL, Cancel G, Abbas N, Durr A, Didierjean O, Stevanin G, Agid Y, Brice A (1996) Cloning of the gene for spinocerebellar ataxia 2 reveals a locus with high sensitivity to expanded CAG/glutamine repeats. *Nat Genet* 14: 285-91
- Izumi Y, Maruyama H, Oda M, Morino H, Okada T, Ito H, Sasaki I, Tanaka H, Komure O, Udaka F, Nakamura S, Kawakami H (2003) SCA8 repeat expansion: large CTA/CTG repeat alleles are more common in ataxic patients, including those with SCA6. *Am J Hum Genet* 72: 704-9

- Juvonen V, Hietala M, Paivarinta M, Rantamaki M, Hakamies L, Kaakkola S, Vierimaa O, Penttinen M, Savontaus ML (2000) Clinical and genetic findings in Finnish ataxia patients with the spinocerebellar ataxia 8 repeat expansion. *Ann Neurol* 48: 354-61
- Kawaguchi Y, Okamoto T, Taniwaki M, Aizawa M, Inoue M, Katayama S, Kawakami H, Nakamura S, Nishimura M, Akiguchi I, et al. (1994) CAG expansions in a novel gene for Machado-Joseph disease at chromosome 14q32.1. *Nat Genet* 8: 221-8
- Kaytor MD, Duvick LA, Skinner PJ, Koob MD, Ranum LP, Orr HT (1999) Nuclear localization of the spinocerebellar ataxia type 7 protein, ataxin-7. *Hum Mol Genet* 8: 1657-64
- Kim YK, Jang SK (2002) Continuous heat shock enhances translational initiation directed by internal ribosomal entry site. *Biochem Biophys Res Commun* 297: 224-31
- Kitsu M, Izumi T, Hara M, Mitsuishi Y, Kobayashi N, Fukuyama Y (1992) [Progressive cerebellar ataxia with diencephalic symptoms (Toyokura)--a case report]. *No To Hattatsu* 24: 273-7
- Koide R, Ikeuchi T, Onodera O, Tanaka H, Igarashi S, Endo K, Takahashi H, Kondo R, Ishikawa A, Hayashi T, et al. (1994) Unstable expansion of CAG repeat in hereditary dentatorubral-pallidoluysian atrophy (DRPLA). *Nat Genet* 6: 9-13
- Koide R, Kobayashi S, Shimohata T, Ikeuchi T, Maruyama M, Saito M, Yamada M, Takahashi H, Tsuji S (1999) A neurological disease caused by an expanded CAG trinucleotide repeat in the TATA-binding protein gene: a new polyglutamine disease? *Hum Mol Genet* 8: 2047-53

- Koob MD, Moseley ML, Schut LJ, Benzow KA, Bird TD, Day JW, Ranum LP (1999) An untranslated CTG expansion causes a novel form of spinocerebellar ataxia (SCA8). *Nat Genet* 21: 379-84
- Koshy B, Matilla T, Burreight EN, Merry DE, Fischbeck KH, Orr HT, Zoghbi HY (1996) Spinocerebellar ataxia type-1 and spinobulbar muscular atrophy gene products interact with glyceraldehyde-3-phosphate dehydrogenase. *Hum Mol Genet* 5: 1311-8
- Kozak M (1991) Structural features in eukaryotic mRNAs that modulate the initiation of translation. *J Biol Chem* 266: 19867-70
- Kumada S, Hayashi M, Mizuguchi M, Nakano I, Morimatsu Y, Oda M (2000) Cerebellar degeneration in hereditary dentatorubral-pallidoluysian atrophy and Machado-Joseph disease. *Acta Neuropathol (Berl)* 99: 48-54
- Lai EC (2002) Micro RNAs are complementary to 3' UTR sequence motifs that mediate negative post-transcriptional regulation. *Nat Genet* 30: 363-4
- Li AW, Seyoum G, Shiu RP, Murphy PR (1996) Expression of the rat BFGF antisense RNA transcript is tissue-specific and developmentally regulated. *Mol Cell Endocrinol* 118: 113-23
- Lin HY, Shiau HC, Chen CM, Hsieh-Li HM, Lee-Chen GJ, Su MT. Spinocerebellar ataxia type 8 RNA has internal ribosome entry segment activity. *BMC Mol Biol*: submitted
- Mahadevan M, Tsilfidis C, Sabourin L, Shutler G, Amemiya C, Jansen G, Neville C, Narang M, Barcelo J, O'Hoy K, et al. (1992) Myotonic dystrophy mutation: an unstable CTG repeat in the 3' untranslated region of the gene. *Science* 255: 1253-5

- Mangiarini L, Sathasivam K, Mahal A, Mott R, Seller M, Bates GP (1997) Instability of highly expanded CAG repeats in mice transgenic for the Huntington's disease mutation. *Nat Genet* 15: 197-200
- Marz P, Probst A, Lang S, Schwager M, Rose-John S, Otten U, Ozbek S (2004) Ataxin-10, the spinocerebellar ataxia type 10 neurodegenerative disorder protein, is essential for survival of cerebellar neurons. *J Biol Chem* 279: 35542-50
- Marz P, Stetefeld J, Bendfeldt K, Nitsch C, Reinstein J, Shoeman RL, Dimitriades-Schmutz B, Schwager M, Leiser D, Ozcan S, Otten U, Ozbek S (2006) Ataxin-10 interacts with O-linked beta-N-acetylglucosamine transferase in the brain. *J Biol Chem* 281: 20263-70
- Masino L, Musi V, Menon RP, Fusi P, Kelly G, Frenkiel TA, Trottier Y, Pastore A (2003) Domain architecture of the polyglutamine protein ataxin-3: a globular domain followed by a flexible tail. *FEBS Lett* 549: 21-5
- Matilla A, Koshy BT, Cummings CJ, Isobe T, Orr HT, Zoghbi HY (1997) The cerebellar leucine-rich acidic nuclear protein interacts with ataxin-1. *Nature* 389: 974-8
- Matilla A, Gorbea C, Einum DD, Townsend J, Michalik A, van Broeckhoven C, Jensen CC, Murphy KJ, Ptacek LJ, Fu YH (2001) Association of ataxin-7 with the proteasome subunit S4 of the 19S regulatory complex. *Hum Mol Genet* 10: 2821-31
- Matsuura T, Yamagata T, Burgess DL, Rasmussen A, Grewal RP, Watase K, Khajavi M, McCall AE, Davis CF, Zu L, Achari M, Pulst SM, Alonso E, Noebels JL, Nelson DL, Zoghbi HY, Ashizawa T (2000) Large

- expansion of the ATTCT pentanucleotide repeat in spinocerebellar ataxia type 10. *Nat Genet* 26: 191-4
- Mattson MP, Rychlik B, Chu C, Christakos S (1991) Evidence for calcium-reducing and excito-protective roles for the calcium-binding protein calbindin-D28k in cultured hippocampal neurons. *Neuron* 6: 41-51
- McGeer PL, McGeer EG (1995) The inflammatory response system of brain: implications for therapy of Alzheimer and other neurodegenerative diseases. *Brain Res Brain Res Rev* 21: 195-218
- McMahon SJ, Pray-Grant MG, Schieltz D, Yates JR, 3rd, Grant PA (2005) Polyglutamine-expanded spinocerebellar ataxia-7 protein disrupts normal SAGA and SLIK histone acetyltransferase activity. *Proc Natl Acad Sci U S A* 102: 8478-82
- Miyashita T, Nagao K, Ohmi K, Yanagisawa H, Okamura-Oho Y, Yamada M (1998) Intracellular aggregate formation of dentatorubral-pallidoluysian atrophy (DRPLA) protein with the extended polyglutamine. *Biochem Biophys Res Commun* 249: 96-102
- Moseley ML, Benzow KA, Schut LJ, Bird TD, Gomez CM, Barkhaus PE, Blindauer KA, Labuda M, Pandolfo M, Koob MD, Ranum LP (1998) Incidence of dominant spinocerebellar and Friedreich triplet repeats among 361 ataxia families. *Neurology* 51: 1666-71
- Moseley ML, Schut LJ, Bird TD, Koob MD, Day JW, Ranum LP (2000) SCA8 CTG repeat: en masse contractions in sperm and intergenerational sequence changes may play a role in reduced penetrance. *Hum Mol Genet* 9: 2125-30
- Moseley ML, Zu T, Ikeda Y, Gao W, Mosemiller AK, Daughters RS, Chen G, Weatherspoon MR, Clark HB, Ebner TJ, Day JW, Ranum LP (2006) Bidirectional expression of CUG and CAG expansion

- transcripts and intranuclear polyglutamine inclusions in spinocerebellar ataxia type 8. *Nat Genet* 38: 758-69
- Mutsuddi M, Marshall CM, Benzow KA, Koob MD, Rebay I (2004) The spinocerebellar ataxia 8 noncoding RNA causes neurodegeneration and associates with staufen in *Drosophila*. *Curr Biol* 14: 302-8
- Mutsuddi M, Rebay I (2005) Molecular genetics of spinocerebellar ataxia type 8 (SCA8). *RNA Biol* 2: 49-52
- Nakamura K, Jeong SY, Uchihara T, Anno M, Nagashima K, Nagashima T, Ikeda S, Tsuji S, Kanazawa I (2001) SCA17, a novel autosomal dominant cerebellar ataxia caused by an expanded polyglutamine in TATA-binding protein. *Hum Mol Genet* 10: 1441-8
- Narang MA, Waring JD, Sabourin LA, Korneluk RG (2000) Myotonic dystrophy (DM) protein kinase levels in congenital and adult DM patients. *Eur J Hum Genet* 8: 507-12
- Nemes JP, Benzow KA, Moseley ML, Ranum LP, Koob MD (2000) The SCA8 transcript is an antisense RNA to a brain-specific transcript encoding a novel actin-binding protein (KLHL1). *Hum Mol Genet* 9: 1543-51
- Nordquist DT, Kozak CA, Orr HT (1988) cDNA cloning and characterization of three genes uniquely expressed in cerebellum by Purkinje neurons. *J Neurosci* 8: 4780-9
- O'Callaghan JP, Rogers TS, Rodman LE, Page JG (1996) Acute and chronic administration of ibogaine to the rat results in astrogliosis that is not confined to the cerebellar vermis. *Ann N Y Acad Sci* 801: 205-16
- O'Hearn E, Holmes SE, Calvert PC, Ross CA, Margolis RL (2001) SCA-12: Tremor with cerebellar and cortical atrophy is associated with a CAG repeat expansion. *Neurology* 56: 299-303

- Oberdick J, Levinthal F, Levinthal C (1988) A Purkinje cell differentiation marker shows a partial DNA sequence homology to the cellular sis/PDGF2 gene. *Neuron* 1: 367-76
- Oberdick J, Smeyne RJ, Mann JR, Zackson S, Morgan JI (1990) A promoter that drives transgene expression in cerebellar Purkinje and retinal bipolar neurons. *Science* 248: 223-6
- Oma Y, Kino Y, Sasagawa N, Ishiura S (2004) Intracellular localization of homopolymeric amino acid-containing proteins expressed in mammalian cells. *J Biol Chem* 279: 21217-22
- Ophoff RA, Terwindt GM, Vergouwe MN, van Eijk R, Oefner PJ, Hoffman SM, Lamerdin JE, Mohrenweiser HW, Bulman DE, Ferrari M, Haan J, Lindhout D, van Ommen GJ, Hofker MH, Ferrari MD, Frants RR (1996) Familial hemiplegic migraine and episodic ataxia type-2 are caused by mutations in the Ca²⁺ channel gene CACNL1A4. *Cell* 87: 543-52
- Orr HT, Chung MY, Banfi S, Kwiatkowski TJ, Jr., Servadio A, Beaudet AL, McCall AE, Duvick LA, Ranum LP, Zoghbi HY (1993) Expansion of an unstable trinucleotide CAG repeat in spinocerebellar ataxia type 1. *Nat Genet* 4: 221-6
- Orr MS, Reinhold W, Yu L, Schreiber-Agus N, O'Connor PM (1998) An important role for the retinoblastoma protein in staurosporine-induced G1 arrest in murine embryonic fibroblasts. *J Biol Chem* 273: 3803-7
- Otten AD, Tapscott SJ (1995) Triplet repeat expansion in myotonic dystrophy alters the adjacent chromatin structure. *Proc Natl Acad Sci USA* 92: 5465-9
- Palhan VB, Chen S, Peng GH, Tjernberg A, Gamper AM, Fan Y, Chait BT, La Spada AR, Roeder RG (2005) Polyglutamine-expanded ataxin-7

- inhibits STAGA histone acetyltransferase activity to produce retinal degeneration. *Proc Natl Acad Sci U S A* 102: 8472-7
- Paulson HL, Perez MK, Trottier Y, Trojanowski JQ, Subramony SH, Das SS, Vig P, Mandel JL, Fischbeck KH, Pittman RN (1997) Intranuclear inclusions of expanded polyglutamine protein in spinocerebellar ataxia type 3. *Neuron* 19: 333-44
- Pelletier J, Sonenberg N (1988) Internal initiation of translation of eukaryotic mRNA directed by a sequence derived from poliovirus RNA. *Nature* 334: 320-5
- Prescott EM, Proudfoot NJ (2002) Transcriptional collision between convergent genes in budding yeast. *Proc Natl Acad Sci USA* 99: 8796-801
- Price NE, Mumby MC (1999) Brain protein serine/threonine phosphatases. *Curr Opin Neurobiol* 9: 336-42
- Pulst SM, Nechiporuk A, Nechiporuk T, Gispert S, Chen XN, Lopes-Cendes I, Pearlman S, Starkman S, Orozco-Diaz G, Lunke A, DeJong P, Rouleau GA, Auburger G, Korenberg JR, Figueroa C, Sahba S (1996) Moderate expansion of a normally biallelic trinucleotide repeat in spinocerebellar ataxia type 2. *Nat Genet* 14: 269-76
- Ragothaman M, Sarangmath N, Chaudhary S, Khare V, Mittal U, Sharma S, Komatireddy S, Chakrabarti S, Mukerji M, Juyal RC, Thelma BK, Muthane UB (2004) Complex phenotypes in an Indian family with homozygous SCA2 mutations. *Ann Neurol* 55: 130-3
- Rasmussen A, Matsuura T, Ruano L, Yescas P, Ochoa A, Ashizawa T, Alonso E (2001) Clinical and genetic analysis of four Mexican families with spinocerebellar ataxia type 10. *Ann Neurol* 50: 234-9

- Reid SJ, Rees MI, van Roon-Mom WM, Jones AL, MacDonald ME, Sutherland G, During MJ, Faull RL, Owen MJ, Dragunow M, Snell RG (2003) Molecular investigation of TBP allele length: a SCA17 cellular model and population study. *Neurobiol Dis* 13: 37-45
- Reid SJ, van Roon-Mom WM, Wood PC, Rees MI, Owen MJ, Faull RL, Dragunow M, Snell RG (2004) TBP, a polyglutamine tract containing protein, accumulates in Alzheimer's disease. *Brain Res Mol Brain Res* 125: 120-8
- Robinson DN, Cooley L (1997) *Drosophila kelch* is an oligomeric ring canal actin organizer. *J Cell Biol* 138: 799-810
- Rogers JH, Resibois A (1992) Calretinin and calbindin-D28k in rat brain: patterns of partial co-localization. *Neuroscience* 51: 843-65
- Sasagawa N, Takahashi N, Suzuki K, Ishiura S (1999) An expanded CTG trinucleotide repeat causes trans RNA interference: a new hypothesis for the pathogenesis of myotonic dystrophy. *Biochem Biophys Res Commun* 264: 76-80
- Scherzinger E, Lurz R, Turmaine M, Mangiarini L, Hollenbach B, Hasenbank R, Bates GP, Davies SW, Lehrach H, Wanker EE (1997) Huntingtin-encoded polyglutamine expansions form amyloid-like protein aggregates in vitro and in vivo. *Cell* 90: 549-58
- Seng S, Avraham HK, Jiang S, Venkatesh S, Avraham S (2006) KLHL1/MRP2 mediates neurite outgrowth in a glycogen synthase kinase 3beta-dependent manner. *Mol Cell Biol* 26: 8371-84
- Serot JM, Christmann D, Dubost T, Couturier M (1997) Cerebrospinal fluid transthyretin: aging and late onset Alzheimer's disease. *J Neurol Neurosurg Psychiatry* 63: 506-8

- Shan DE, Soong BW, Sun CM, Lee SJ, Liao KK, Liu RS (2001) Spinocerebellar ataxia type 2 presenting as familial levodopa-responsive parkinsonism. *Ann Neurol* 50: 812-5
- Shaw G, Morse S, Ararat M, Graham FL (2002) Preferential transformation of human neuronal cells by human adenoviruses and the origin of HEK 293 cells. *Faseb J* 16: 869-71
- Sherrill KW, Byrd MP, Van Eden ME, Lloyd RE (2004) BCL-2 translation is mediated via internal ribosome entry during cell stress. *J Biol Chem* 279: 29066-74
- Silveira I, Alonso I, Guimaraes L, Mendonca P, Santos C, Maciel P, Fidalgo De Matos JM, Costa M, Barbot C, Tuna A, Barros J, Jardim L, Coutinho P, Sequeiros J (2000) High germinal instability of the (CTG)_n at the SCA8 locus of both expanded and normal alleles. *Am J Hum Genet* 66: 830-40
- Silveira I, Miranda C, Guimaraes L, Moreira MC, Alonso I, Mendonca P, Ferro A, Pinto-Basto J, Coelho J, Ferreirinha F, Poirier J, Parreira E, Vale J, Januario C, Barbot C, Tuna A, Barros J, Koide R, Tsuji S, Holmes SE, Margolis RL, Jardim L, Pandolfo M, Coutinho P, Sequeiros J (2002) Trinucleotide repeats in 202 families with ataxia: a small expanded (CAG)_n allele at the SCA17 locus. *Arch Neurol* 59: 623-9
- Skinner PJ, Koshy BT, Cummings CJ, Klement IA, Helin K, Servadio A, Zoghbi HY, Orr HT (1997) Ataxin-1 with an expanded glutamine tract alters nuclear matrix-associated structures. *Nature* 389: 971-4
- Sobrido MJ, Cholfin JA, Perlman S, Pulst SM, Geschwind DH (2001) SCA8 repeat expansions in ataxia: a controversial association. *Neurology* 57: 1310-2

- Sonenberg N (1994) Regulation of translation and cell growth by eIF-4E. *Biochimie* 76: 839-46
- Soong BW, Lu YC, Choo KB, Lee HY (2001) Frequency analysis of autosomal dominant cerebellar ataxias in Taiwanese patients and clinical and molecular characterization of spinocerebellar ataxia type 6. *Arch Neurol* 58: 1105-9
- Srivastava AK, Choudhry S, Gopinath MS, Roy S, Tripathi M, Brahmachari SK, Jain S (2001) Molecular and clinical correlation in five Indian families with spinocerebellar ataxia 12. *Ann Neurol* 50: 796-800
- Stevanin G, Fujigasaki H, Lebre AS, Camuzat A, Jeannequin C, Dode C, Takahashi J, San C, Bellance R, Brice A, Durr A (2003) Huntington's disease-like phenotype due to trinucleotide repeat expansions in the TBP and JPH3 genes. *Brain* 126: 1599-603
- Stevanin G, Hahn V, Lohmann E, Bouslam N, Gouttard M, Soumphonphakdy C, Welter ML, Ollagnon-Roman E, Lemainque A, Ruberg M, Brice A, Durr A (2004) Mutation in the catalytic domain of protein kinase C gamma and extension of the phenotype associated with spinocerebellar ataxia type 14. *Arch Neurol* 61: 1242-8
- Stevanin G, Herman A, Durr A, Jodice C, Frontali M, Agid Y, Brice A (2000) Are (CTG)_n expansions at the SCA8 locus rare polymorphisms? *Nat Genet* 24: 213; author reply 215
- Stoneley M, Willis AE (2004) Cellular internal ribosome entry segments: structures, trans-acting factors and regulation of gene expression. *Oncogene* 23: 3200-7
- Takano H, Cancel G, Ikeuchi T, Lorenzetti D, Mawad R, Stevanin G, Didierjean O, Durr A, Oyake M, Shimohata T, Sasaki R, Koide R, Igarashi S, Hayashi S, Takiyama Y, Nishizawa M, Tanaka H, Zoghbi

- H, Brice A, Tsuji S (1998) Close associations between prevalences of dominantly inherited spinocerebellar ataxias with CAG-repeat expansions and frequencies of large normal CAG alleles in Japanese and Caucasian populations. *Am J Hum Genet* 63: 1060-6
- Taneja KL, McCurrach M, Schalling M, Housman D, Singer RH (1995) Foci of trinucleotide repeat transcripts in nuclei of myotonic dystrophy cells and tissues. *J Cell Biol* 128:995-1002
- Tang B, Liu C, Shen L, Dai H, Pan Q, Jing L, Ouyang S, Xia J (2000) Frequency of SCA1, SCA2, SCA3/MJD, SCA6, SCA7, and DRPLA CAG trinucleotide repeat expansion in patients with hereditary spinocerebellar ataxia from Chinese kindreds. *Arch Neurol* 57: 540-4
- Tazon B, Badenas C, Jimenez L, Munoz E, Mila M (2002) SCA8 in the Spanish population including one homozygous patient. *Clin Genet* 62: 404-9
- Toru S, Murakoshi T, Ishikawa K, Saegusa H, Fujigasaki H, Uchihara T, Nagayama S, Osanai M, Mizusawa H, Tanabe T (2000) Spinocerebellar ataxia type 6 mutation alters P-type calcium channel function. *J Biol Chem* 275: 10893-8
- Tufarelli C, Stanley JA, Garrick D, Sharpe JA, Ayyub H, Wood WG, Higgs DR (2003) Transcription of antisense RNA leading to gene silencing and methylation as a novel cause of human genetic disease. *Nat Genet* 34: 157-65
- Uchihara T, Duyckaerts C, Iwabuchi K, Iwata M, Yagishita S, Hauw JJ (2004) Was the ataxia of Pierre Marie Machado-Joseph disease?: A reappraisal based on the last autopsy case from la Salpetriere Hospital. *Arch Neurol* 61: 784-90

- van Dellen A, Deacon R, York D, Blakemore C, Hannan AJ (2001) Anterior cingulate cortical transplantation in transgenic Huntington's disease mice. *Brain Res Bull* 56: 313-8
- van de Warrenburg BP, Verbeek DS, Piersma SJ, Hennekam FA, Pearson PL, Knoers NV, Kremer HP, Sinke RJ (2003) Identification of a novel SCA14 mutation in a Dutch autosomal dominant cerebellar ataxia family. *Neurology* 61: 1760-5
- Vandaele S, Nordquist DT, Feddersen RM, Tretjakoff I, Peterson AC, Orr HT (1991) Purkinje cell protein-2 regulatory regions and transgene expression in cerebellar compartments. *Genes Dev* 5: 1136-48
- Vig PJ, Fratkin JD, Desai D, Currier RD, Subramony SH (1996) Decreased parvalbumin immunoreactivity in surviving Purkinje cells of patients with spinocerebellar ataxia-1. *Neurology* 47: 249-53
- Vig PJ, Subramony SH, Burright EN, Fratkin JD, McDaniel DO, Desai D, Qin Z (1998) Reduced immunoreactivity to calcium-binding proteins in Purkinje cells precedes onset of ataxia in spinocerebellar ataxia-1 transgenic mice. *Neurology* 50: 106-13
- Vig PJ, Subramony SH, Qin Z, McDaniel DO, Fratkin JD (2000) Relationship between ataxin-1 nuclear inclusions and Purkinje cell specific proteins in SCA-1 transgenic mice. *J Neurol Sci* 174: 100-10
- Vincent JB, Yuan QP, Schalling M, Adolfsson R, Azevedo MH, Macedo A, Bauer A, DallaTorre C, Medeiros HM, Pato MT, Pato CN, Bowen T, Guy CA, Owen MJ, O'Donovan MC, Paterson AD, Petronis A, Kennedy JL (2000) Long repeat tracts at SCA8 in major psychosis. *Am J Med Genet* 96: 873-6
- Virshup DM (2000) Protein phosphatase 2A: a panoply of enzymes. *Curr Opin Cell Biol* 12: 180-5

- Werner A, Berdal A (2005) Natural antisense transcripts: sound or silence? *Physiol Genomics* 23: 125-31
- Worth PF, Houlden H, Giunti P, Davis MB, Wood NW (2000) Large, expanded repeats in SCA8 are not confined to patients with cerebellar ataxia. *Nat Genet* 24: 214-5
- Wutz A, Smrzka OW, Schweifer N, Schellander K, Wagner EF, Barlow DP (1997) Imprinted expression of the *Igf2r* gene depends on an intronic CpG island. *Nature* 389: 745-9
- Xu Z, Chang LW, Slikker W, Jr., Ali SF, Rountree RL, Scallet AC (2000) A dose-response study of ibogaine-induced neuropathology in the rat cerebellum. *Toxicol Sci* 57: 95-101
- Xue F, Cooley L (1993) *kelch* encodes a component of intercellular bridges in *Drosophila* egg chambers. *Cell* 72: 681-93
- Yabe I, Sasaki H, Chen DH, Raskind WH, Bird TD, Yamashita I, Tsuji S, Kikuchi S, Tashiro K (2003) Spinocerebellar ataxia type 14 caused by a mutation in protein kinase C gamma. *Arch Neurol* 60: 1749-51
- Yang Q, Hashizume Y, Yoshida M, Wang Y, Goto Y, Mitsuma N, Ishikawa K, Mizusawa H (2000) Morphological Purkinje cell changes in spinocerebellar ataxia type 6. *Acta Neuropathol (Berl)* 100: 371-6
- Zhuchenko O, Bailey J, Bonnen P, Ashizawa T, Stockton DW, Amos C, Dobyns WB, Subramony SH, Zoghbi HY, Lee CC (1997) Autosomal dominant cerebellar ataxia (SCA6) associated with small polyglutamine expansions in the alpha 1A-voltage-dependent calcium channel. *Nat Genet* 15: 62-9
- Zuhlke C, Gehlken U, Hellenbroich Y, Schwinger E, Burk K (2003) Phenotypical variability of expanded alleles in the TATA-binding protein gene. Reduced penetrance in SCA17? *J Neurol* 250: 161-3

Zuhlke C, Hellenbroich Y, Dalski A, Kononowa N, Hagenah J, Vieregge P, Riess O, Klein C, Schwinger E (2001) Different types of repeat expansion in the TATA-binding protein gene are associated with a new form of inherited ataxia. *Eur J Hum Genet* 9: 160-4

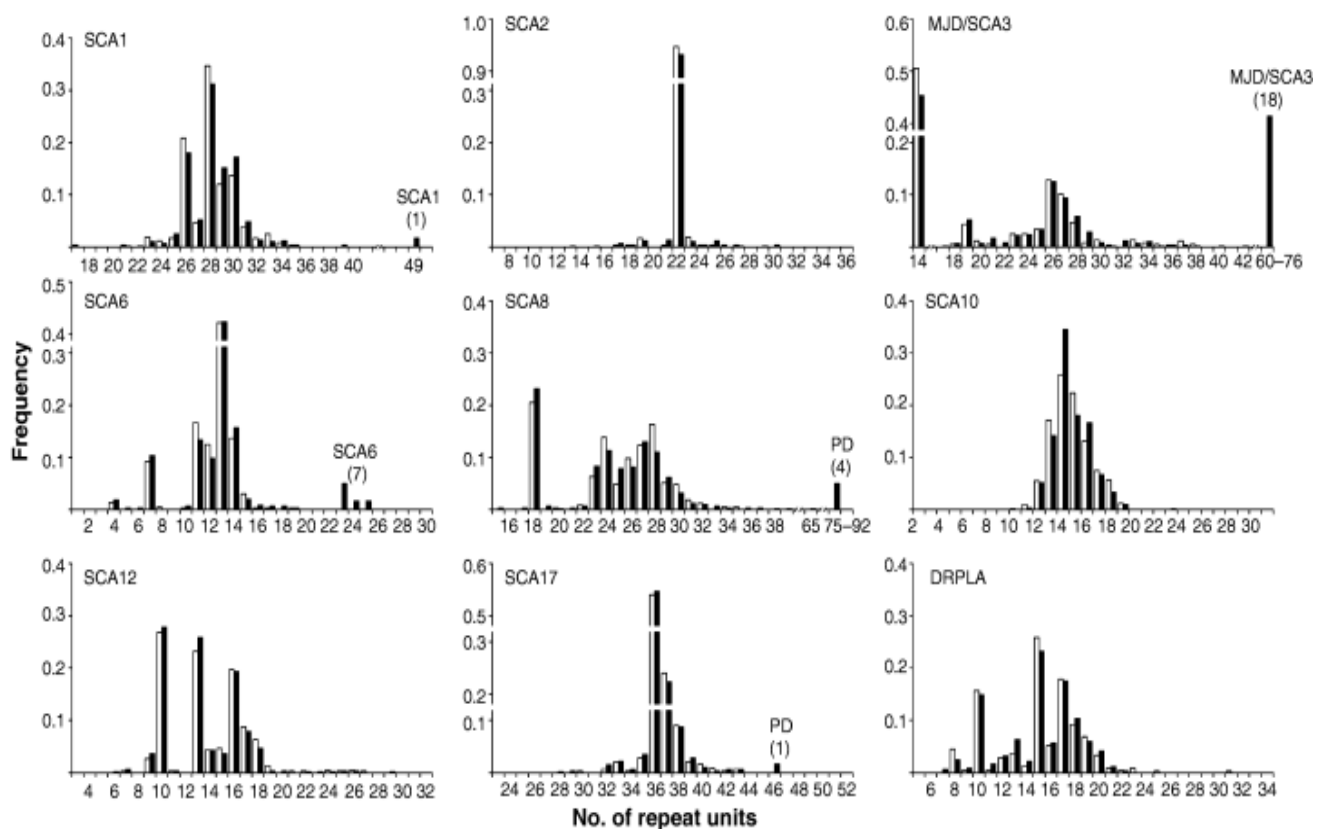


Figure 1. Frequency distribution of (CAG/CTG/ATTCT)-repeat lengths in patients with ataxia and Parkinson's disease (■) and controls (□) at the nine SCA loci examined. The expanded alleles in SCA1, MJD/SCA3, SCA6, SCA8, and SCA17 are indicated in the enlarged closed bars with number indicated below in parenthesis.

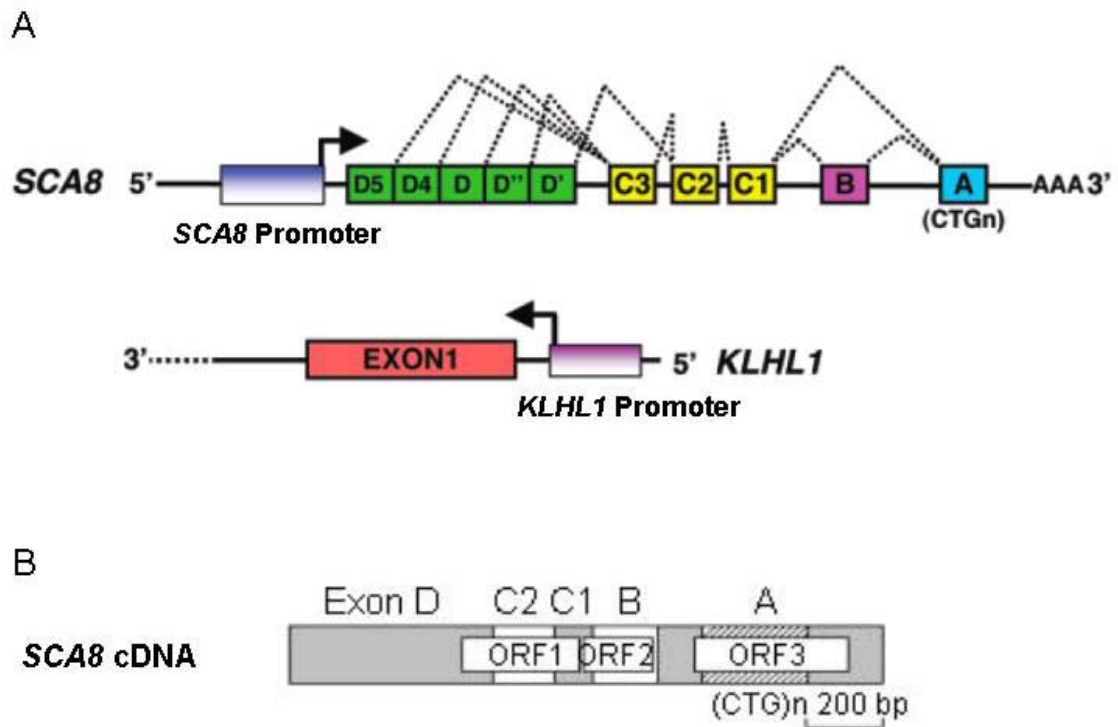


Figure 2. (A) *SCA8* genomic organization and its relation to *KLHL1*. (Adapted from Mutsuddi and Rebay 2005) (B) The *SCA8* cDNA contains exons D, C2, C1, B, and A. The three putative ORFs are indicated by the open boxes inside the cDNA. The combined repeats (CTG)_n inside ORF3 are represented by striped box.

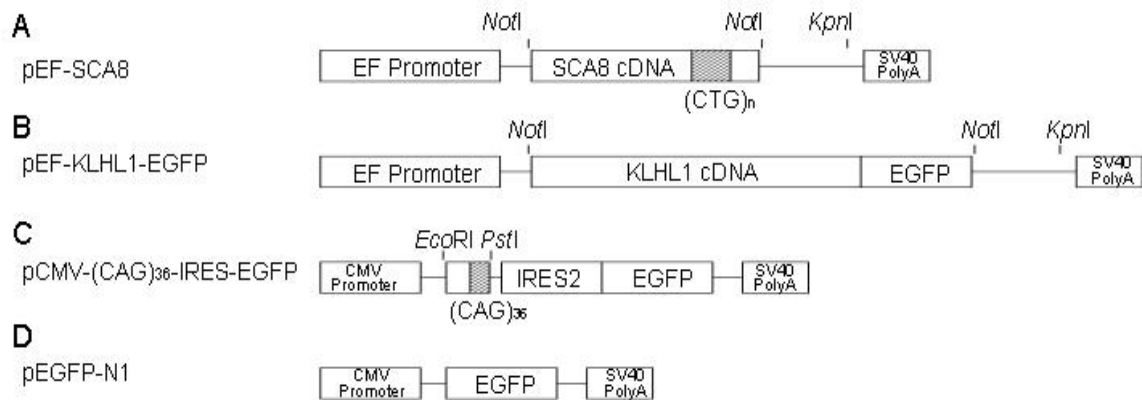


Figure 3. Schematic diagrams of pEF-SCA8 (A), pEF-KLHL1-EGFP (B), pCMV-(CAG)₃₆-IRES-EGFP (C) and pEGFP-N1 (D) constructs. pEF-SCA8: SCA8 alleles of 0, 23, 88 and 157 CTA/CTG repeats were placed in the *NotI* site of the pEF-IRES/hrGFP vector in which the *KpnI* fragment containing IRES/hrGFP gene was removed. pEF-KLHL1-EGFP: the in-framed KLHL1-EGFP fusion gene was inserted into the *NotI* site of the modified pEF vector. pCMV-(CAG)₃₆-IRES-EGFP: the 5' region of *TBP* cDNA was placed between the *EcoRI* and *PstI* sites of the pIRES2-EGFP vector. pEGFP-N1 from Clontech was used as a negative control to show the specificity of SCA8 *trans* RNA interference.

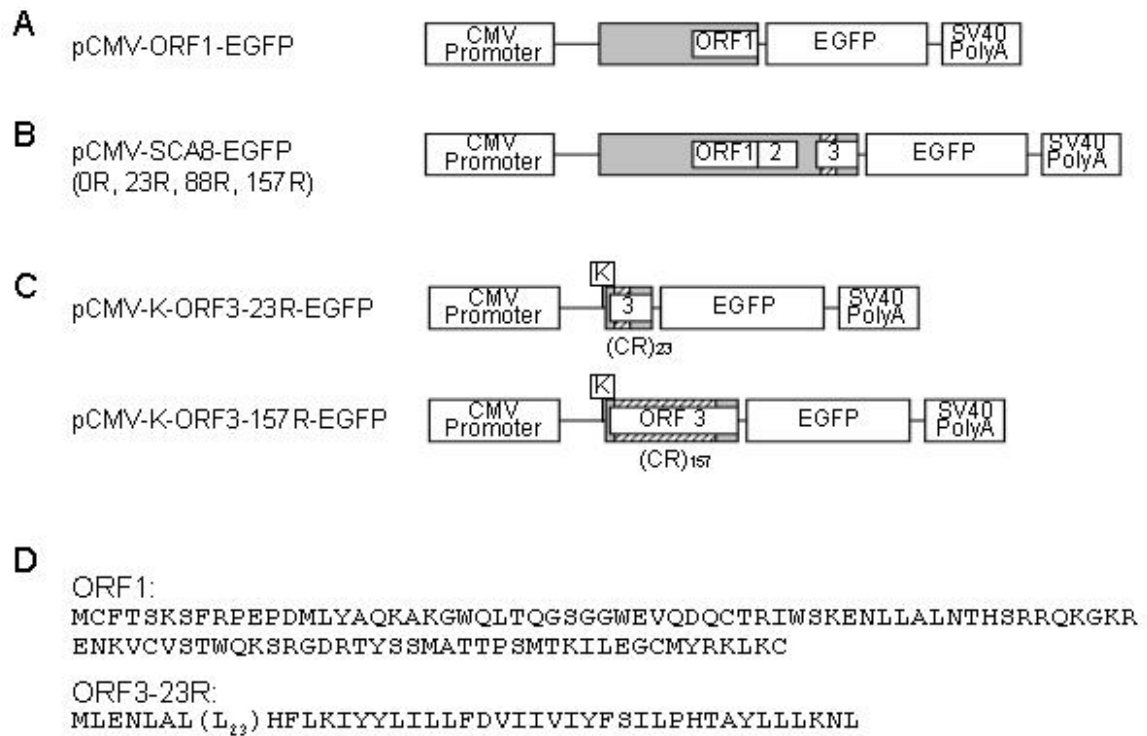


Figure 4. Schematic diagrams of pCMV-ORF1-EGFP (**A**), pCMV-SCA8-EGFP (**B**), pCMV-K-ORF3-23R-EGFP and pCMV-K-ORF3-157R-EGFP (**C**) constructs. K: Kozak consensus sequence. (**D**) Predicted amino acid sequences of the SCA8 ORF1 and ORF3-23R.

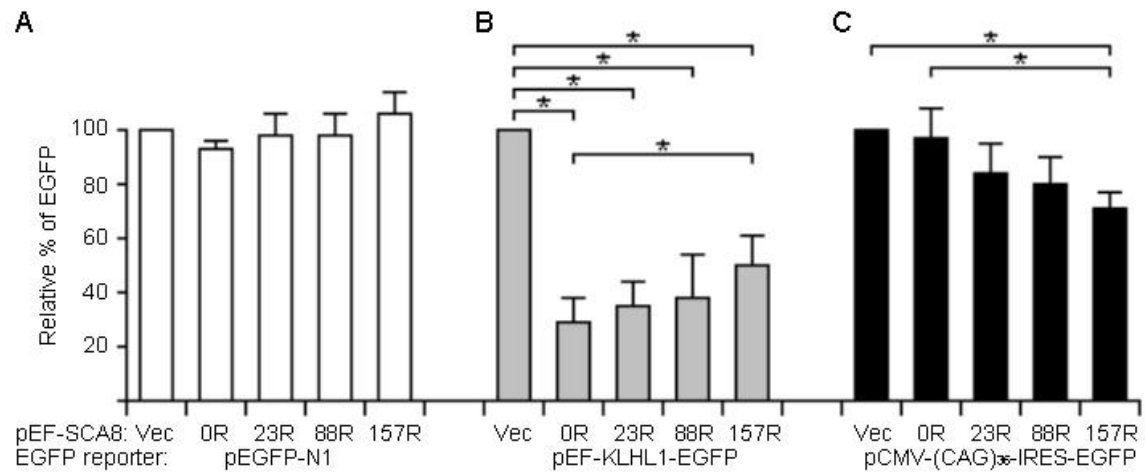


Figure 5. Regulation of the *KLHL1* and CAG repeat-containing transcript expression by *SCA8*. Co-transfection of pEGFP-N1 (A), pEF-KLHL1-EGFP (B), pCMV-(CAG)₃₆-IRES-EGFP (C) and pEF-SCA8-0R, -23R, -88R, -157R constructs in HEK293 cells. The amounts of EGFP expressed were analyzed by FACS analysis 48 hr after transfection. Levels of EGFP were expressed as percentages of EGFP reporter, which was set at 100%. Each value is the mean ± SD of three independent experiments each performed in duplicate. An asterisk (*) depicts significant difference ($P < 0.05$) between comparisons.

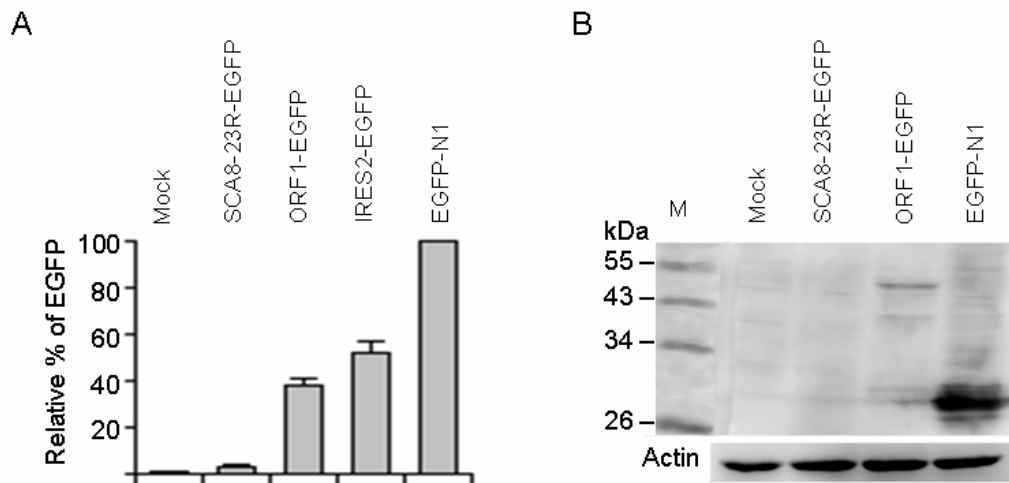


Figure 6. (A) Transient expression of pEGFP-N1 vector and pCMV-ORF1-EGFP, pCMV-SCA8-EGFP-23R-EGFP and pIRES2-EGFP constructs in HEK293 cells. Levels of EGFP were expressed as percentages of the control vector, which was set at 100%. Each value is the mean \pm SD of three independent experiments each performed in duplicate. (B) Western blot analysis of HEK293 cells transiently transfected with pEGFP-N1 vector and pCMV-ORF1-EGFP, pCMV-SCA8-EGFP-23R-EGFP constructs using GFP (top) and β -actin (bottom) antibodies.

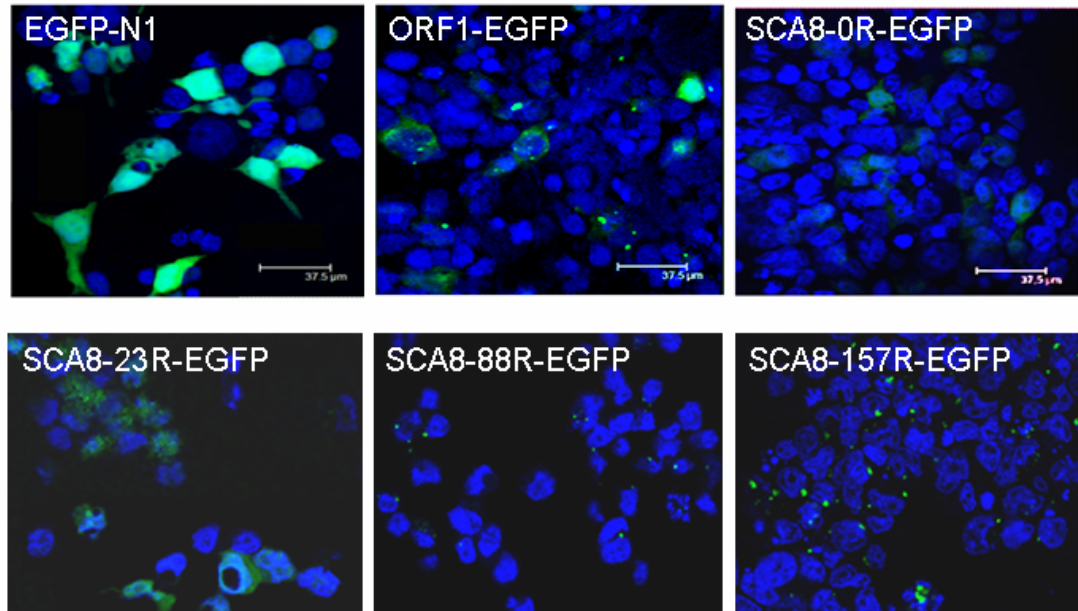


Figure 7. Distributions of SCA8-ORF1 and ORF3 protein. Confocal microscopy examination of cells expressing GFP-tagged ORF1 and ORF3 carrying 0, 23, 88, or 157 combined repeats or EGFP-N1 vector (green). Nuclei were counterstained with DAPI (blue). (The scale bar = 37.5 μm)

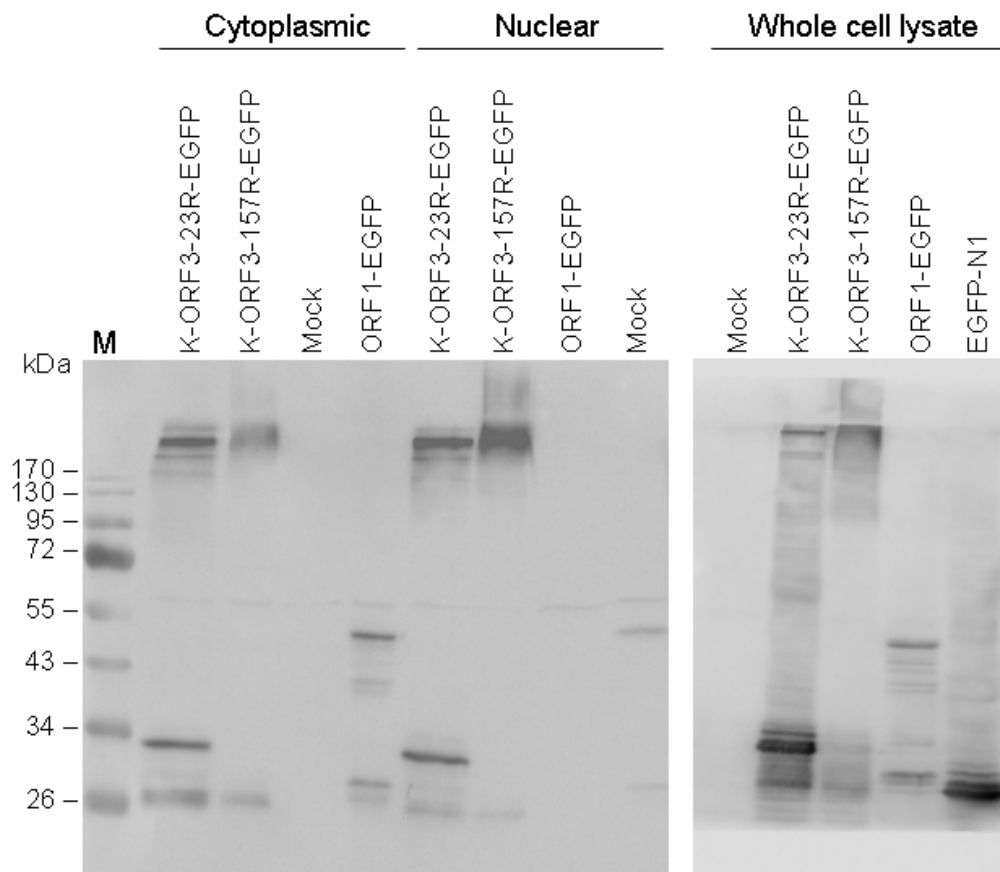


Figure 8. Subcellular localization of SCA8 ORF1-EGFP and ORF3-EGFP proteins. HEK293 cells were transfected with indicated plasmids. Whole cell lysates, cytoplasmic and nuclear extracts were prepared. Total proteins were analyzed by Western blotting using GFP antibody.

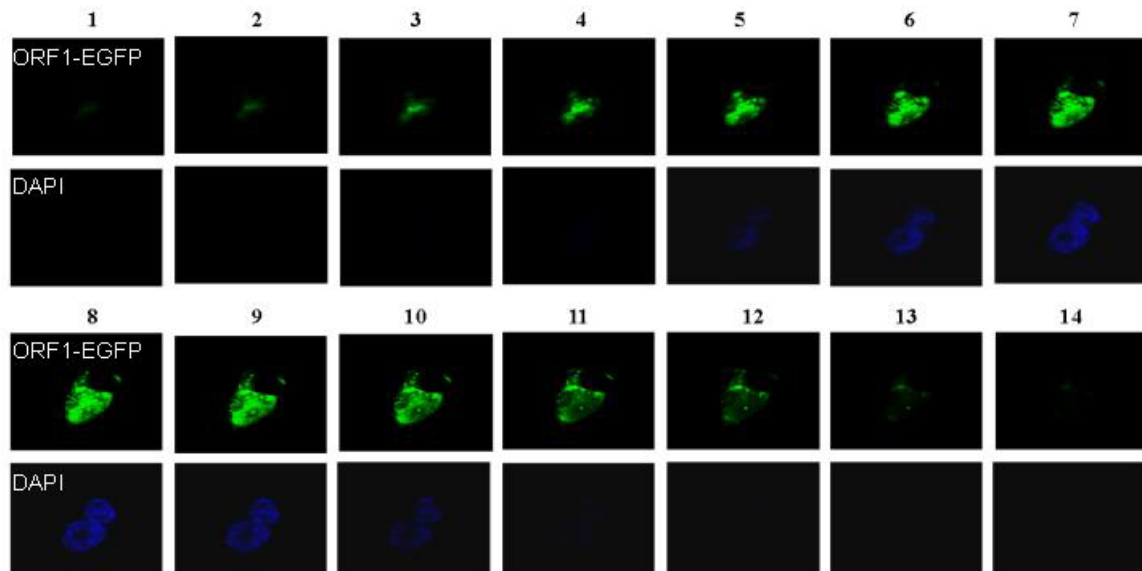


Figure 9. Observation of ORF1-EGFP distribution form continuous focal planes. The scanning was performed from apical to bottom end (plane number 1 to 14) of two transfected cells. Each plane represents an individual 2 μ m thick section. Nuclei were counterstained with DAPI (blue).

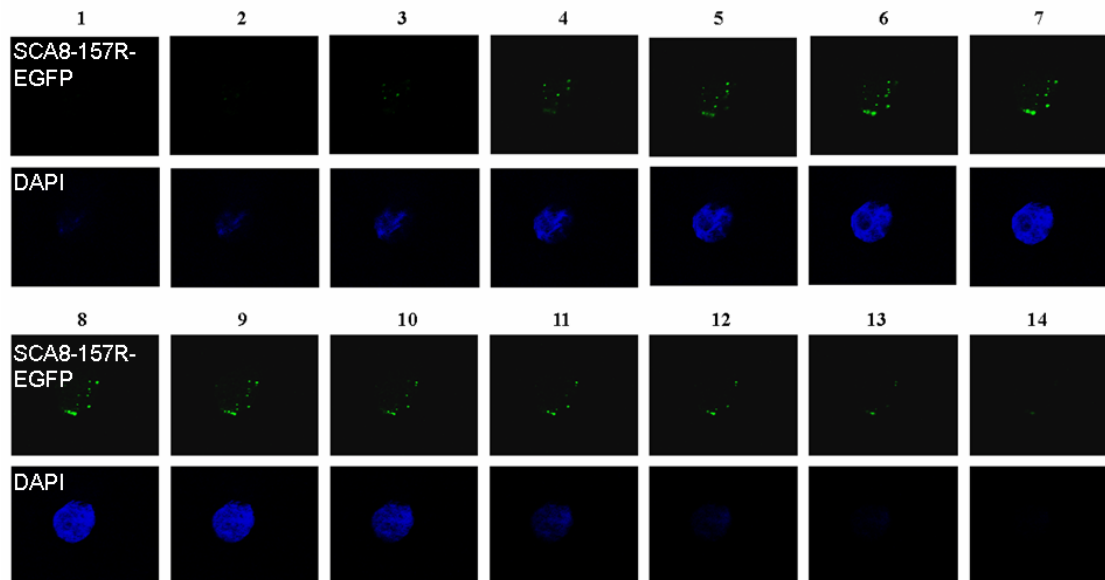


Figure 10. Observation of SCA8-157R-EGFP distribution form continuous focal planes. The scanning was performed from apical to bottom end (plane number 1 to 14) of a transfected cell. Each plane represents an individual 2 μm thick section. Nuclei were counterstained with DAPI (blue).

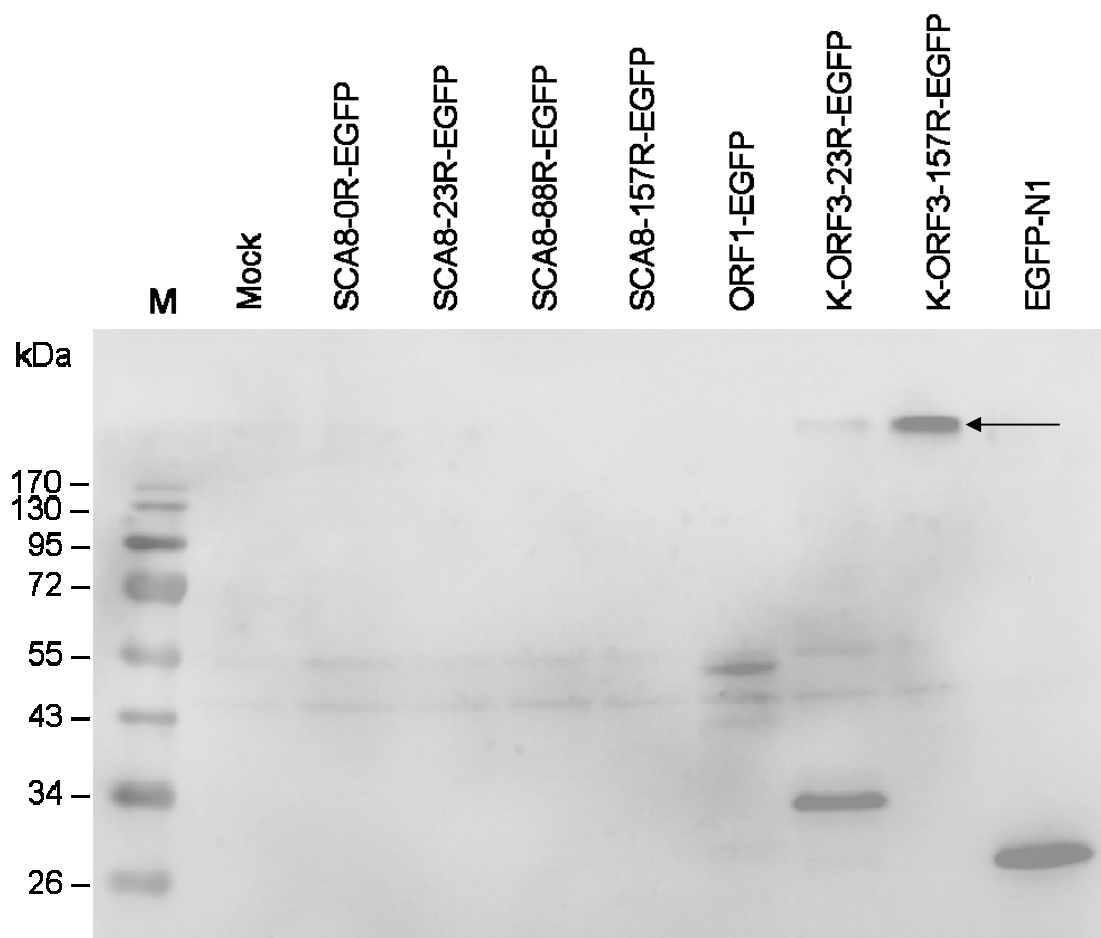


Figure 11. Western blot analysis of IMR-32 cells transiently transfected with various pCMV-SCA8-EGFP constructs, pCMV-ORF1-EGFP, pCMV-K-ORF3-EGFP, or pEGFP-N1 vector using GFP antibodies. The arrow indicates that insoluble proteins stall at the boundary of separatin gel.

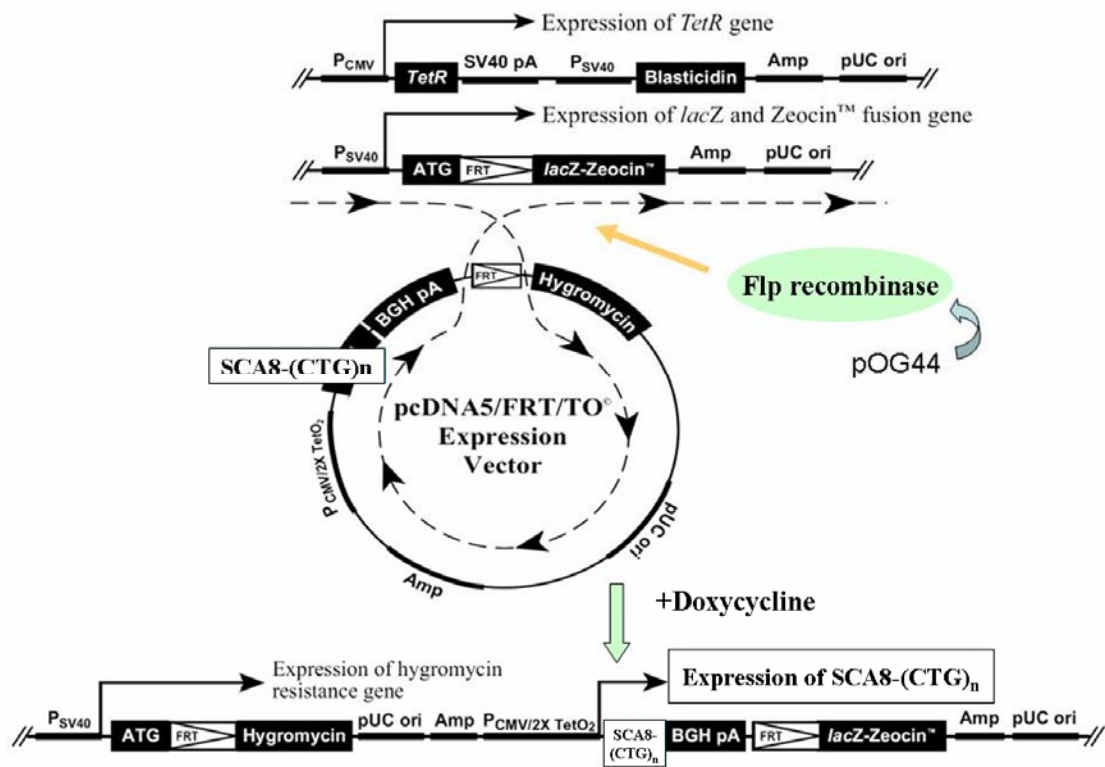


Figure 12. Diagram of Flp-In system. (Modified from the manual of Flp-In system, Invitrogen)

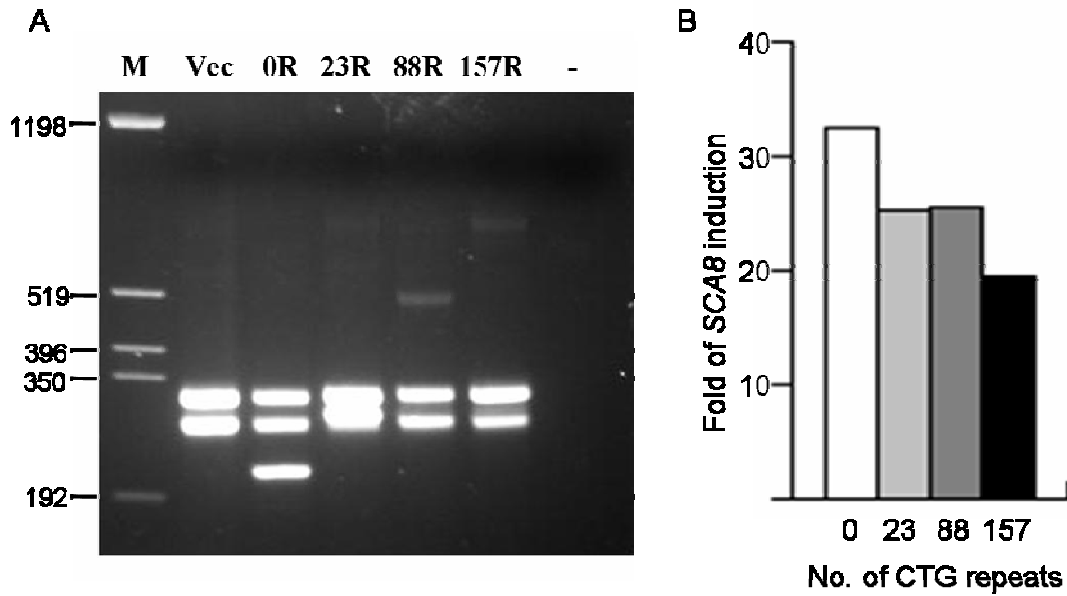


Figure 13. Characterization of isogenic and inducible *SCA8* cell lines. **(A)** Genotyping of these cell lines by PCR amplification for the region spanning CTA/CTG combined repeats. (-, negative control) **(B)** Expression levels of *SCA8* mRNA relative to 18s rRNA by real-time PCR assays. The results are shown with mean for duplicate determinations.

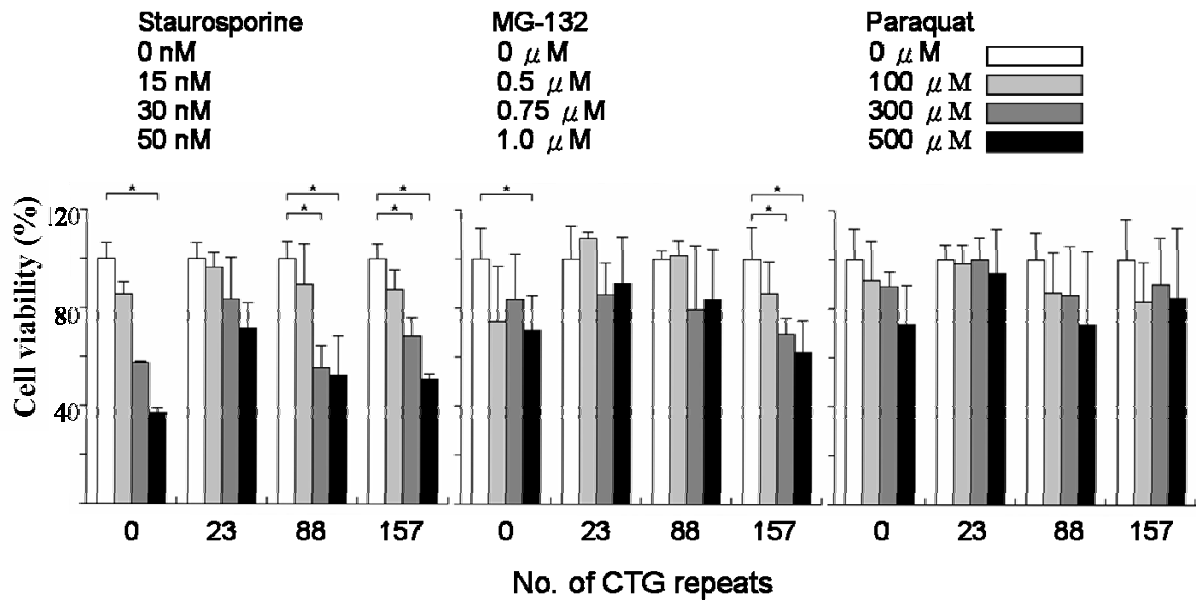


Figure 14. The effects of staurosporin, MG-132, and paraquat on the survival of SCA8-0, 23, 88, and 157R containing cells grown without doxycycline. The * indicates the difference between the indicated samples are statistically significant ($p < 0.05$).

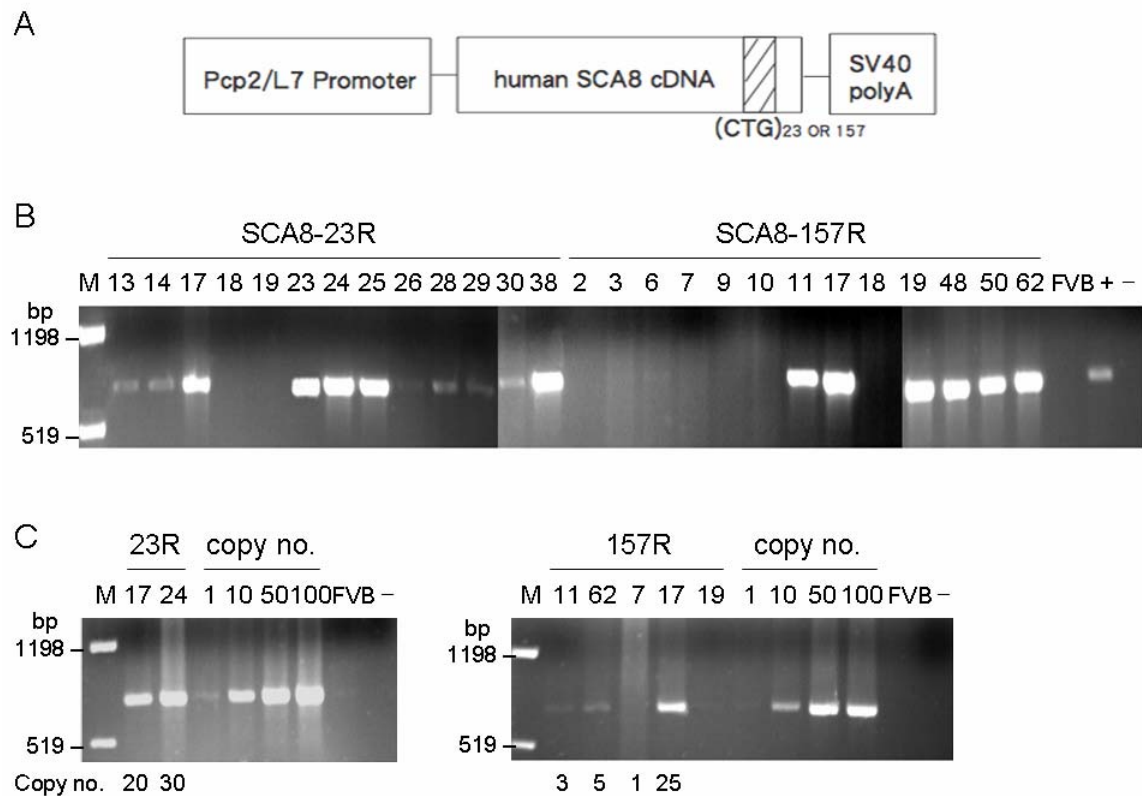


Figure 15. (A) Transgene constructs. The human *SCA8* cDNA carrying either 23 or 157 CTG trinucleotide repeats was placed downstream to the *Pcp2/L7* promoter. (B) Genotyping of *SCA8-23R* and *SCA8-157R* transgenic mice. (C) The transgene copy numbers were estimated by comparing to the PCR products intensity of standards of 1, 10, 50, and 100 copies. (+, positive control; -, negative control)

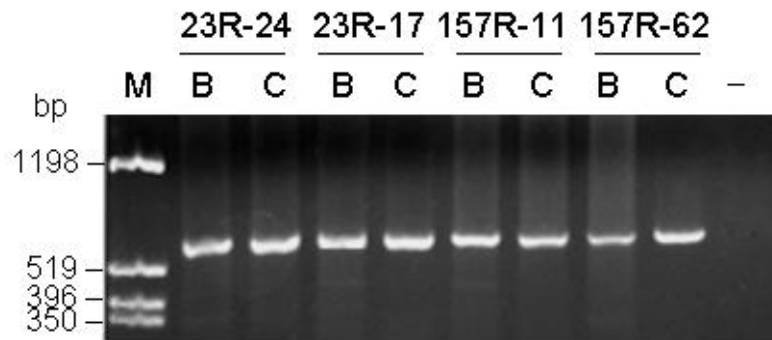


Figure 16. Estimation of the expression of *SCA8* transgene by RT-PCR. C, the cerebellum; B, brain regions other than the cerebellum; -, negative control.

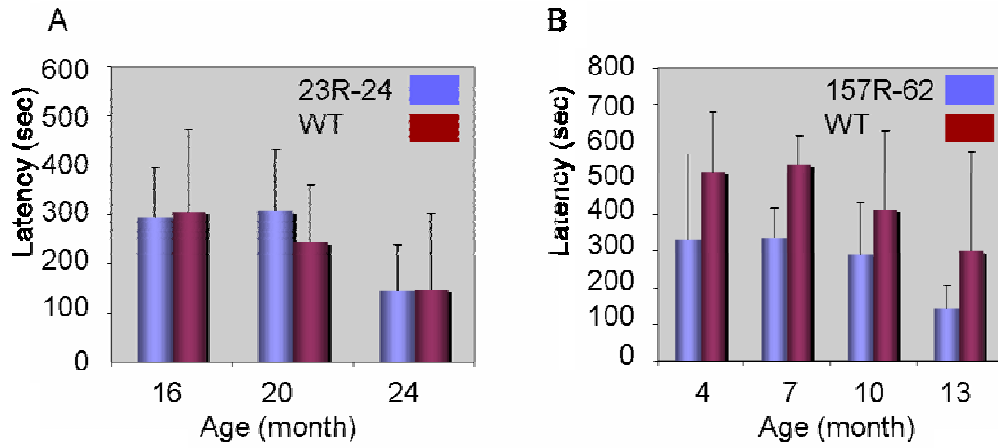


Figure 17. Rotarod performance of SCA8 transgenic mice. At the early life, there were no significant differences in latencies between SCA8 transgenic and wild type (WT) control littermates.

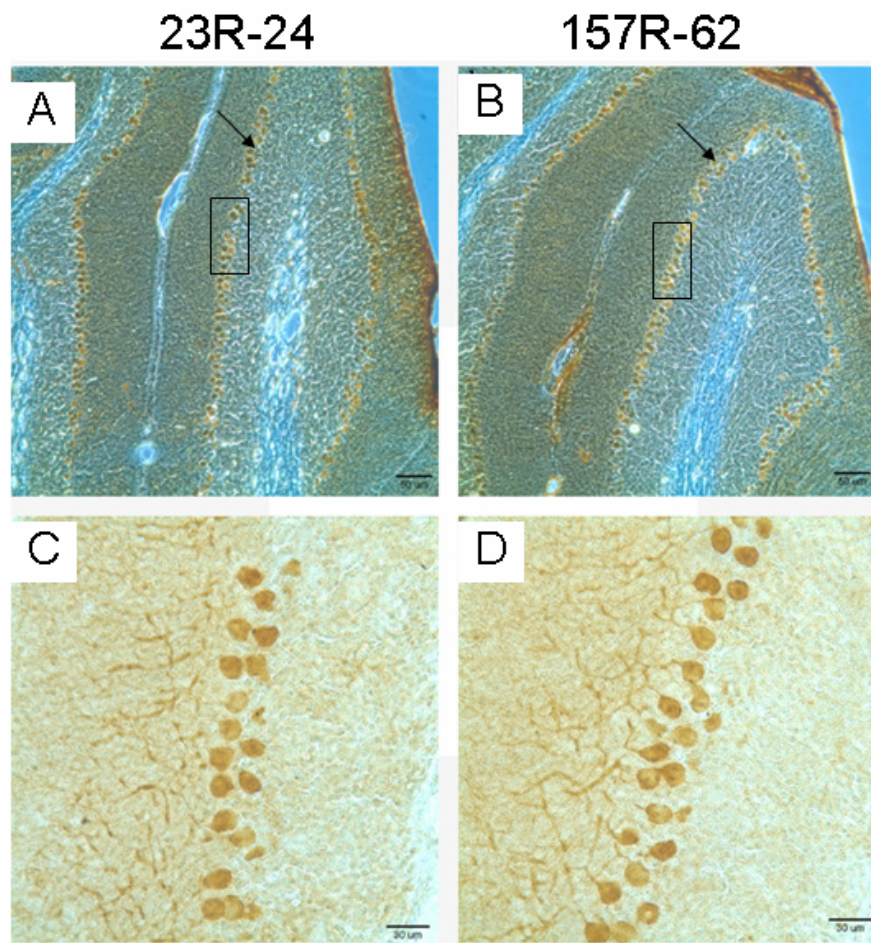


Figure 18. Immunohistochemical analyses of the SCA8 transgenic mouse cerebella. The brown staining of line 23R-24 (**A**) and 157R-62 (**B**) with arrowheads showing the calbindin-immunoreactivity of Purkinje cells. (**C**) and (**D**) are higher magnification of the framed areas of (**A**) and (**B**). (**A** and **B**, bar=50 μm; **C** and **D**, bar=30 μm)



Figure 19. The clasp phenotype of SCA8 transgenic mouse. **(A)** SCA8-157R mouse (left) exhibited a paw clasping phenotype when suspended by the tail. A nontransgenic control is shown in the right. **(B)** This phenotype is similar to that observed in the HD R6/2 mice. (Adapted from Mangiarini et al. 1995)

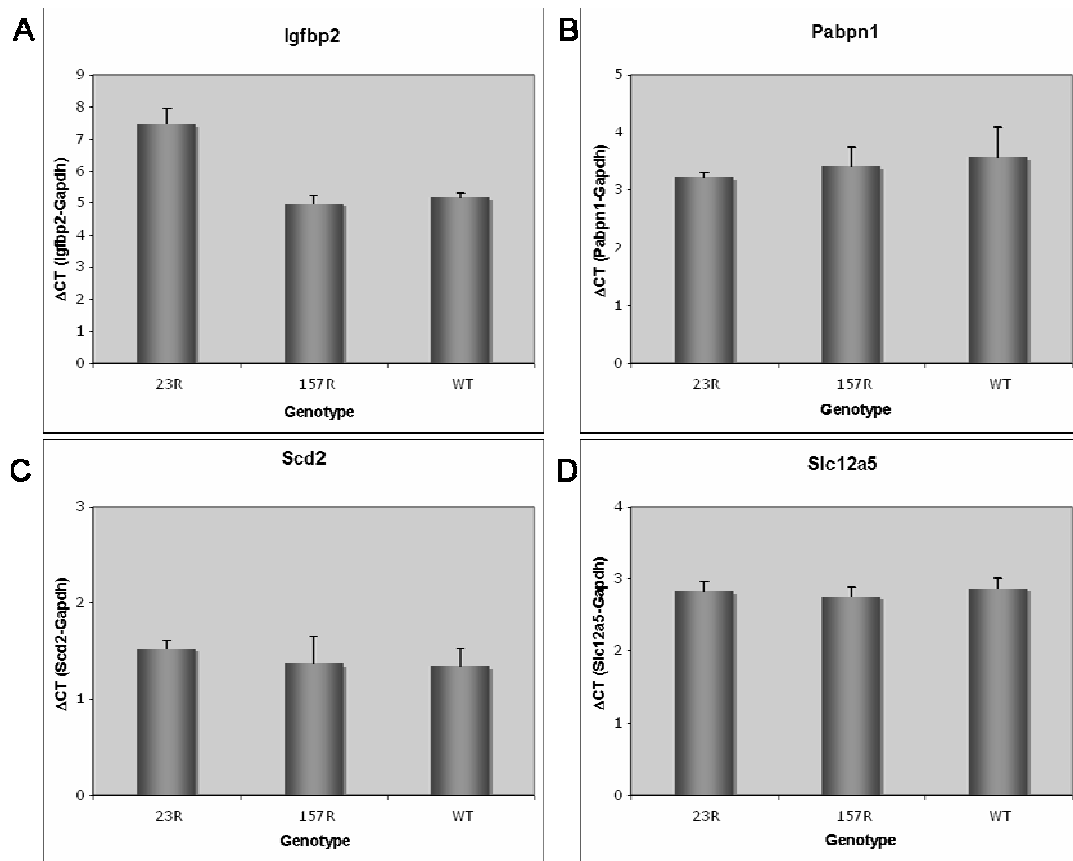


Figure 20. Real-time RT-PCR analyses of cerebella from SCA8 transgenic mice and wild type littermates. (A), (B), (C), and (D) Expression of Igfbp2, Pabpn1, Scd2, and Slc12a5 mRNA relative to Gapdh mRNA, respectively.

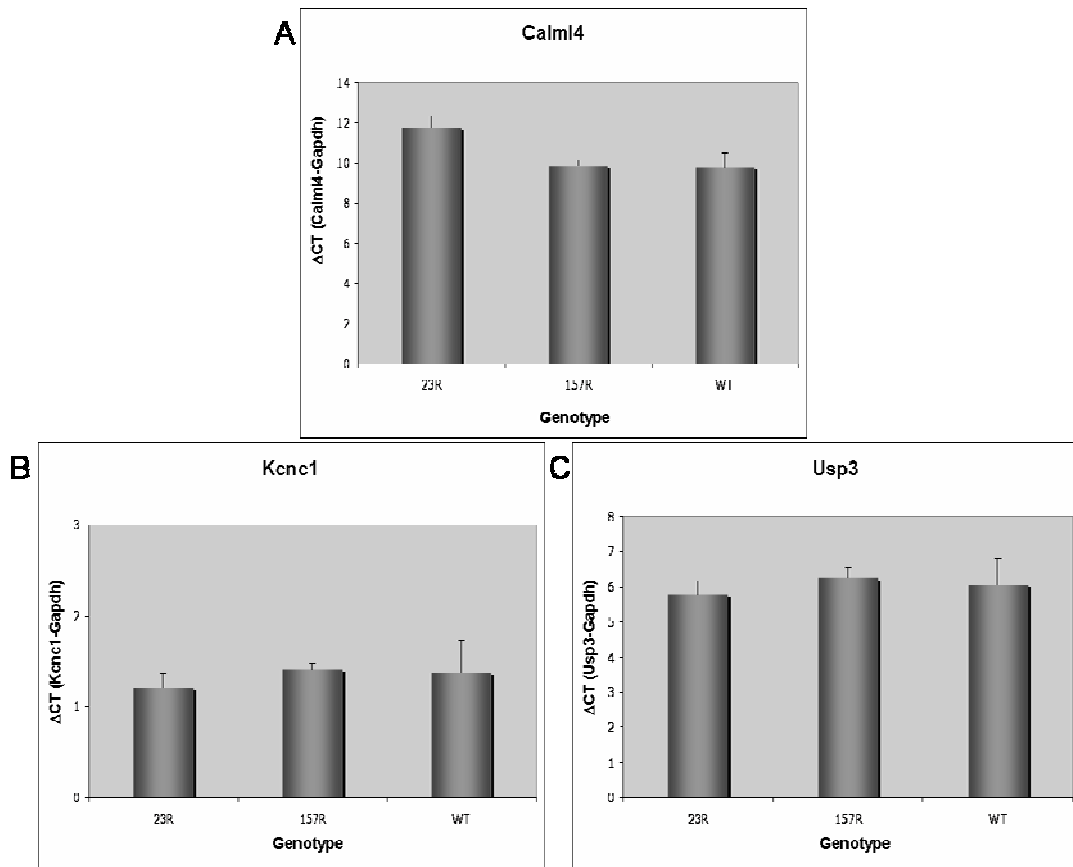


Figure 21. Real-time RT-PCR analyses of cerebella from SCA8 transgenic mice and wild type littermates. (A), (B), and (C) Expression of Calml4, Kcnc1, and Usp3 mRNA relative to Gapdh mRNA, respectively.

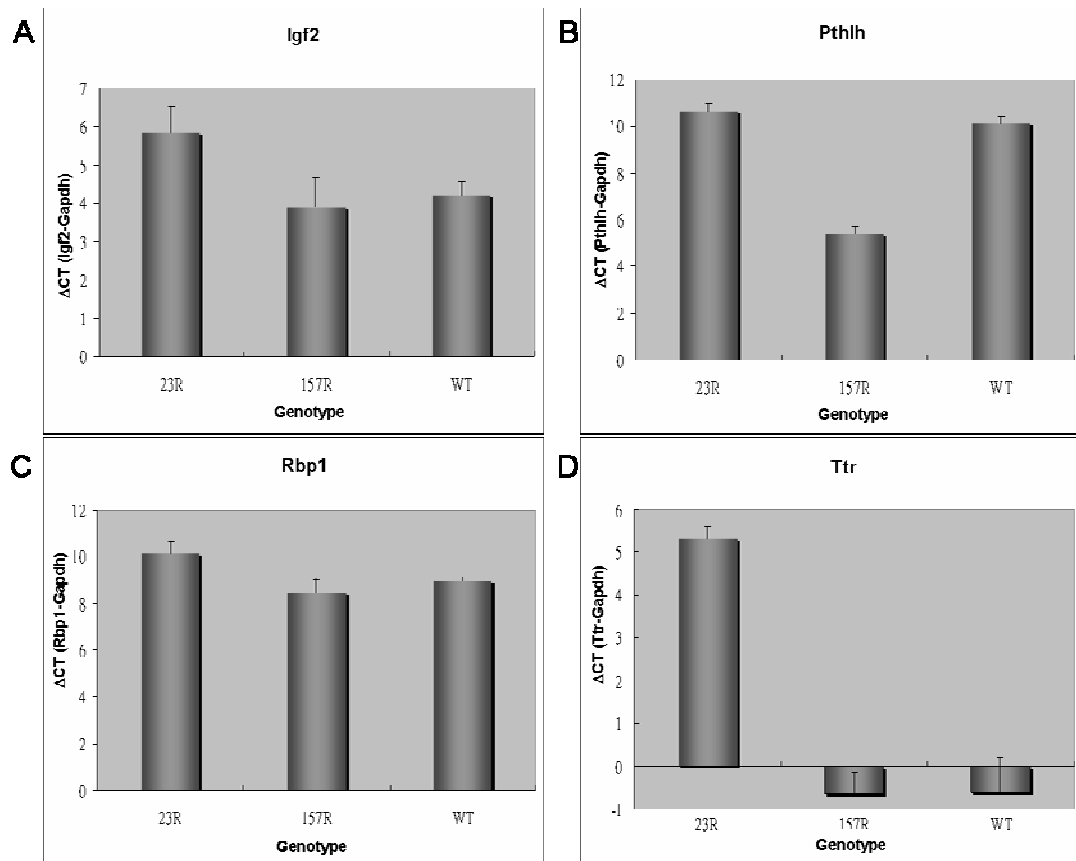


Figure 22. Real-time RT-PCR analyses of cerebella from SCA8 transgenic mice and wild type littermates. (A), (B), (C), and (D) Expression of Igf2, Pthlh, Rbp1, and Ttr mRNA relative to Gapdh mRNA, respectively.

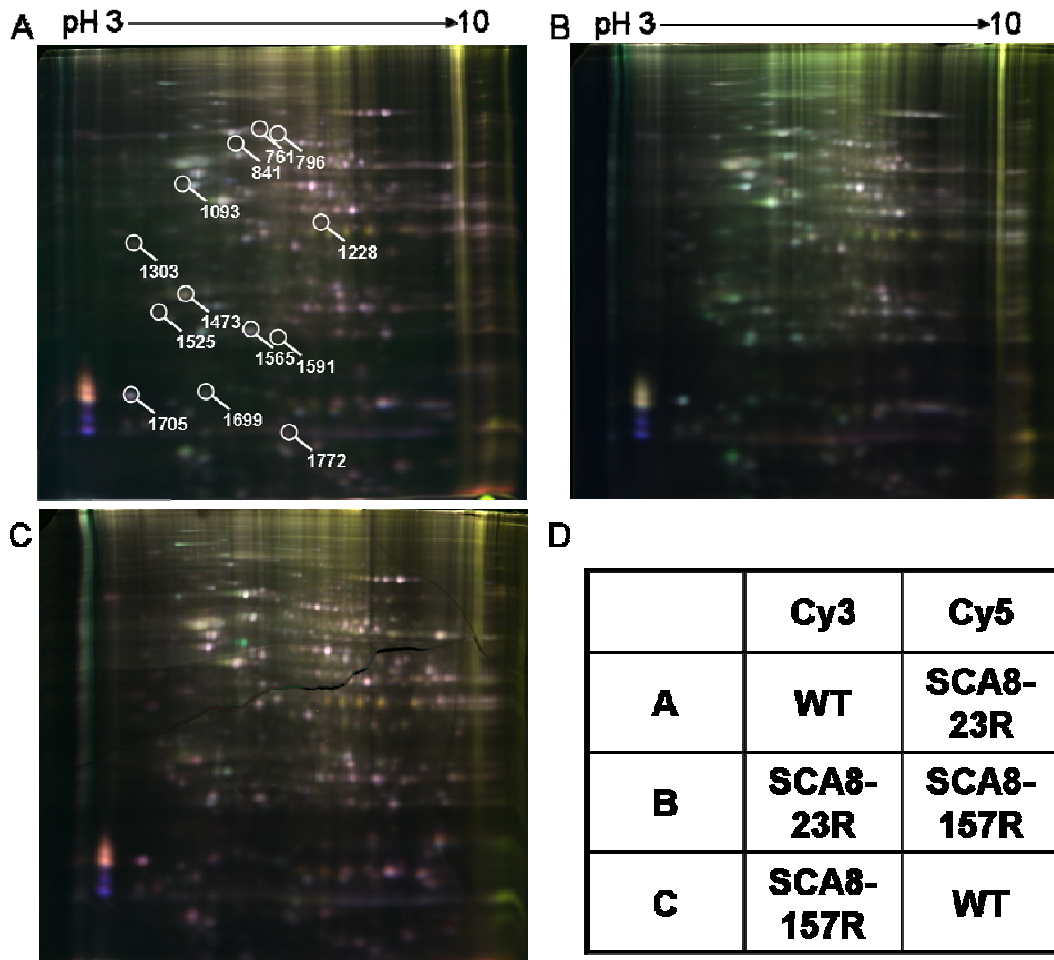


Figure 23. Two-dimensional difference gel electrophoresis (2-D DIGE) gels. A 50 μ g aliquot of each of samples was labelled with either Cy3 or Cy5 (A, B and C), performing a so-called dye swap as shown in (D). Positions of significantly differentially expressed proteins are shown in (A) with white circles and match IDs are indicated with white numbers.

Table 1. Genetics of SCAs

Disease	Gene locus	Gene, gene product	Mutation pattern
SCA1	6p22-p23	<i>SCA1</i> , ataxin-1	CAG expansion
SCA2	12q24.1	<i>SCA2</i> , ataxin-2	CAG expansion
SCA3	14q32.1	<i>SCA3</i> , ataxin-3	CAG expansion
SCA4	16q22.1	<i>PLEKHG4</i> , Puratrophin-1	5'-UTR 1 nt substitution
SCA5	11q13	<i>SPTBN2</i> , β III spectrin	Deletion, missense mutation
SCA6	19p13	<i>CACNA1A</i> , α_{1A} subunit of voltage-gated calcium channels type P/Q	CAG expansion
SCA7	3p21.1-p12	<i>SCA7</i> , ataxin-7	CAG expansion
SCA8	13q21	<i>SCA8</i> , untranslated	CTG expansion
SCA10	22q13.3	<i>SCA10</i> , ataxin-10	ATTCT expansion
SCA11	15q14-q21.3	Undefined	
SCA12	5q31-33	<i>PPP2R2B</i> , protein phosphatase 2, regulatory subunit B, β	CAG expansion
SCA13	19q13.3-q13.4	Undefined	
SCA14	19q13.4-qter	<i>PRKCG</i> , protein kinase C γ	Missense mutation
SCA15	3p24.2-pter	Undefined	
SCA16	8q22.1-q24.1	Undefined	
SCA17	6q27	<i>TBP</i> , TBP	CAG expansion
SCA18	7q22-q32	Undefined	
SCA19	1p21-q21	Undefined	
SCA20	11p13-q11	Undefined	
SCA21	7p21.3-p15.1	Undefined	
SCA22	1p21-q23	Undefined	
SCA23	20p13-12.3	Undefined	
SCA25	2p15-21	Undefined	
SCA26	19p13.3	Undefined	
SCA27	13q34	<i>FGF14</i> , fibroblast growth factor 14	Missense mutation
SCA28	18p11.22-q11.2	Undefined	
DRPLA	12p13.31	<i>DRPLA</i> , atrophin-1	CAG expansion

Table 2. Primers and conditions for PCR amplification of tri- or pentanucleotide repeat region in SCA genes

<i>Gene</i>	Primer	T _m (°C)	MgCl ₂ / dNTP (mM)	Amplicon(bp) (repeats)
<i>SCA1</i>	Tamra-CAACATGGGCAGTCTGAG AACTGGAAATGTGGACGTAC	60	1.5 / 0.2	194-293 (6-39)
<i>SCA2</i>	CGTGCGAGCCGGTGTATGGG Hex-GGCGACGCTAGAAGGCCGCT	60	1.5 / 0.2	145-196 (14~31)
<i>SCA3</i>	Tamra-CCAGTGACTACTTTGATTCG CTTACCTAGATCACTCCCAA	60	1.5 / 0.2	235-319 (12-40)
<i>SCA6</i>	Hex-CCACACGTGTCCTATCCCCTG TACCTCCGAGGGCCGCTGGTG	65	1.0 / 0.2	110-149 (3-16)
<i>SCA8</i>	Fam-GCTTGTGAGGACTGAGAATG CCCTGGGTCCTTCATGTTAG	60	1.5 / 0.2	277-349 (16-40)
<i>SCA10</i>	Tamra-AGAAAACAGATGGCAGAATGA GCCTGGGCAACATAGAGAGA	54	0.8 / 0.2	177-237 (10-22)
<i>SCA12</i>	Tamra-TGCTGGGAAAGAGTCGTG GCCAGCGCACTCACCCTC	54	1.0 / 0.2	<209 (29)
<i>SCA17</i>	Hex-ATGCCTTATGGCACTGGACTG CTGCTGGGACGTTGACTGCTG	58	1.0 / 0.2	186-237 (25-42)
<i>DRPLA</i>	Hex-CAGTGGGTGGGGAAATGCTC CACCAGTCTCAACACATCAC	65	1.0/0.2	114-189 (10-35)

Tamra, Hex, Fam represent the fluorescence dyes labeled in the forward primers

Table 3. Trinucleotide and pentanucleotide repeat lengths in nine disease genes in neurodegenerative patient* and control groups

Locus	<u>Patient</u>			<u>Control</u>			<i>P</i>
	Mean (SD)	Median	Range	Mean (SD)	Median	Range	
<i>SCA1</i>	28.28 (2.01)	28	21-39	28.07 (2.11)	28	17-35	0.094
<i>SCA2</i>	21.99 (0.99)	22	13-30	21.98 (0.65)	22	17-27	0.516
<i>SCA3</i>	20.34 (6.55)	14	14-42	20.05 (6.75)	14	14-38	0.327
<i>SCA6</i>	12.08 (2.48)	13	4-19	12.06 (2.22)	13	4-19	0.340
<i>SCA8</i>	24.66 (5.85)	25	15-88	24.91 (4.20)	26	18-37	0.071
<i>SCA10</i>	14.66 (1.52)	14	11-23	14.69 (1.65)	15	10-19	0.765
<i>SCA12</i>	13.39 (3.08)	13	6-29	13.77 (3.24)	13	7-27	0.064
<i>SCA17</i>	36.43 (1.57)	36	28-46	36.52 (1.35)	36	30-43	0.280
<i>DRPLA</i>	14.92 (3.26)	15	7-22	15.02 (3.51)	15	8-31	0.799

*SCA patients were excluded.

Table 4. Prevalence and frequency of large normal alleles in Taiwanese, Japanese and Caucasians*

Locus	Prevalence (%)	Frequency (repeat no.)
	Taiwanese / Japanese / Caucasians	Taiwanese / Japanese / Caucasians
<i>SCA1</i>	4 / 3 / 15	0.09 / 0.09 / 0.26 (>30)
		0.05 / 0.04 / 0.16 (>31)
<i>SCA2</i>	0 / 5 / 14	0.03 / 0.01 / 0.12 (>22)
		0.01 / 0.01 / 0.03 (>23)
<i>SCA3</i>	36 / 43 / 30	0.07 / 0.11 / 0.04 (>28)
		0.06 / 0.07 / 0.02 (>29)
<i>SCA6</i>	18 / 11 / 5	0.17 / 0.20 / 0.04 (>13)
		0.04 / 0.08 / 0.00 (>14)
<i>DRPLA</i>	0 / 20 / 0	0.05 / 0.10 / 0.03 (>19)
		0.01 / 0.08 / 0.01 (>20)

*Prevalence of SCA and frequency of large normal alleles in Japanese and Caucasians according to Takano et al. 1998.

Table 5. Expanded trinucleotide repeat sequences and numbers in PD patients

Subject	Age/Sex	SCA: repeat no.	Repeat sequence	Diagnosis
H31	71/F	SCA8: 88	CTA ₈ CCACTACTGCTACTGCTA CTG ₇₄	PD
H168	79/F	SCA8: 75	CTA ₂₀ CTG ₂ CTCCTG ₅₂	PD
H327	68/F	SCA8: 82	CTA ₁₂ CTG ₇₀	PD
H600	60/F	SCA8: 92	CTA ₇ CTG ₂ CTACTGCTACTG ₈₀	PD
H115	76/M	SCA17: 46	CAG ₃ CAA ₃ CAG ₆ CAACAGCAAC AG ₂₉ CAACAG	PD

Table 6. Summary of copy numbers, RNA expression, and clasping phenotype of SCA8 transgenic mice. (-, not detected; +++ and +++++, mild and severe extent of clasping phenotype, respectively)

Founder line	Copy #	RNA expression in CNS (offspring)	Clasping (founder)
23R-17	20	+	-
23R-24	30	+	-
157R-11	3	+	+++
157R-62	5	+	+++++
157R-17	25	-	-
157R-7	1	+	+++++

Table 7. List of TaqMan gene expression assays

Assay ID	Gene Symbol	Gene Name	Accession No.
Mm00492632_m1	Igfbp2	insulin-like growth factor binding protein 2	NM_008342.2
Mm01208542_m1	Scd2	stearoyl-Coenzyme A desaturase 2	NM_009128.1
Mm00803929_m1	Slc12a5	solute carrier family 12, member 5(K-Cl cotransporter)	NM_020333.1
Mm00479791_m1	Pabpn1	poly(A) binding protein, nuclear 1	NM_019402.1
Mm00657708_m1	Kcnc1	potassium voltage gated channel, Shaw-related subfamily, member 1	NM_008421.2
Mm00454956_m1	Usp3	ubiquitin specific peptidase 3	NM_144937.2
Mm00460360_m1	Calml4	calmodulin-like 4	NM_138304.1
Mm00439564_m1	Igf2	insulin-like growth factor 2	NM_010514.2
Mm00443267_m1	Ttr	transthyretin	NM_013697.1
Mm00436057_m1	Pthlh	parathyroid hormone-like peptide	NM_008970.1
Mm00441119_m1	Rbp1	retinol binding protein 1, cellular	NM_011254.4
Mm99999915_g1	Gapdh	glyceraldehyde-3-phosphate dehydrogenase	NM_00804.2

Table 8. Summary of microarray analysis at the age of 20-month. ↑ and ↓ represent greater than 1.5- fold or smaller than 0.7-fold changes when comparing to the wild type littermate, respectively. Compared to 157R-62 line, transcript expressions of *Pthlh* and *Rbp1* are significantly down-regulated in 23R-24 line.

Gene name	Product	Transgenic line	
		157R-62	23R-24
S100a9	S100 calcium-binding protein A9 (calgranulin B)		↑
S100a8	S100 calcium binding protein A8 (calgranulin A)		↑
Slc12a5	K-Cl cotransporter	↑	↑
Actb	actin, beta, cytoplasmic	↑	↑
Scd2	stearoyl-Coenzyme A desaturase 2	↑	↑
Pabpn1	poly(A) binding protein, nuclear 1	↑	
Usp3	Similar to ubiquitin specific protease 3	↑	
Kcnc1	potassium voltage gated channel, Shaw-related subfamily, member 1	↑	
Hnrpa2b1	heterogeneous nuclear ribonucleoprotein A2/B1	↑	
SOD3	extracellular superoxide dismutase		↓
Calml4	calmodulin-related protein		↓
Gh	growth hormone	↓	↓
Igf2	insulin-like growth factor 2		↓
Igfbp2	insulin-like growth factor binding protein 2	↓	↓
Ttr	transthyretin		↓
Pthlh	parathyroid hormone-like peptide		
Rbp1	retinol binding protein 1, cellular		

Table 9. Summary of relative changes of protein abundance among 157R-62, 23R-24 and wild type (WT) littermates. ↑, increased protein level when comparing with the other mouse line. The bold numbers indicate that the levels of same proteins in 23R-24 and the wild type littermate were significantly abundant than in 157R-62 transgenic mouse line.

Match ID	Comparison between		Comparison between	
	157R-62	23R-24	157R-62	WT
1772	↑			
1705		↑		↑
1699				↑
1591				↑
1565		↑		↑
1525				↑
1473		↑		↑
1303		↑		↑
1228	↑			
1093		↑		
841				↑
796	↑			
761		↑		↑

Table 10. MALDI-TOF analysis of the protein spots

Match ID	Identified protein	Mascot Score	Difference	MS Coverage	Protein MW	pI value
1565	ATP synthase D chain, mitochondrial	102	59	56	18607	5.41
1525	Calbindin (Vitamin D-dependent calcium-binding protein)	102	69	32	29844	4.56
1473	Calretinin (CR)	132	83	47	31353	4.8
841	Heterogeneous nuclear ribonucleoprotein K	93	66	38	50944	5.26
761	Serum albumin precursor	126	79	32	68648	5.7